Alma Mater Studiorum – Università di Bologna

DOTTORATO DI RICERCA IN

Chimica

Ciclo XXVII

Settore Concorsuale di afferenza: 03/C2

Settore Scientifico disciplinare: CHIM/04

THE SYNTHESIS OF MALEIC ANHYDRIDE: STUDY OF A NEW PROCESS AND IMPROVEMENT OF THE INDUSTRIAL CATALYST

Presentata da: Giulia Pavarelli

Coordinatore Dottorato **Relatore**

Prof. Aldo Roda **prof. Fabrizio Cavani**

Esame finale anno 2015

Summary

1 Aim of work

Nowadays the industrial production of maleic anhydride (MA) is achieved principally by the selective oxidation of *n*-butane, a process catalyzed by V/P/O-based materials, namely the vanadyl pyrophosphate (VPP), a compound with formula $(VO)_2P_2O_7$.

Although this process has been widely used since the '80s, the importance of MA as a building block in the chemical industry is still largely recognized and this is why the interest for both improving the technology and more deeply studying this reaction has never ended. Within this framework, the first topic of my PhD thesis was investigated in collaboration with a company specialized in the production of organic anhydrides and their derivatives, Polynt SpA, with the aim of improving the performance of the process for the selective oxidation of *n*-butane to maleic anhydride and comparing the behavior of an industrial VPP-based catalysts (produced at an industrial scale by Polynt) when utilized either in the industrial plant or in lab-scale reactor. In particular, we investigated how the catalysts are affected by the reaction conditions (for example the hydrocarbon concentration) and how the addition of a dopant (specifically, Nb) could enhance the catalytic performance. Moreover, we monitored the ageing of the catalyst and we correlated the gradual deactivation process with the modifications occurring on the catalyst surface and in the bulk.

The second topic of my PhD thesis was produced within the Seventh Framework (FP7) European Project "EuroBioRef". The study was focused on a new route for the synthesis of maleic anhydride starting from non-petroleum based reactants, in particular from renewable raw materials. The project intended to utilize an alternative reactant produced by fermentation of biomass, "bio-1-butanol". In this field, my PhD was dedicated to the investigation of three possible catalytic configurations for the feasibility of the process; in particular, the process was divided into two main reactions: the dehydration of 1-butanol to butenes and the selective oxidation of butenes to maleic anhydride. We investigated the features needed to catalyze the reactions successfully and we proposed different materials as catalysts, namely Keggin-type

polyoxometalates, $VOPO_4 \cdot 2H_2O$ and $(VO)_2P_2O_7$. The reactivity of 1-butanol was tested under different conditions, in order to optimize the performances and understand the interaction between the alcohol and the catalyst surface. Then, we studied the key intermediates in the mechanism of 1-butanol oxidehydration to MA, in order to understand the possible reaction mechanism. Lastly, we compared the reactivity of the chemical 1-butanol with the behaviour of different types of bio-butanols produced by biomass fermentation.

2 Introduction

2.1 Maleic anhydride

Maleic anhydride (MA) is the acid anhydride of maleic acid and its formula is $C_4H_2O_3$. It is an organic compound with four atoms of carbon in a cyclic structure and at room temperature is a white solid with an acrid odor (Figure 2.1).

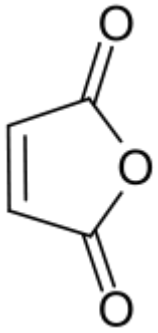

Figure 2.1: Maleic anhydride structure

Physical and chemical characteristics of MA are reported in Table 2.1.

Molecular weight (g/mol)	98.057
Melting point (°C)	52.56
Boiling point (°C)	202
Density (g/cm^3)	1.314
Specific gravity at 60°C (g/cm^3)	1.31
Specific gravity, solid (g/cm^3)	1.43
Viscosity at 70°C (mPa·s)	1.53
Vapor Pressure at 70°C (mmHg)	6.2
Vapor Density (air=1)	3.4
Flash point, closed cup (°C)	103
Flash point, open cup (°C)	102
Autoignition temperature (°C)	447
Flammable limits (%)	Lower: 1.4 Upper: 7.1
Heat of combustion (Kcal/mol)	333.9
Heat of formation, solid (Kcal/mol)	112.2
Heat of fusion (Kcal/mol)	3.26
Heat of hydration to maleic acid (Kcal/mol)	8.33
Heat of Vaporization (Kcal/mol)	13.1
Specific Heat, solid (cal/g/°C)	0.285

Specific Heat, liquid (cal/g/°C)	0.396
Refractive index	1.515
Solubility in xylene at 30°C (g/L)	163.2
Solubility in water at 30°C (g/L)	572
Solubility in acetone at 30°C (g/L)	227
Solubility in benzene at 30°C (g/L)	439.4
Exposure limits (ppm)	PEL: 0.25 REL: 0.25 TLV: 0.1

Table 2.1: Physical and chemical properties of MA [1, 2, 3]

MA is a very versatile molecule, that lends itself to many applications; indeed with three active sites (two carboxylic groups and one double bond C=C) it is an excellent joining and cross-linking material, that make MA a bifunctional and a platform molecule. World production and consumption of maleic anhydride in 2010 were reported to be approximately 1.7 million metric tons and its demand was expected to grow on an average of 3-6 % by 2020 [4]. The main use of MA is as monomer in the manufacture of polymers, representing more than 50% for the production of unsaturated polyester resins and about 20% to produce alkyd resins. In the remaining part MA is utilized in different end-use applications as intermediate molecule to obtain other important organic compounds, such as 1,4 butandiol (BDO).

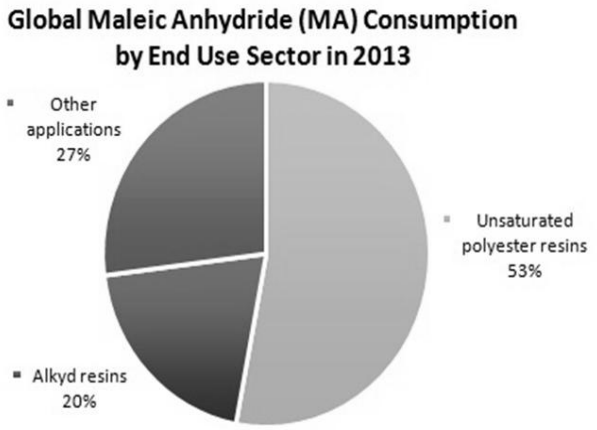

Figure 2.2: World consumption of MA by end use sector in 2013 [5]

MA could be transform to obtain special anhydrides, such as succinic anhydrides (by hydrogenation) and tetrahydrophthalic anhydride (by Diels-Alder reaction with butadiene). Furthermore, succinic ahydride is hydrolyzed to succinic acid and converted to γ-butyrolactone (GBL) [6], tetrahydrofuran (THF) [7, 8] and 1,4

butandiol (BDO) [8, 9]. On the other hand, tetrahydrophthalic anhydride could be hydrogenated to esahydrophthalic anhydride, that is used together with methyl-esahydrophthalic as vulcanizer agent and as hardener in the production of epoxy resins. MA is also an important intermediate in the fine chemical industry, particularly in the manifacture of agricultural chemicals (pesticides) and lubrication oil additives. It is also a component of several copolymers (MA-styrene, MA-acrylic acid) and paints. Moreover, MA could be hydrolyzed to maleic acid and fumaric acid, which are used as additives to adjust the acid flavor; fumaric acid is also utilized as drug in the treatment of psoriasis and as intermediate in the synthesis of tartaric acid. Finally, MA is utilized for the production of aspartic acid, an intermediate of aspartame production. In Figure 2.3 the applications of MA are summarized:

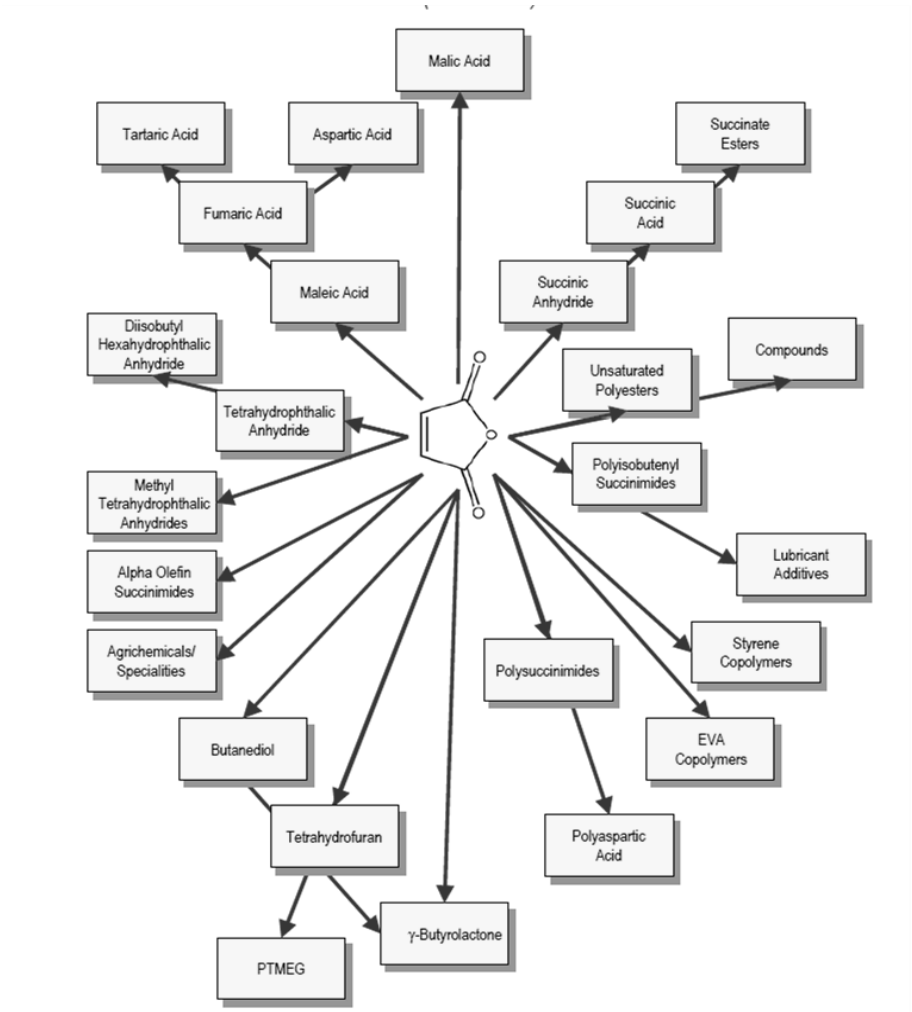

Figure 2.3: Applications of MA [10]

2.2 Maleic anhydride production

The industrial production of MA is achieved either by the selective oxidation of benzene or the selective oxidation of *n*-butane.

The selective oxidation of benzene (Figure 2.4) is the oldest process and even if it has been replaced by *n*-butane, it continues to be used in Far East countries, namely in China. The reactor technology is a fixed-bed configuration: the reaction occurs in gas phase, at 400-450°C, in a multi tubular plug flow reactor [11].

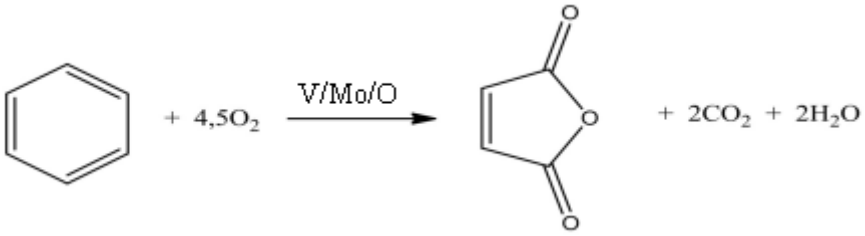

Figure 2.4: Selective oxidation of benzene to MA

The catalyst is composed by V/Mo oxides (V_2O_5 and MoO_3) supported on an inert and high-conductive material, in order to better remove the heat of reaction. Reaction gas passes through the tubes over the catalysts, the process pressure being adjusted to an optimim value of 0.15 – 0.25 MPa. A considerable amount of heat is produced during the reaction (ΔH = - 1875 kJ/mol) and the undesirable secondary reactions of combustion to CO_x are strongly exothermic and ‘‘hot spots’’ of 340-500 °C can occur on the catalyst surface [12]. The advantage of this process is that benzene conversion is almost total (about 96%) and MA selectivity can reach 73%; because of its toxicity, the unreacted benzene is catalytically incinerated. Indeed, benzene is classified as a carcinogen so its emission are strictly controlled by environmental legislations. These rules differ very much in various countries: nowadays the limit emission in air of benzene in Italy is established by D. Lgs. 155/2010 and it is fixed at 5 $\mu g/m^3$ per year [13]. In Figure 2.5 the process of benzene oxidation to maleic anhydride is reported: after reaction the gases are cooled by salts melts and crude MA is recovered by partial condensation and by water scrubbing as maleic acid solution. Then, the water solution

is dehyderated and pure MA is obtained by a batchwise distillation (*o*-xylene is added as entraining agent for the azeotropic distillation).

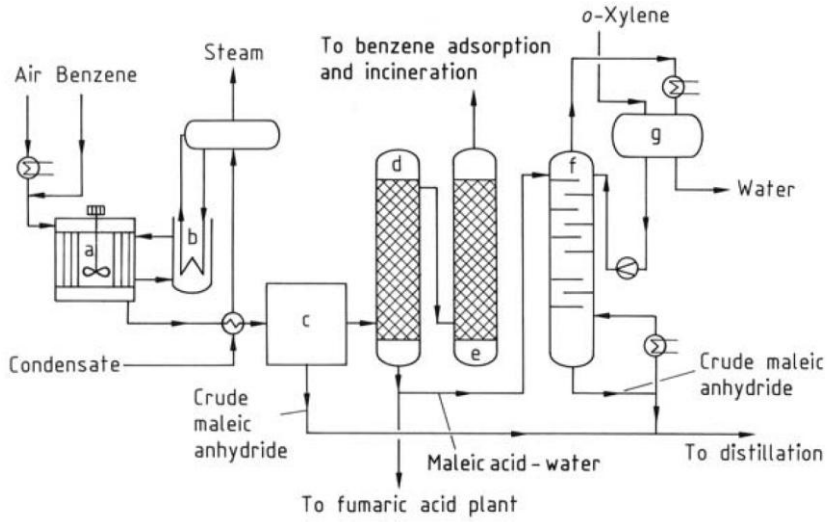

Figure 2.5: Plant for the production of maleic anhydride by benzene oxidation: a) reactor; b) salt bath cooler; c) partial condense; d) acid scrubber; e) alkali scrubber; f) dehydration column; g) phase separator

Since the 70's *n*-butane has gradually been replaced benzene as reactant for the synthesis of MA and nowadays approximately 80% of MA is produced starting from *n*-butane (Figure 2.6). The major incentives of the C4 hydrocarbon are the lower cost and the lower environmental impact, that render *n*-butane an inexpensive and non-toxic feedstock.

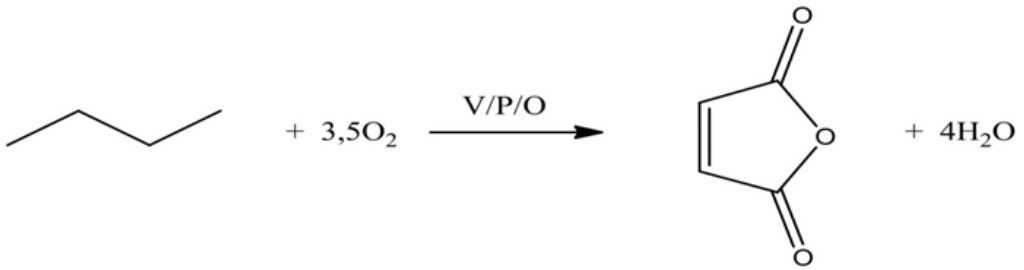

Figure 2.6: Selective oxidation of *n*-butane to MA

A list of the advantages is reported below:

1. Cost: *n*-butane is cheaper than benzene (*n*-butane: 750 €/ton; benzene: 1000 €/ton);
2. Toxicity: *n*-butane is a non-toxic reagent, instead of benezene that is a proven carcinogenic compound;
3. Atom economy (E factor): ratio between atoms of carbons of the target product and the reactant; for *n*-butane the ratio is 1 (C4/C4), for benzene is C6/C4 (2 atoms of carbon lose in CO_2)
4. Separation and purification: starting from benzene many heavy compounds are formed as by-products;
5. Heat removal: starting from *n*-butane the reaction is less exothermic (-1260 kJ/mol instead of -1875 kJ/mol [12]).

The success of the process was the the discovery of a suitable and highly selective catalyst, the vanadyl pyrophosphate $(VO)_2P_2O_7$ (VPP), that is one of the most successful example of an industrial catalyst used for the synthesis of a bulk chemical compound starting from an alkane.
Nevertheless, the selective oxidation of *n*-butane has many disadvantages, as all alkane oxidation process:

1. Total oxidation: CO and CO_2 are formed by parallel and consecutive combustion reactions involving unreacted *n*-butane and products formed; in order to limit the combustion the *n*-butane conversion has to be maintained lower than 80%;
2. Exothermicy: the reaction is highly exothermic and run-away must be avoided by an efficient heat removal;
3. Flammable mixtures: the composition of reactive mixture *n*-butane/air must be controlled and maintained under its flammability limit, in order to guarantee the safety of the process.

In order to have a successful industrial process, a simultaneous fine-tuning of the catalyst and of the reactor technology is required [14].

2.3 Commercial Maleic Anhydride Technologies

Several reactor configurations have been developed for commercial maleic anhydride production [14]:

1. Fixed bed: practised and licensed by Huntsman (formerly Monsanto) Scientific Design and Technobell;
2. Fluidized bed: practised and licensed by Polynt (formerly Lonza), Ineos (formerly BP) and BOC/Mitsubishi;
3. Transported bed: Circulating Fluidized Bed Reactor (CFBR), developed by DuPont and recently abandoned [15].

In every kind of technology the basic plant configuration could be summarized in a common scheme reported in Figure 2.7.

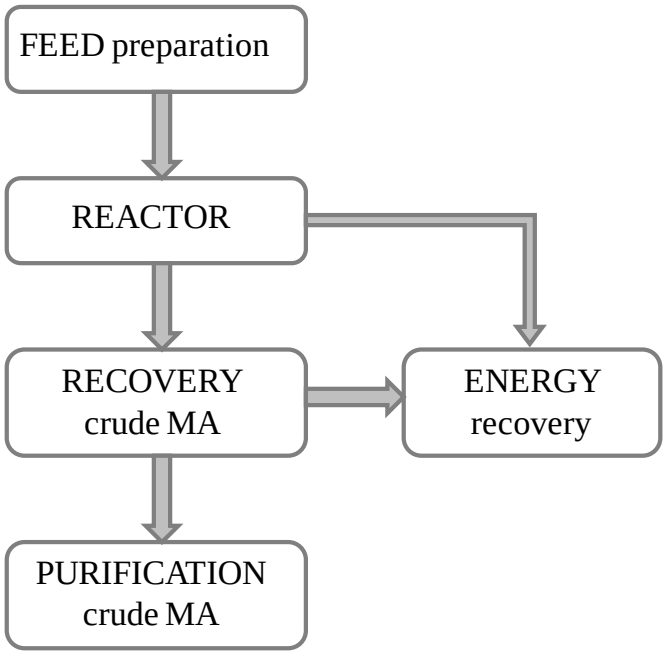

Figure 2.7: Basic MA plant configuration

MA plants are distinguished by type of reactor, method for the recovery of crude MA and feed composition (percentage of *n*-butane in air). In Table 2.2 the most important industrial technologies used for the synthsis of MA starting from *n*-butane are reported.

Process	**Reactor**	**Recovery**	**Feed composition**
ALMA (Polynt)	Fluidized bed	Anhydrous	3.6-5% *n*-butane
BOC/Mitsubishi	Fluidized bed	Aqueous	3.6-5% *n*-butane
Sohio-UCB	Fluidized bed	Aqueous	3.6-5% *n*-butane
Monsanto (Huntsman)	Fixed bed	Anhydrous	1.8% *n*-butane
Scientific Design	Fixed bed	Aqueous	1.8% *n*-butane
Technobell	Fixed bed	Aqueous	1.8% *n*-butane
DuPont	Transported bed (CFBR)	Aqueous	<4% of n-butane in air

Table 2.2: Industrial technologies for the synthesis of MA from n-butane [16, 17, 18]

2.3.1 Fixed bed

In a fixed bed configuration the catalyst is loaded in pellets or in various shapes in a multi tubular reactor containing several thousand reaction tubes, tipically either 3 or 6.5 m long and with 21-25 mm as diameter. Because of its explosion hazards *n*-butane has to be fed in limited inlet concentrations, lower than 1.85% mol in air (lower explosion limit). With this technology, feeding 1.7% *n*-butane in air at 400°C, the highest MA yield obtained is around 60% and *n*-butane conversion is 80%.

The crude MA could be recovered by adsorption in water or in organic solvent. In water MA is hydrolyzed to maleic acid, then the acid is dehydrated (at temperature below 130°C to minimize the isomerization to fumaric acid) and finally crude MA is purified by distillation. In the recovery with organic solvent *o*-xylene is tipically used and in such way about 98% of the MA produced is recovered, avoiding fumaric acid formation.

The advantages of fixed bed reactors are:

1. MA yield: it is higher than that one obtained by fluidized bed;
2. Larger plant: it is possible to build plants in parallel;
3. Retrofitting of benzene plants: outdates plants used for the synthesis of MA by benzene route could be transformed in *n*-butane based plants.

2.3.2 Fluidized bed

Fixed bed reactor was the first technology used for the synthesis of MA starting from benzene; for this reason it was applied also for the *n*-butane route and it has been conventionally practiced since several decades. The main advantage is the possibility to easly convert benzene based plant to *n*-butane based ones. However, fluidized bed reactors offer many advantages:

1. Higher productivity: possibility to work with higher inlet *n*-butane concentrations with low risk of explosion (due to quenching effects of particles on free radicals in the bed);
2. More efficient heat removal: the formation of hot sposts is minimized and the runaway combustion risk is suppressed;
3. Lower investment cost;
4. Lower cost of post-reactor treatment, because of the more concentrated streams;
5. Efficient energy recovery: the process provides the export of high pressure steam, working with an air rate lower than the fixed bed;
6. Shorter downtime for catalyst replacement: in the fluidized bed technology the time spent to load and download the catalyst is shorter because it is replaced by a continuous make-up of fresh catalyst.

One of the most advanced fluidized bed technology is the ALMA process (Alusuisse Italia-Lummus Crest), licensed by Polynt SpA (formerly Lonza). In this process *n*-butane and air are fed to a fluidized bed catalytic reactor working at 400-430 °C. Cooling coils are merged in the bed to generate high-pressure steam. In the recovery section, an organic solvent is used to remove the MA from the reaction effluent gas; a

conventional absorption/stripping scheme is used. Crude MA is refined by continuous distillation to separate light compounds and heavy impurities. Tail gas is sent to an incinerator, which converts residual hydrocarbon (and CO) and the developed energy is recovered for producing extra steam. The *n*-butane in the feed composition is about 4% mol; conversion is typically 80-85%, with a molar yield to MA of about 50% [17].

The bulk VPO catalyst is treated by spray-drying with a low amount of additives in order to improve its mechanical resistance. To limit the abrasion of bulk catalyst particles, different techniques can be employed:

1. Impregnation of the active components on an inert support characterized by good fluidization properties and high attrition resistance;
2. Addition of additives;
3. Encapsulation of the active phase in a silica structure.

However fluidized bed reactor has also some disadvantages:

1. Lower MA selectivity, because of feed back-mixing;
2. High mechanical stress and abrasion of the catalyst;
3. Greater catalyst inventory;
4. More complex scale-up.

In order to maintain the necessary particle size distribution of the catalyst, an amount of new catalyst is refilled by make-up.

2.3.3 Transported bed

Latest reactor technology is the circulating fluidized bed reactor (CFBR), developed by DuPont [15], in which the VPP catalyst was circulated between two different separated vessels, the regeneration and the reaction zones (oxidizing and reducing zones). The main objective has been to maximize the utilization of selective catalyst lattice oxygen: *n*-butane and oxygen are fed separately, so higher *n*-butane concentrations (20%) could be fed, giving an enhancement of MA productivity. The

process could be schematically divided into two parts: (1) the riser reactor, where *n*-butane is fed (without air) and where the catalyst transforms the hydrocarbon to MA by means of lattice oxygen the, being itself consequently reduced; (2) the re-oxidation part, where the catalyst is recovered by a cyclone and transported to the regenerator reactor, where solely air is fed to restore the oxidation state of the catalyst. Then MA is recovered using water; after the hydrolysis, aqueous MA and maleic acid are reduced to tetrahydrofuran in a hydrogenation reactor. In CFBR technology the *n*-butane conversion is about 50% and MA yield is about 37%. Because of the riser reactor system, it has to be used a catalyst highly resistant to the attrition: indeed, VPP was coated by silica, which gives a very high mechanical resistance and does not cause any selectivity decreasing. The DuPont plant worked from 1996 to 2004 for tetrahydrofuran (THF) production and in 2005 it was shut down.

2.4 Vanadyl pyrophosphate catalyst

The best-suited catalyst known for the selective oxidation of *n*-butane to MA is vanadyl pyrophosphate $(VO)_2P_2O_7$ (VPP), a bulk vanadium-phosphorus mixed oxide with a particular crystalline structure [17, 19, 20, 21]. In the scientific literature many different preparation methods are reported, however there is a general agreement on these following common steps:

1. Synthesis of the catalyst precursor: vanadyl hydrogenphosphate emihydrated, $VOHPO_4 \cdot 0.5H_2O$ (VHP); in the synthesis, the most common reactants used are vanadium pentoxide V_2O_5 as source of V^{5+} and phosphoric acid H_3PO_4 as source of P^{5+};
2. Thermal treatment (calcination) of the precursor to generate the active catalyst $(VO)_2P_2O_7$ (VPP);
3. Activation of the catalyst vanadyl pyrophosphate.

2.4.1 Synthesis of the precursor $VOHPO_4 \cdot 0.5H_2O$

The method of synthesis of the catalyst precursor $VOHPO_4 \cdot 0.5H_2O$ consists of refluxing a mixture of vanadium pentoxide and phosphoric acid in either an organic or aqueous medium. In the reaction, V^{5+} is reduced to V^{4+} species and the reducing agent is oxidised: this it could be hydrogen chloride (HCl) in aqueous solution or an organic solvent, tipically alcohols such as isobutanol or benzyl alcohol. The catalyst precursor precipitates and then it is further dehydrated to produce the active phase (VPP): the reaction produce also water and the oxidative products derivated from the alchol.

Concerning the synthesis, at least three kinds of preparation could be distinguished: VPA, VPO and VPD routes [22].
The VPA route is the oldest precursor synthesis made in aqueous medium with a reducing agent like HCl or hydrazine [23, 24, 25]. In these strong acid conditions the solid is soluble in the aqueous medium: at first it is solubilized as $VOCl_3$ and then it reduced to V_2O_4; the final VHP is obtained by solvent evaporation, together with an amorphous phase, or after a crystallization process, adding water [19]. In

Figure 2.8 the scheme of the VPA method is reported.

$$V_2O_5 + 2HCl \longrightarrow V_2O_4 + Cl_2 + H_2O$$
$$0{,}5V_2O_4 + H_3PO_4 \longrightarrow VO(HPO_4)\cdot 0{,}5H_2O + 0{,}5H_2O$$

Figure 2.8: Scheme of the VPA method

The VPO route is the synthesis with organic reductant (a single alcohol – generally isobutanol - or a mixture of alcohols) and this is the most common preparation [26, 27]. In the organic medium V_2O_5 is solubilized forming vanadium alcoholates, which are reduced by the organic solvent to V_2O_4. Thus, H_3PO_4 is added and it reacts with V_2O_4 at the liquid-solid interface forming the VHP. The choise of the alchols greatly affects the catalyst behaviour: in particular, the addition of glycols, like 1,2- ethandiol, 1,3-propandiol, 1,3-butandiol and 1,4-butandiol, has a considerable effect on the

morphological features of the vanadyl orthophosphate hemihydrate, because the organic compounds are trapped in the structure [31]. In Figure 2.9 the scheme of the VPO method is reported.

$$V_2O_5 + \text{i-}C_4H_9OH \longrightarrow V_2O_4 + \text{i-}C_4H_8O + H_2O$$
$$0{,}5V_2O_4 + H_3PO_4 \longrightarrow VO(HPO_4)\cdot 0{,}5H_2O + 0{,}5H_2O$$

Figure 2.9: Scheme of the VPO method

Finally there is the VPD route, composed by two-steps, where the VHP is formed by the reduction of dihydrate vanadyl phosphate ($VOPO_4 \cdot 2H_2O$) with alcohol [28, 29]. In Figure 2.10 the scheme of the VPO method is reported.

$$0{,}5\ V_2O_5 + H_3PO_4 + 0{,}5H_2O \longrightarrow VOPO_4 \cdot 2H_2O$$
$$2VOPO_4 \cdot 2H_2O + \text{i-}C_4H_9OH \longrightarrow 2VO(HPO_4)\cdot 0{,}5H_2O + \text{i-}C_4H_8O + 3H_2O$$

Figure 2.10: Scheme of the VPD method

The synthesis of the precursor is a fundamental step in the overall process because it strictly affects the catalytic behaviour of the active phase (VPP). For these reasons, there are many scientific papers and patents dealing with the catalyst manifacture [30, 31, 32]. Indeed, one of the main innovations in the industrial synthesis of MA has been the replacement of the corrosive HCl with organic reducing agent, beeing the organic medium a solvent for the phosphoric acid but not for the V/P oxide. With the catalyst synthetized by the VPO route an important improvement in terms of MA yield was achieved, from 43% with the VPA route to 54% with VPO route [32].

Mainly the three methods differ for the morphology and the surface area of the catalyst obtained. By the VPA route a catalyst with low surface area is formed (3-5 m^2/g) and often an impurity phase $VO(H_2PO_4)_2$ is co-produced. With the VPO method, higher values of surface area (10 m^2/g) a more defective structure are possibile; the presence of defects is known to improve the catalyst performances in terms of MA yield. These aspects are a consequence of alcohols molecules, retained

inside the VHP layers: these organic residues ("intercalated") trapped into the crystalline structure are responsible of a thin platelet structure. Moreover, the precursors samples obtained by VPO method are less crystalline and preferentially expose (001) planes, correspondent to (100) planes of vanadyl pyrophosphate, which possess higher density of active sites [16, 31]. The VPD route has been attracting attention recently: the morphology of the material is markedly different from those synthetized via VPA and VPO method: the the particles have a "rosette" morphology and an higher surface area (30 m^2/g). This method permits a good control of the precursor morphology but the low crystallinity and the dominance of non-selective planes (220) make this route not so suitable; this is why the most used industrial method of synthesis of VHP remains the VPO one.

Nevertheless, in the scientific literature other methods of preparation are reported [22], differing for alternative V and P sources: i) the hydrothermal synthesis, using V_2O_4 instead of V_2O_5, H_3PO_4 or $H_4P_2O_7$ in an autoclave at 145°C); ii) NH_4VO_3, with oxalic acid and H_3PO_4; iii) a mixture of VCl_3 and V_2O_5, or even iv) vanadium metal to reduce V_2O_5; finally, also v) V_4O_9 was utilized as a vanadium source.

2.4.2 Thermal treatment of the precursor $VOHPO_4 \cdot 0.5H_2O$: mechanism of transformation of VHP to VPP

The crystal structure of the precursor $VOHPO_4 \cdot 0.5H_2O$ is made of pairs of $[VO_6]$ octahedra sharing a face, linked together by an hydrogenphosphate tetrahedral groups (Figure 2.11). The molecule of water is bridge-connected and shared between the two neighbor vanadium atoms, oriented in *trans* position to the atom of oxygen of the vanadyl group (V=O): the water is responsible of the layered structure of the precursor [33]. The layers are kept together in the c direction through strong hydrogen bonds involving the water molecules and the P-OH groups: this relatively strong network is reflected in the high temperature required for water loss of the precursor. In this tridimensional structure interconnected by hydrogen bonds, the nature of the organic alcohol used in the VPO preparation is strictly connected to the intercalation properties (see previous paragraph): indeed, the alcohol could reduce distance

between the planes, allowing the formation of crystals with the predominant exposure of (001) planes [34, 35, 36].

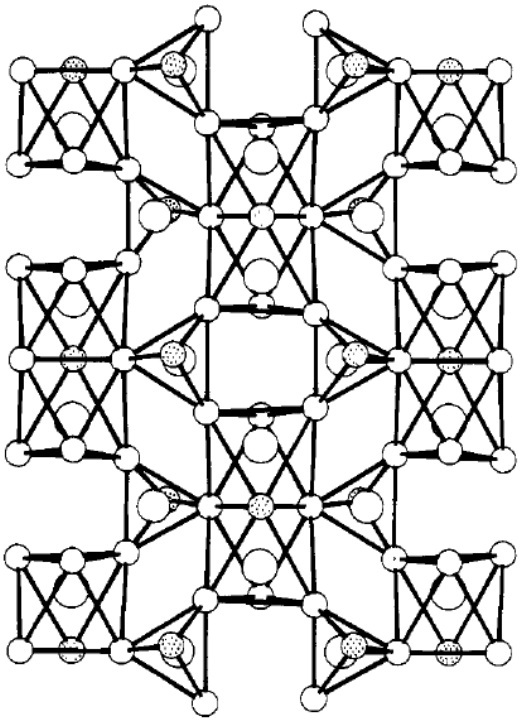

Figure 2.11: $VOHPO_4 \cdot 0.5H_2O$ structure [29]

After the synthesis of vanadyl hydrogen phosphate hemihydrate the material has to be thermally treated to generate the active phase, $(VO)_2P_2O_7$. This transformation involves two molecules of water lost in two dehydration steps [29]; the reaction is summarized in Figure 2.1.

$$2\ VOHPO_4 \cdot 0{,}5H_2O \rightarrow 2\ VOHPO_4 + H_2O$$
$$2\ VOHPO_4 \rightarrow (VO)_2P_2O_7 + H_2O$$

Figure 2.12: Scheme of the synthesis of VPP starting from the precursor VHP

The first dehydration forms an amorphous or microcrystalline compound, having still typical functional groups of hemihydrate vanadyl acid orthophosphate; the second step involves the condensation of orthophosphate groups to form the typical pyrophosphate groups. In the traditional lab-scale synthesis the transformation of

VHP to VPP occurs by a calcination in air at 350°C, followed by a calcination in nitrogen at 550°C. The thermal treatment of the precursor is a multi-steps method composed by:

1. Drying at temperature under 300°C, in order to remove organic residues (in case of VPO route) or Cl^- ions (in case of VPA route) avoiding water removal;
2. Dehydration and/or calcination with formation of the active phase VPP.

Several methods of dehydration are reported in literature, namely differing for the temperature and for the gas phase composition. A list of the most used treatment is reported below.

1. *In-situ* dehydration (inside the reactor): at 280°C, feeding a lean *n*-butane/air mixture at low residence time; temperature and reactive mixture are increased until reaching the common reaction conditions (this procedure is completed in one day);
2. Oxygen-free dehydration at high temperature (>400°C) followed by a treatment with *n*-butane/air reactive mixture [29, 37];
3. Calcination at high temperature (>400°C) and then feeding of *n*-butane/air reactive mixture [38, 39]
4. Hydrothermal treatment, composed by a flow of air and water at 275°C (pre-calcination) and after nitrogen at 390°C [40]

Compared with the precursor, the active phase $(VO)_2P_2O_7$ has a different crystal structure; this was solved by Gorbunova et al. in 1979 [41] and later refined by Nguyen et al. 1995 [42]. Vanadyl pyrophosphate is built of pairs of $[VO_6]$ octahedra linked through a common hedge, forming double chains of octahedral connected by the hedge-oxygen in the *c* direction and by pyrophosphate groups, with a phosphorous-bridge bond (Figure 2.13). Along the chains, single bond V-O and double bond V=O are alternate, respectively 1.60 Å and 2.30 Å long. The unit cell of VPP is orthorhombic [43].

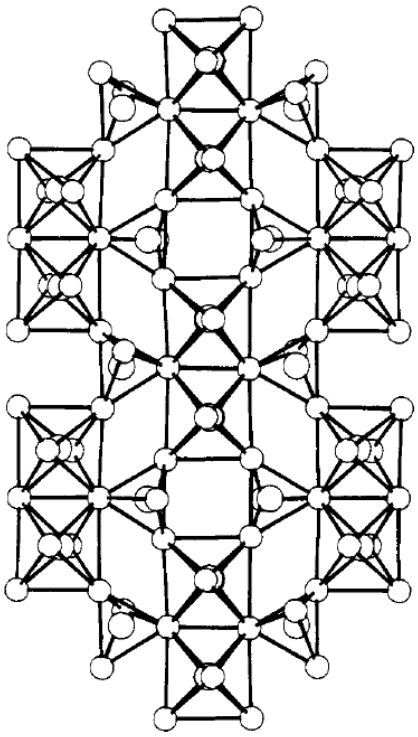

Figure 2.13: ($(VO)_2P_2O_7$ structure [29]

Several hypothesis have been proposed for the mechanism of transformation of VHP to VPP, however all agree that vanadyl pyrophosphate retains the morphology of the precursor [28, 44, 45]. The relation between the two crystalline structures indicates that a topotactic transformation occurs, since the conversion takes place without breaking V-O-P bonds, while weak V-OH_2 and e P-OH_2 bonds are broken and a couple of [HPO_4] unit condense into pyrophosphate groups. There mechanism was studied by Torardi et al. [46] and by Bordes et al. [35, 47, 48, 49] and was confirmed by in situ XRD, SEME-TEM and XPS experiments [45, 36, 50]. In the topotactic transformation the face-shared octahedra are converted in edge-shared ones, resulting in a small expansion (about 12%) of the *a* axis and with the inversion of the central atom of phosphorous. The structural (001) basal planes and (220) planes of the precursor are transformed, respectively, in the correspondent (200) parallel to the basal planes and (024) planes of VPP, maintaining further the same relative broadening. Because of this strong relationship, it is possible to control the structure of vanadyl pyrophosphate by a fine-tuning of the emihydrate synthesis.

It is worth to note that physical and chemical characteristics of the final VPP catalyst are affected by several parameters involving not only the precursor synthesis:

1. Temperature, time and thermal treatment conditions;
2. Reductant agent (VPO, VPA or VPD route)
3. Precursor morphology;
4. Addition of dopants;
5. Structural defects;
6. P/V ratio
7. Optimal V^{4+}/V^{5+} ratio

In particular, the latter point is the result of a combination of effects involving the precursor synthesis, the P/V ratio, the presence of dopants and the working conditions of the catalyst, i.e the reactive *n*-butane/air mixture composition. Even though vanadium is present as V^{4+} in stoichiometric vanadyl pyrophosphate, after the thermal treatment of precursor some crystalline and amorphous vanadium phosphates different from $(VO)_2P_2O_7$ are formed [51, 52, 53]. Indeed, the calcination process could lead to the formation of oxidized V^{5+} species, $VOPO_4$ phase, and vanadyl metaphosphate $VO(PO_3)_2$ phase, that may coexist together with VPP. For this reason in the scientific literature there are several hypothesis concerning the identification of the real active phase of the V/P/O based catalyst. Nevertheless, there is a general agreement on considering that the active phase of the catalyst for the selective oxidation of *n*-butane to maleic anhydride is a core of crystalline $(VO)_2P_2O_7$ covered with little isolated amount of $VOPO_4$ phases [54, 55]. The relative amount of each compound mostly depends on the preparation and the thermal treatment/calcination of the precursor. Otherwise, while VPP catalyst is working in the reaction conditions, it may undergo some surface transformations without substantial structural change, but however playing an active roles in the catalytic cycle [56].

2.4.3 Activation of $(VO)_2P_2O_7$ catalyst

After the thermal treatment $(VO)_2P_2O_7$ does not possess yet the proper characteristics of an optimal catalyst. In order to achieve stable catalytic performances, VPP has to undergo to a time of equilibration under *n*-butane/air reaction mixture at 400°C for several hours, typically 50-100 hours. The catalyst could be considered "equilibrated" or "activated" when it has reached a steady behavior in terms of *n*-butane conversion and MA yield/selectivity. During the equilibration time on stream, the chemical structure of VPP gains stability thought a preferential exposure of (001) planes. These are recognized to be the structure-sensitive planes for the formation of MA [19], while the side faces give low selectivity because of the difficulty of the reoxidation of vanadium atoms to V^{5+} in these planes [57, 58]. Typically an equilibrated catalyst as an average oxidation state of vanadium between 4.00 and 4.04, a surface area of 16-25 m^2/g and a slight excess of phosphorous through a P/V ratio between 1.00 and 1.05 [16]. The equilibration period could be more or less long depending on the evolution of the *n*-butane conversion vs. time; generally the fresh catalyst is more active but less selective than the equilibrated one and the initial high conversion decreases during the equilibration time (with an increasing MA selectivity). If the fresh catalyst is highly reduced (containing only V^{4+}), it is necessary an equilibration period longer than 100 hours (200-300h), while in case of an highly oxidised sample (containing also V^{5+}) at least 500 hours are needed to activate vanadyl pyrophosphate. For this reason, the equilibration process inside the reactor is very expensive in terms of commercial cost and for an industrial application it has to be preferred a shorter process in which a stable, active and selective catalyst is obtained directly into the reactor. This is why many patents concerning the activation of the industrial VPP catalyst have been published, for example by Lonza [59] and Hunsman [60]. The improvement could be achieved by a control of the catalyst shape, forming the material into pellets or tablets before the calcination with the combined addition of dopants: the final catalyst is has a P/V ratio in the range 1.03-1.10 and a surface area between 25-40 m^2/g [60]. Another type of innovation was realized by activating the catalyst directly inside the fluidized bed reactor: the

ageing was carried out under reaction conditions, with the advantages of obtaining an activated catalyst even at the beginning, giving stable performances and a better V^{4+}/V^{5+} control [59].

2.4.4 P/V ratio

One of the most important parameter affecting the catalytic performance of vanadyl pyrophosphate is P/V ratio, which is the atomic ratio between the V source and the P source used in the preparation of the precursor. Several studies concerning this topic are reported in literature [61, 62, 63] and the general agreement is that a slight excess of phosphorous is necessary to optimize VPP catalytic performances in the selective oxidation of maleic anhydride. This amount is proposed to affect V^{4+}/V^{5+} ratio, stabilizing V^{4+} phase: P/V ratio lower than 1.0 gives a catalyst active but not selective because the oxidation takes place easier than in samples with a P/V ratio > 1.0; on the other hand, catalysts with P/V ratio between 1.0 and 1.2 show a lower activity but an higher selectivity to MA, because the oxidation of V^{4+} in $(VO)_2P_2O_7$ is limited [16]. Generally on the catalyst surface the P/V ratio is higher than in the bulk [54, 64] and this phosphorous enrichment on the surface layer is considered the responsible of the selective oxidation to MA. However, too much P content leads to the formation of $VO(PO_3)_2$ which is detrimental for the catalytic activity [65].

In conclusions, the variation of the P content modifies the redox properties of VPP catalyst, affecting the rate of V^{4+} oxidation to V^{5+} and the rate of V^{4+}reduction to V^{3+}. For this reason the redox properties of the catalyst are correlated also with the reducing or oxidizing power of the reactive mixture: at low conversion (< 10%), when the reactive mixture is more reducing, P-rich and P-poor catalysts behave in the same way. However, at high conversion (> 80%), when the reactive mixture is more oxidizing, P-poor catalysts form preferentially carbon oxides becoming less selective, because of their increased ability to oxidize V^{4+} to V^{5+}; on the other hand, P-rich catalysts, even if they show low activity and low selectivity at low conversion, they keep more stable performances, avoiding a strong decline of MA selectivity at high conversion [63].

2.4.5 Vanadium oxidation state: V^{4+}/V^{5+} ratio

The selective oxidation of *n*-butane to maleic anhydride is a redox reaction, where *n*-butane is oxidized and oxygen is reduced apparently. In fact, it is the lattice oxygen of the catalyst structure that is actually involved in the redox mechanism, while the oxygen fed in the reactive mixture is necessary to restore the oxidised state of vanadium and the redox cycle. This mechanism follows the Mars-Van Krevelen scheme [66]: in the first step the lattice oxygen of the catalyst oxides the *n*-butane and V^{4+} ions are reduced to V^{3+}; in the second step, the catalyst is re-oxidized by molecular O_2 co-fed with the C4 hydrocarbon. Many species of V^{3+} and V^{5+} could be present either as amorphous or crystalline phosphates or as defects of the vanadyl pyrophosphate structure; the thermal treatment adopted for the precursor plays an important role in determine the final ratio of these compounds.

For this reason, the oxidation state of V in VPP catalyst has an important role in the catalyst behavior and its function has been debated for several years [67, 44, 68]. Volta et al. pointed out that the optimal V^{5+}/V^{4+} ratio has to be equal to 0.25, so defined and isolated amount of V^{5+} over a core of V^{4+} should be the key of the success of the VPP catalyst [69, 70, 71]. Several authors have supported the hypothesis of the strategic role of V^{5+} [72, 73, 74]: isolated V^{5+} sites interacting with VPP are able to provide the optimal surface concentration of sites which permit the alkane activation and O-insertion; on the other hand, if $VOPO_4$ are formed as bulk phases, they become detrimental for the catalyst selectivity [71]. Bordes have asserted that the two oxidation states of V are related to two distinct steps: the activation of *n*-butane by oxygen is associated with V^{4+} species, while the insertion of oxygen to form MA is associated to V^{5+} species [75].

Several forms of $VOPO_4$ phases have been identified: α_I, α_{II}, β, δ, ε, γ, ω and hydrated phases $VOPO_4 \cdot nH_2O$ [76, 77, 78, 79]. The δ and γ $VOPO_4$ were the first structures identified after the precursor treatment in O_2 or air [80] and in used catalysts [81], but they were finely described some years later, together with the other polymorphic and hydrated phases [82, 83]. In general $VOPO_4$ structures consist of $[VO_6]$ octahedra and $[PO_4]$ tetrahedra held together by V-O bond and hydrogen bonds, only connected

through a corner (no edge-sharing, as VPP): the different allotropic forms are distinguished by the arrangement of octahedral and tetrahedra inside the layer. For example, α_I-$VOPO_4$, α_{II}-$VOPO_4$, $VOPO_4 \cdot 2H_2O$ and δ-$VOPO_4$ have a tetragonal structure, even if the δ one was supposed to be orthorhombic for many years and its structure was resolved recently [82]. It is worth to note that δ-$VOPO_4$ phase shows a significant long V-O bond (3.1 Å) and an high O=V—O angle (168°), factors that are supposed to be the causes of its activity in the selective cycle of MA production. According to literature papers, the frequency of these phases in VPP-based catalysts decreases along this series: α_{II}, $\beta > \delta > \gamma$, $\alpha_I > \omega >> \varepsilon$.

Different is the debate concerning the role of V^{3+}: the scientific literature generally agrees about its negative effect on the selectivity, while the generation of a discrete number of these species in the lattice of the VPP associated with anionic vacancies have been proposed to play a positive role on catalytic activity [84, 85]. Generally, the reduced vanadium species are generated during the thermal treatment of the precursor: their concentration is function of the amount of organics trapped in the precursor and of the heat treatment.

As reported in the previous paragraph in case of P/V ratio, also V^{4+}/V^{5+} ratio is function of the reaction conditions, i.e the reducing/oxidizing power of the gas phase atmosphere. Mallada et al. analyzed the effect of hydrocarbon-rich and hydrocarbon-lean conditions on the oxidative state of the catalyst surface [86]: in the first case, V^{3+} surface phases developed together with amounts of C deposits. The same conclusions were reached by Volta et al. [87]: the reduction of V^{5+} and the formation of C deposits are responsible for the decrease of the selectivity to MA. However, the deactivation is not so rapid when the catalyst is pre-oxidized at mild temperature. One way to overcome these limitations is to add promoters, which helps to maintain a higher V oxidation state through either the formation of specific compounds or through the mediation of V re-oxidation in the redox mechanism.

2.4.6 Acidity of the catalyst

Vanadyl pyrophosphate catalyst is considered a multifunctional system because it possesses acid and redox properties both. The acidity occurs in Lewis acid sites (V^{4+}) and in Brønsted ones (P—OH). These sites were detected by IR experiments with probe molecule, like NH_3, pyridine and acetonitrile [88, 89, 90]. It has been hypothesized that the two types of acidity played a different role in the reaction mechanism: in particular, Lewis sites could take part in the hydrogen abstraction, while the Brønsted sites could play a key role in the selective path to MA; the presence of these letter sites was also confirmed by the P-enrichment on the catalyst surface. A more thorough analysis was given by Centi et al. [91], who supposed that Brønsted sites act as a combination of effects, namely through the stabilization of the intermediates and of the adsorbed oxygen species, favoring the oxygen-insertion.
The acidity of VPP catalyst was also studied by density functional theory (DFT) [92, 93]: as expected, the terminal P—O oxygen species are the most basic surface oxygen, in both P-poor and P-rich samples. Moreover, they are involved in the post-activation step, i.e the selective oxidation to non-combustion products: this could be considered another explanation of the positive effect of P-enrichment for promoting selectivity to MA. DFT calculations also indicate that the P—O—V oxygen is as nucleophic as the terminal P—O, explaining in that way its role in the rupture of C—H bonds. In conclusions, it is possible to affirm that the specificity of VPP catalyst is strictly related also to its acidic properties.

2.4.7 Redox properties and effect of the gas phase composition

The redox properties of the feed influence the surface oxidation state of the catalyst, which greatly affects its behavior. The oxidation state of vanadium depends on (i) redox potential of the feed, (ii) rate of reduction and (iii) rate of oxidation of the catalyst. These parameters were studied in literature varying the feed composition, the catalyst residence time, the temperature, the pressure and the reactor technology [86, 94, 95]. In general, it was confirmed that the key point for an active and selective catalyst is to keep the surface at an optimized oxidation state: this could be achieved

not only by a fine-tuning of catalyst preparation, but also by regeneration procedures, by supplying a proper oxygen content during the reaction, by addition of dopants [96]. Since the VPP performances are largely correlated to the operating conditions, also the conversion of *n*-butane is a variable parameter to take into account. In fixed bed reactors the mixture is typically 1-2% *n*-butane in air while in fluidized bed the hydrocarbon is more concentrated, 4-5% *n*-butane in air: in the latter case it is possible to recycle the unconverted reactant, reducing the operative costs and increasing the productivity of the process. Otherwise, as the feed becomes more reducing, a drop in MA selectivity and in *n*-butane conversion could happen: this means that the hydrocarbon activation occurs through reaction with nucleophilic lattice oxygen or adsorbed lattice oxygen. Since the oxygen partial pressure decreases, the number of available surface O^{2-} species, which should be supplied through the inlet oxygen, becomes non insufficient and the MA selectivity tends to decrease as the feed composition becomes more reducing. In conclusion, when the catalyst is adequately oxidized, catalytic performances could be kept constant.

2.5 New catalyst systems

It is known that the maximum yield to MA is limited by:

1. Parallel reactions of *n*-butane combustion and oxidative degradation to acetic and acrylic acids;
2. Consecutive reactions of combustion, becoming more relevant when the alkane conversion reaches 70-80%. This has been attributed to local catalyst overheating due to reaction exothermicity and to the poor heat-transfer properties of the material.

In order enhance the catalytic performances, several pathways could be chosen:

1. Improvement of the heat removal: use of highly heat-conductive supports for VPP catalyst;

2. Control of oxygen concentration in the feed, in order to maintain an high $C4/O_2$ ratio over the catalytic bed;
3. Addition of dopants.

2.5.1 Supported systems

In general, the supports employed for systems used in oxidation reaction should have the following characteristics:

1. Good mechanical properties, to improve the attrition resistance of the catalyst;
2. High thermal conductivity, to avoid hot spots on the catalyst surface;
3. Low surface area, to avoid high residence times that favor the total oxidation reactions of the reactant;
4. Chemical inertia to reactants and to the active phase, to avoid changes in its morphology.

Initially, vanadyl pyrophosphate was supported on oxides materials such as TiO_2 and Al_2O_3 [97],:in the complex all VPP-supported systems showed worse performances than the VPP-bulk systems, probably because in these systems the reaction does not follow the Mars van Krevelen mechanism. In particular, the TiO_2-supported showed both activity and selectivity lower than commercial VPO catalysts. This behavior was investigate by Overbeek at al. [98, 99], which suggested that the activity worsening of titania-supported VPO catalysts was related to a strong interaction between VPP and TiO_2, and a different reducibility of VPP on support. Ruitenbeek et al. [100] observed no changes in average vanadium oxidation state during equilibration, since they concluded that the lattice VPP oxygen species were not involved in *n*-butane oxidation and the reaction does not follow the Mars van Krevelen mechanism.
For the SiO_2-supported systems a weaker interaction than the titania-ones was observed. However, the silica-supported catalyst was less active, but more selective to MA: this behavior was attributed to the non-reducible nature of silica support and to the higher surface P/V ratio found. On the other hand, in the VPP-supported on Al_2O_3

an high affinity between Al and P limited the dispersion of active phase and consequently the catalysts showed poor catalytic performances [101].

Recently, highly heat-conducting supports were studied, namely β-SiC, Si_3N_4 and BN, respectively with thermal conductivity of 140-270 $W \cdot m^{-1} \cdot K^{-1}$, 6 $W \cdot m^{-1} \cdot K^{-1}$ and 31 $W \cdot m^{-1} \cdot K^{-1}$ [102]. This characteristic together with their relatively high surface area (>20 m^2/g for β-SiC, prepared via the "shape memory synthesis") renders them potential useful supports for oxidation catalyst. The advantages given by a better heat transfer permits a significant gain in MA yield; moreover, the chemical inertness of these supports did not modify the morphology of VPP active phase [103]. For example, with β-SiC-supported VPO (30 wt.% of active phase) it was possible to reach the best result in MA selectivity under hydrocarbon-rich conditions ever reported: 54% of yield at 72% of conversion at 485 °C.

2.5.2 Addition of dopants

One of the most common route to improve the performance of a catalyst is the addition of dopants. Since the '80, together with the study of active phase, several promoters elements for vanadyl pyrophosphate employed for the selective oxidation of *n*-butane to MA were studied [104, 105, 106, 107, 108] and addressed in patent literature [109, 196, 197]. A vast array of metals has been studied and this work was summarized by Ye at al. [110, 111] in a list of the elements in order of activity to MA (not the specific activity, the surface areas show a large variation 26-51 m^2/g):

Zr>Ce>La>Fe>Co>Cu>Nb>Ti>Mo>Ca>Si>W>Ni>Ge>K

This work was continued by Hutchings [112] who plotted the activity of the dopants in function of the surface area: the major part followed a linear correlation.

The scientific literature reported that Ce, Co, Ce, Cu, Fe, Hf, La, Mo, Nb, Ni, Ti, Zr are elements commonly used to enhance activity: these cations are suggested to form solid solutions with the catalyst, $[(VO)_xM_{1-x}]_2P_2O_7$ (where M is the promoter metal) causing defects on VPP lattice, which can function as active sites for the *n*-butane oxidation. More in detail, the addition of Zr have been found to improve activity: despite other metals, it is not incorporated into the VPP lattice, but it forms an

amorphous phase that probably is responsible of the activity improvement [113, 114]. Moreover, it was found that a low concentration of Zr permits to lower the temperature required to reach the maximum MA yield; also, it has been proposed that Zr creates acidic surface sites that prevent the desorption of the reaction intermediates (butenes, butadiene and furan) facilitating the desorption of MA. The effect of promoters was summarized by Ballarini et al. [115] and it is reported in Table 2.3.

Dopant/V ratio	Promotional effect	Reasons for promotion
Co, Co/V 0.77	C: 15 → 25% S: 0 → 11% under hydrocarbon-rich conditions	Control of the optimal V^{5+}/V^{4+} surface ratio; stabilization of an amorphous Co/V/P/O compound
Co, Co/V >2	C: 55 → 79% S: 43 → 35% at 653K	Optimal surface Lewis acidity
Ce+Fe	C: 44 → 60% S: 63 → 66% in absence of O_2	Improvement of redox properties
Fe, Fe/V 0.08	Increase of catalytic activity	Fe replaces V^{4+} in $(VO)_2P_2O_7$ Re-oxidation rate is increased
Ga, Ga/V 0.10	C: 22 → 73% S: 55 → 51%	Increase of surface area + increase of intrinsic activity (electronic effect)
Nb, 0.25 wt%	C: 20 → 17% S: 35 → 53%	Increase of surface acidity promotes desorption of MA
Nb, Nb/V 0.01	C: 58 → 75% S: 70 →70%	Nb concentrates at the surface, where defects are generated. Nb acts a n-type dope; development of a more oxidized surface

Table 2.3: Summary of dopants for VPP catalyst: 2° column C = conversion and S = selectivity, for un-doped (left values) and doped catalyst (right value) in selective oxidation of *n*-butane to MA.

In recent years, one of the most studied dopant is Nb: the great interest has leaded to its successful implementation in industrial scale [109, 196] and its role in VPP catalyst has been widely discussed in literature in the last two decades. Many hypothesis have been suggested:

1. Increase of acidity associated with the generation of defects responsible for C—H activation [116,117];
2. Improvement of MA selectivity by a structural incorporation within V phosphate, preventing overoxidation of the products [118];
3. Shortening of the activation time of the catalyst;
4. Action as n-type dopant for the p-type VPP semiconductor [119];
5. Control of the V^{4+}/V^{5+} ratio, by modification of the redox properties of vanadium [96];
6. Formation of solid solution $V_{1-x}Nb_xOPO_4$ and mixed oxides $[(VO)_{2-x}(Nb)_x(P_2O_7)_{1-x}(PO_4)_{2x}$, which increase the conductivity and the charge transfer properties of the catalyst [120].

2.6 Mechanism of *n*-butane oxidation to maleic anhydride

The selective oxidation of *n*-butane to maleic anhydride is a demanding reaction because it involves the exchange of 14 electrons and 7 oxygens on the surface of the catalyst, coproducing water. During the reaction, the catalytic redox couple of V is reduced, while the *n*-butane is oxidized. At the steady state the rate of reduction of the catalyst is equal to the rate of oxidation, $r_{red}=r_{ox}$. The catalytic cycle follows the Mars-Van Krevelen mechanisms, that is reported below:

reduction: $R\text{-}CH + 2KO \rightarrow R\text{-}C\text{-}O + H_2O + 2K$

oxidation: $2K + O_2(gas) \rightarrow 2KO$

where R-CH e R-C-O are respectively the reactant and the products, while KO e K are the oxidized and reduced catalysts.

The selectivity to the target molecule is due to the participation of lattice oxygens, while the oxygen co-fed is needed to refill the oxygen vacancies reproducing the proper oxidation state of vanadium. These weakly adsorbed oxygen species are strongly electrophilic and they are responsible of total oxidation [121].

2.6.1 Reaction scheme

Several hypothesis regarding the reaction mechanism were suggested, otherwise the most proposed reaction scheme is represented in Figure 2.14: *n*-butane is transformed into MA through different sequential steps of oxidative dehydrogenation and oxygen insertion [16, 19, 122, 123, 124, 125].

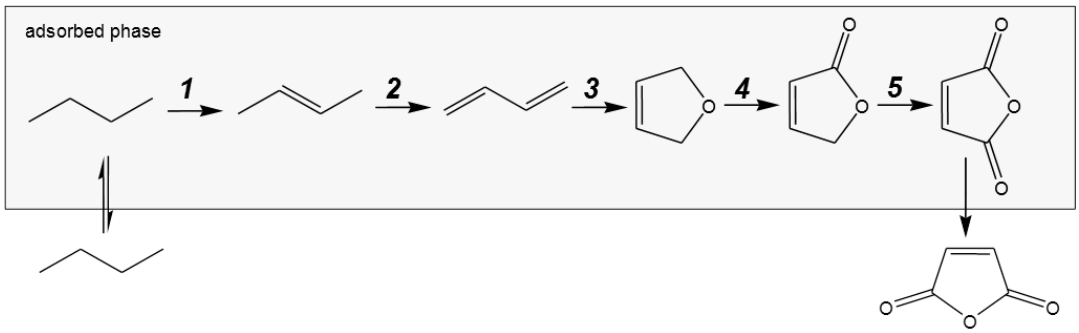

Figure 2.14: Reaction intermediate steps of selective oxidation of *n*-butane to MA

1) *n*-butane + 1/2 O_2 → butenes + H_2O (oxidative dehydrogenation)

2) butenes + 1/2 O_2 → butadienes + H_2O (allylic H extraction)

3) butadienes + 1/2 O_2 → 2,5-dihydrofurane (1,4-oxygen insertion)

4-5) 2,5-dihydrofurane +2 O_2 → MA + 2 H_2O (o-allylic insertion lactone mediated)

6a) 2,5-dihydrofurane + 1/2 O_2 → furan + H_2O (allylic extraction)

6b) furan + 3/2 O_2 → AM + H_2O (electrophilic oxygen insertion)

This proposed mechanism was derived by experiments dealing with the isolation of some intermediates at unusual reaction conditions (such as under high $C4/O_2$ ratio or at low residence time) [126, 127]; also, the intermediates butene, butadiene and furan were identified by Rodemerck et al. under vacuum conditions [73].

In Figure 2.15 an alternative reaction scheme is reported: the activation of *n*-butane occurs on the VPP surface with the production of olefins; then, the oxidation goes through the formation of non-cyclic carbonylic compounds, which are subjcted to oxygen-insertion and give MA finally.

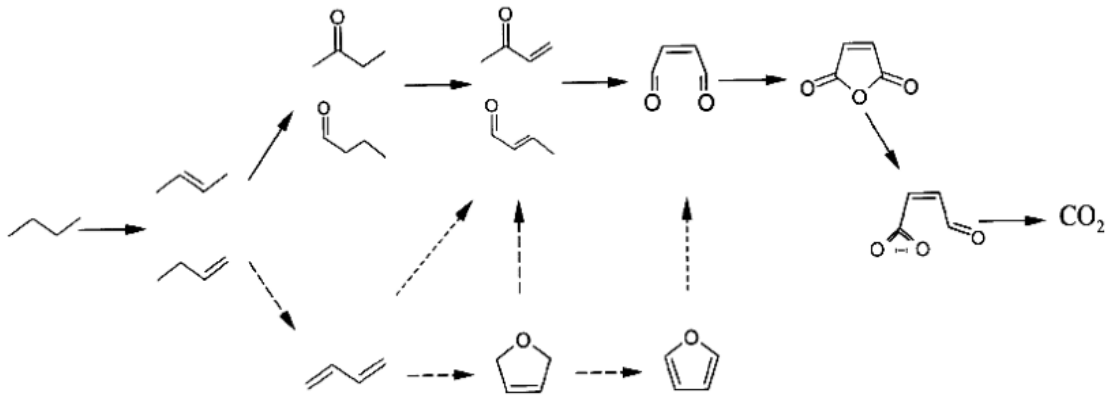

Figure 2.15: Alternative reaction scheme for the synthesis of MA through carbonylic intermediates

The rate determining step is the activation of *n*-butane and its oxidative deydrogenation to butenes. In order to obtain high MA selectivity, the rate of the oxidative dehydrogenation has to be higher than the oxygen insertion one, because olefins formation (butene and butadiene) has be favorited instead of molecules formed through oxidative path, such as crotonaldehyde and methylvinylketone, which are precursors of CO_X and lead to a drop of MA selectivity. However, recent computational calculation have revealed that probably 1-butene does not interact with VPP catalyst so its key role as first intermediate in the mechanism scheme has to be revised [128, 129].

2.6.2 Nature of active sites

Vanadyl pyrophosphate catalyst is a complex system because of the great variety of phases and species involved in the catalytic process. The multifunctionality is its peculiarity, because both redox and acid sites are present: acidity is necessary to activate alkane and to quickly desorb the acid products; at the same time the electrons transfer needs metal atoms that have to be active in redox mechanism and in oxygen insertion, avoiding over-oxidation reactions [89, 28, 130]. For this reason, only with

some isolated oxidizing centers the partial oxidation of the reagent could be reached, and a proper V^{4+}/V^{5+} ratio is needed to limit the consecutive oxidation reactions of the intermediates and to allow their desorption from the catalyst surface.

It is worth to note that the complexy of VPP catalyst is reflected in its ability to be active and selective not only in the synthesis of MA but also in different oxidation reactions, involving alkanes, olefins, anhydrides and aromatics. A list of the reactions catalyzed by VPP is reported in Table 2.4.

Type of reaction	Reagent	Product
Oxidative dehydrogenation	Isobutyric acid	Methacrilic acid
	Ciclohexane	Benzene
	Succinic anydride	Maleic anhydride
	Alkanes	olefins
Allylic oxidation (H-abstraction)	Olefins	Diolefins
	2,5-dihydrofuran	furan
Electrophilic O-insertion	Methacrolein	Methacrilic acid
	o-xylene	Phtalic anhydride
	Butadiene	Furan
	Furan	Maleic anhydride

Table 2.4: Reactions catalyzed by VPP

The wide variety of reactions catalyzed by vanadyl pyrophosphate is due to the different natures of its active sites; in Table 2.5 the active species and their functions are summarized.

Active sites	Main function
Lewis acidic sites (Vanadium)	Alkane activation
Bröensted acidic sites (P—OH)	H-abstraction and product desorption
One electron redox couple: V^{5+}/V^{4+}, V^{4+}/V^{3+}	Alkane activation
Two electrons redox couple: V^{5+}/V^{3+}	Several hypothesis
Bridged oxygen: V-O-V e V-O-P	Oxidative dehydrogenation and

	oxygen insertion
Terminal oxygen: $(V=O)^{3+}$, $(V=O)^{2+}$	Oxygen insertion
Adsorbed molecular oxygen: species η^1-peroxo and η^2-superperoxo	Total combustion to CO_x

Table 2.5: Active sites in vanadyl pyrophosphate

1. Lewis acid sites: they are attributed to the presence of V ions coordinatively unsatured in the VPP (100) planes and are identified by FT-IR absorption of basic probe molecules. The main role is to permit the H-abstraction from *n*-butane [16].

2. Bröensted acid sites: they were identified by FT-IR spectroscopy and correspond to P-OH groups in the terminal position of phosphorus tetrahedra. They act facilitating the H removal in the activation of C—H bonds, favoring the H shift toward the H_2O formation and making easy the maleic anhydride desorption [131].

3. V^{5+} species: they are active in the oxygen insertion of activated hydrocarbons producoing oxidized compounds (MA but also to CO_x). Its amount on the surface may vary from 20 to 100%, depending on the several parameters (i.e preparation method, dopants). A controlled amount of V^{5+} is necessary to improve activity, but an excess of oxidized V is detrimental for selectivity (the optimal V^{5+}/V^{4+} ratio is about 0.25) [70, 71].

4. V^{4+} species: thery are responsible for *n*-butane activation; the $(V=O)^{2+}$ species are involved in the H-extraction from *n*-butane and in the allylic oxidation [16]; some authors suggested that they act also in oxygen insertion on butadiene with the formation of the 5-elements ring compounds [132].

5. V^{3+} species: their role is difficult to be clarified; the formation of V^{3+}/P/O compounds is detrimental for the selectivity, otherwise small amount of V^{3+}

and its associated anionic vacancies could be positively affect the catalytic activity [133, 134].

6. Bridge oxygens V-O-P: these species are involved in the oxidative dehydrogenation of activated *n*-butane to butadiene; moreover they play a role in the oxygen insertion reaction on the 5-elements ring compounds.

7. Adsorbed molecular oxygen: molecular oxygen is absorbed in η^1-superoxo and η^2-peroxo species; they are responsible of over-oxidation reactions, because of theier strong and non-selective nucleophilicity. They are also able to interact with the V=O group, thus activating *n*-butane [135].

2.7 Alternative reactant for the synthesis of maleic anhydride: 1-butanol

The industrial synthesis of maleic anhydride has been utilized for many years, otherwise nowadays there is a significant interest dealing with the development of new synthetic routes starting from non-petroleum based reactants. In this field, the production of MA starting from renewable raw materials is demonstrated by recent papers in which either 2,5-hydroxymethylfurfural or furfural are used as reactants for liquid-phase or gas-phase oxidations. In particular in the scientific literature reported these examples of selective oxidation: 2,5-hydroxymethylfurfural with air in liquid phase with an homogeneous catalyst $VO(acac)_2$ based [136]; furfural to maleic acid in liquid phase, with a phosphomolibdic acid-based catalyst [137], or the same reaction in gas phase, with a vanadium oxide catalyst supported on alumina [138]; in these cases reported both furfural and 2,5- hydroxymethylfurfural are aldehydes obtained by sugars rearrangement and transformation.

For the replacement of *n*-butane, it was suggested a reactant derived from biomass fermentation, the simplest alcohol with four atoms of carbon, 1-butanol. This could be easy produced by biomass fermentation and it could be a interesting molecule for the synthesis of building blocks, because of its availability and its competitive cost.

The reaction of synthesis of maleic anhydride starting from 1-butanol is reported in Figure 2.16.

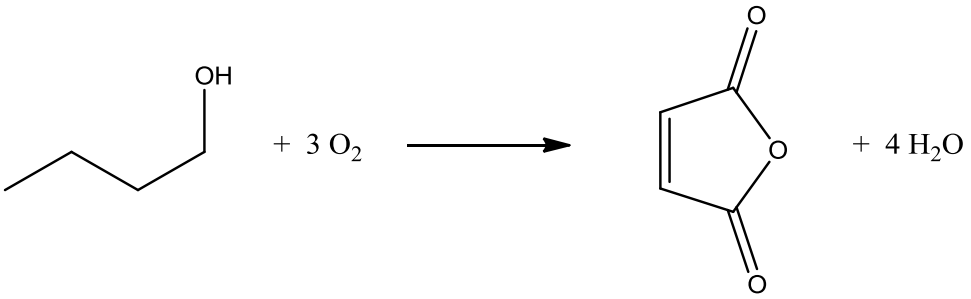

Figure 2.16: Selective oxidation of 1-butanol to maleic anhydride

2.7.1 1-butanol

1-butanol is an organic compound liquid and colorless at room temperature. Its physic and chemical characteristic are reported in Table 2.6.

Formula	C_4H_9OH
Molecular weight (g/mol)	74.12
Melting point (°C)	-89.3
Boling point (°C)	118
Flammable limits (%vol)	Lower: 1.4 Upper: 11.3
Solubility in water (wt% at 30°C)	7.85

Table 2.6: Physical and chemical properties of 1-butanol [2]

1-butanol can be produced by means of various technologies [139]:

1. The most important industrial process is propylene hydroformylation (oxo synthesis) with subsequent hydrogenation of the aldehyde formed, i.e, 1-butyraldehyde (and minor amount of 2-methylpropanal as the by-product).

2. Reppe process, consisting in the direct hydroxycarbonylation of propylene into 1-butanol (with 2-methylpropanol as the by-product).

3. Aldol condensation of acetaldehyde into acetaldol in basic conditions, the dehydration of acetaldol into crotonaldehyde in the presence of an acid, and – lastly - the hydrogenation of the latter into 1-butanol. The source for the process can be bio-ethanol, which can be (oxi)dehydrogenated into acetaldehyde. The multi-step process can occur in a single step starting directly from ethanol (which also serves as internal H-transfer reagent, developing a MPV-type reduction), using a single bifunctional catalyst, and proper reaction conditions (Guerbet alcohol [140, 141, 142, 143]).

4. Catalytic hydrogenation of CO into higher alcohols; nowadays, however, this process has no commercial importance.

5. ABE process: biomass fermentation based on *Clostridium acetobutylicum*, a bacterium leading to the formation of an ABE mixture (acetone, butanol, ethanol). This process was largely used during the first half of the last century; today there is a renewed interest in it, especially with the aim of producing 1-butanol as a biofuel. With regard to the overall biomass use, 1-butanol has an advantage over ethanol, as it can be produced from both five- and six-carbon sugars with no organism modifications; this allows for the efficient use of cellulose and hemicelluloses. Nowadays, various companies supply 1-butanol produced by fermentation.

For this reason recently the ABE process has been revaluated and the research has been focused on the improvement of the process by:

1. Replacement with cheaper raw arterials, for example lignocellulosic waste and algae;
2. Genetic modification of the bacteria or discovery of new, more efficient microorganisms and not sensible to alcohol concentration;
3. Implementation of the fermentation reactor, using continuous plants and increasing the bacteria amount by supporting them on fibres and inorganic materials able to give higher productivity;

4. Reducing of energy costs associated with separation and purification steps, by realization of *in-situ* separation.

Recently, DuPont and BP have developed a new bio-reactor for the specific production of bio-butanol as additive for gasoline, starting from beet; other research are focused on new technologies for the production of alcohols from lignocellulosic biomass, but in the latter case a pre-treatment and an hydrolysis steps (enzymatic or chemical) are necessary in order to obtain sugars.

Bio-butanol could have different applications, for examples as fuel in the automotive industry [144], as reactant in the chemical industry, and this is why it could play a key role in the sustainable growth. Moreover, it gives many advantages, compared with bio-ethanol and other bio-fuels [145]:

1. Higher energetic content than bio-ethanol (+30%) that makes it comparable with gasoline;
2. Easy to transport in the existing oil pipeline: compared with bio-ethanol it has a lower vapour pressure, it is less corrosive and less soluble in water;
3. Lower flammability limit: safer than other fuels;
4. Miscible in gasoline in many ratios.

1-butanol is a versatile molecule because it could be used to synthesize many products; moreover, the availability and relatively low cost of 1-butanol make this compound an interesting bio-platform molecule for the synthesis of chemicals. Alcohols generally decompose by either dehydrogenation to produce a carbonyl or dehydration to produce an alkene; dehydration and dehydrogenation routes are competitive in the gas phase in the absence of O_2 up to 500°C, while dehydrogenation predominates at higher temperatures [146]. On dehydrogenating catalysts, 1-butanol transforms into two main products, butyraldehyde and 4-heptanone (a symmetric ketone: ketonisation reaction) [147] and smaller amounts of hydrocarbons, such as butene, heptene, and 3-methylheptane, as well as of other oxygenated compounds, such as 4-heptanol, dibutylether, and butylbutyrate. Butyraldehyde (like all aldehydes)

may undergo reactions such as Tishchenko dimerisation (to form butylbutyrate), aldolisation, and ketonisation [148, 149, 150, 151]; however, deep dehydrogenation, aromatisation and, lastly, carbonisation may also occur. Depending on the catalyst and conditions used, other reactions may occur, such as either decarbonylation to yield CO, H_2 and C_3H_6, or demethylation to yield propanal and a CH_x radical [152]; the butenes formed by 1-butanol dehydration may decompose to produce propylene and a CH_x radical [153]. In the presence of oxygen, 1-butanol yields butyraldehyde by means of oxidehydrogenation [152, 154]. Acid catalysts for 1-butanol dehydration into butenes include heteropolycompounds [155, 156, 157], $AlPO_4$ [158, 159], sulphated alumina [160], hydroxyapatite [161], Ta-montmorillonite and Ta/Si mixed oxides [162], silica-alumina [163], Al/P and Al/Ga/P oxynitrides [164].

2.7.2 1-butanol to maleic anhydride:

The synthesis of maleic anhydride from 1-butanol requires two reactive steps:

1. Dehydration of 1-butanol to butenes;
2. Selective oxidation of butenes to MA.

To catalyze these two steps two different catalytic properties are needed: the dehydration requires an acid catalyst, while the oxidation needs specific redox properties. The hypothetic reaction scheme for the synthesis of MA from1-butanol is similar to that one proposed for the *n*-butane route and it is reported in Figure 2.17.

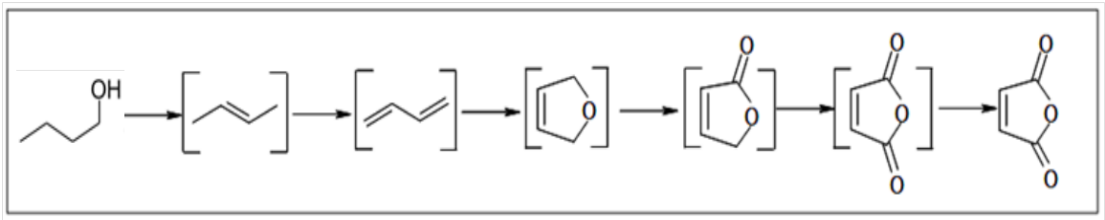

Figure 2.17: Reaction scheme for the synthesis of MA from 1-butanol

The difference is in the first reactive step, where in place of the oxidative dehydrogenation of *n*-butane there is the dehydration of 1-butanol, giving the same

intermediates products, butenes. Because this reaction is formally divided in two steps, it could be hypothesized three possible reactor configurations:

1. **Two-reactors system**: the reaction is carried out in two consecutive reactors: in the first dehydration occurs with an acid catalyst and in the second one the selective oxidation of butenes formed in the previous step is finished with a redox catalyst. Keeping the two reactive steps separated, it is possible to optimize them both in terms of technology (for example the dehydration is endothermic and the oxidation is exothermic), catalyst design and operative conditions, so theoretically, this should be the best configuration for the optimization of the selectivity. Moreover, the purification and the separation of the mixture of butenes produced could be realized after the first reactor, becoming possible to feed the purified olefins to the second reactor. In that way 1-butanol is fed only in the first reactor and air only in the second one; however, higher investment costs are the disadvantage of two-reactors configuration.

2. **One-reactor system**: the reactions take place in only one reactor, arranged with two separated catalytic beds: the first is the acid catalyst for 1-butanol dehydration, below the second redox catalyst is loaded to oxidize butenes. Many papers concerning the selective oxidation of butenes to MA have been published, namely dealing with Fe and Co molibdates-based catalyst [165, 166] and also with VPP, catalyst for MA from *n*-butane [166, 167]. Obviously this configuration is less flexible than the previous one, because it is not possible to diversify the control the operative conditions (temperature, separation). Problematic is also the management of the catalytic beds, because we have only one reactive mixture composed by 1-butanol and air: so the acid catalyst has to be active even in presence of oxygen, while the redox catalyst receiving the products flow coming out from the first bed must be resistant to water poisoning effect (co-produced in large amount in the dehydration) and it must not catalyze secondary reactions on un-reacted 1-butanol. The main

advantage of this configuration is the lower investment cost, thanks to a single-two beds-reactor.

3. **One-reactor and one-pot reaction**: in this case a bi-functional catalysts is required, in order to carry out with only one catalyst and in only one reactor the one-pot reaction; this means that a catalyst with proper acidity and redox properties has to be utilized. Disadvantages described in point 2 are the same for this type of technology, however the advantages given by a one-pot reaction are not only the reduction of the investment costs, but also the a simpler plant management.

In Figure 2.18 the three reactor configurations described above are represented.

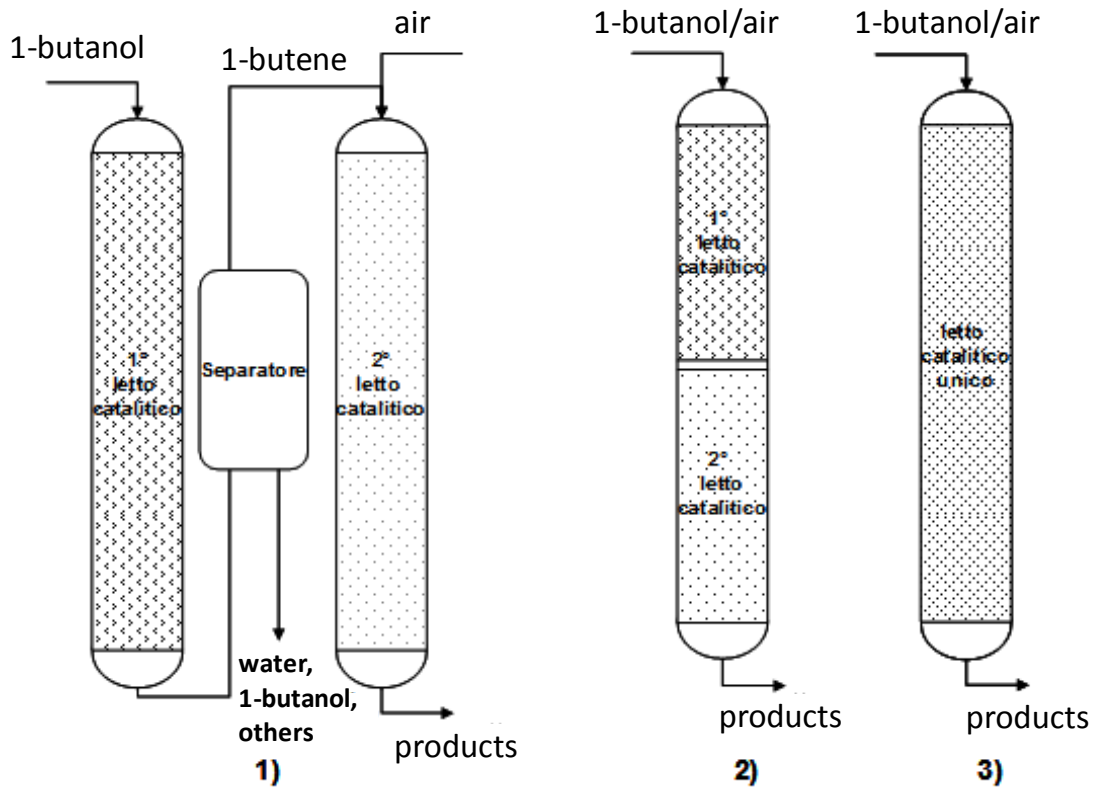

Figure 2.18: Reactor configurations for the synthesis of MA from 1-butanol; 1) Two-reactors 2) One-reactor and two catalysts, 3) One reactor and one-pot reaction

2.7.2.1 1-butanol to butenes

Dehydration of alcohols to olefins is an important and industrially demanded reaction, since the main applications of the alkenes is in the industry of polymers. The elimination of water and the formation of a double bond follow the well-known Zaitsev rule, which affirms that the alkene formed in greatest amount derives from the removal of the hydrogen from the β-carbon having the fewest hydrogen substituents; this means that the most stable alkene is the most substituted one.

In general, the dehydration of alcohols requires an acid environment: indeed the reaction could be catalyzed by a strong acid (H_2SO_4) in acqueos medium, by weaker acid such as $POCl_3$ [167] or by solid materials [168, 169, 170]. More in details, for 1-butanol dehydration, both 1-butene and 2-butenes (cis and *trans*) are formed but the main products are the second ones, since the Zaitsev rule is respected. Moreover, 1-butene is the primary product and it is in equilibrium with *cis* 2-butene and *trans* 2-butenes: these productis are involved in the equilibrium of thermic isomerization, moved preferentially to 2-butenes.

In order to enhance the reactivity of 1-butanol towards dehydration, several acid catalysts could be used and many examples are reported in literature: polyoxometalates, silico-aluminates, alumino-phosphate and zeolites [159, 171, 172, 173]. Janik et al. [171] studied the reaction mechanism for the dehydration of 2-butanol, in presence of Keggin type-polyoxometalates supported catalysts (POM). The reaction goes through an equilibrium adsorption of the alcohol over the Bröensted acid sites in POM surface, forming adsorbed species, which in a second time release water in E1-type elimination mechanism. Similar to this, it is possible to propose an analogous dehydration mechanism for 1-butanol; the scheme is reported in Figure 2.19.

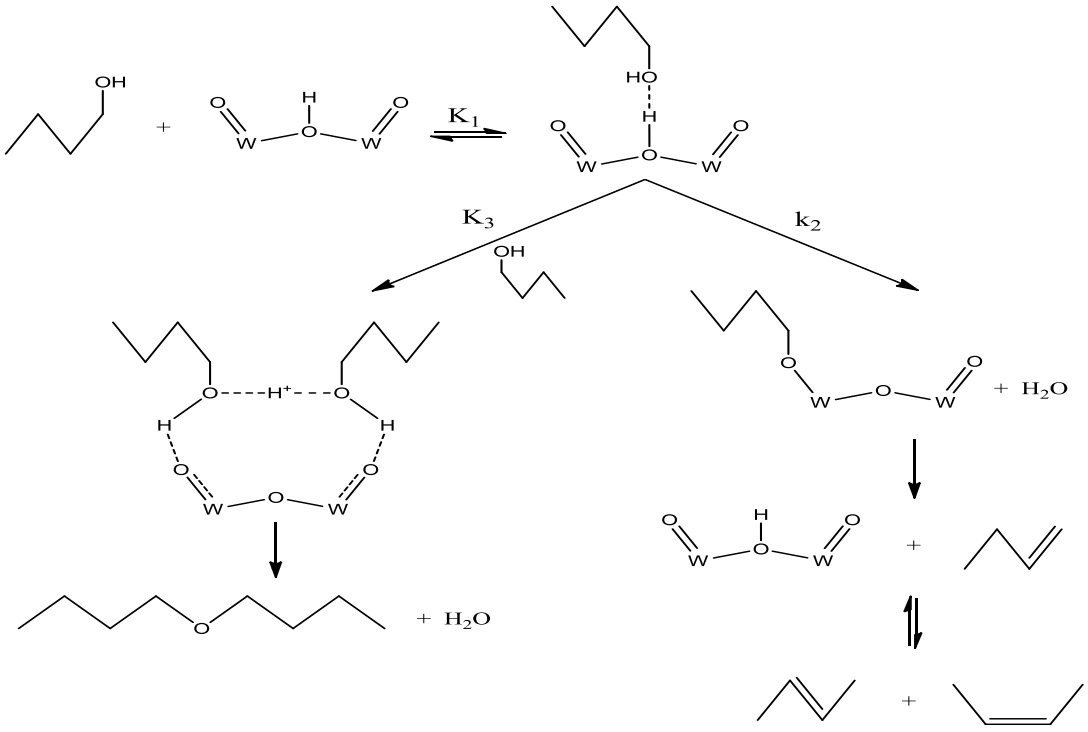

Figure 2.19: Reaction mechanism of 1-butanol dehydration on POM supported catalysts

The first step of the mechanism is the adsorption of 1-butanol molecule on the catalyst surface, which takes place through the establishment of hydrogen bonds between the oxygen O of the alcohol and the acid sites; subsequently, the adsorbed specie is protonated, causing the breaking of C—O bond, the formation of an alkoxy adsorbed specie and the co-prodution of water. Lastly, the dehydration reaction is completed with the desorption of water and the deprotonation of the alkoxy specie to butene. Otherwise, the molecules of 1-butanol on the POM surface could also give a intermolecular reaction, forming dimer species as *n*-butyl ether; these molecules, occupying the acid sites in place of 1-butanol, are detrimental for the efficiency of the catalyst and cause a slowing down of the rate of reaction. This means that the rate of 1-butanol dehydration depends on the ratio between the kinetic constant of the elimination reaction (k_2) and the kinetic constant of the formation of the dimer species (k_3) (see Figure 2.19). According with Matachowski et al. [174] (who have made in evidence the same mechanism for the dehydration of ethanol on POM supported catalysts) these two competitive reactions two different pathways:

1. Intramolecular reaction: the most favourite one, especially at high temperature, leads to butenes;
2. Intermolecular reaction: favourite ad low temperature, it leads to *n*-butyl ether.

2.7.2.2 Keggin-type polyoxomethalates

Polyoxometalates (POM) [175] are special chemical compounds composed by oxygen and metals of the first transition state, namely V, Nb, Ta, Mo, W, in their highest oxidation state; they may contain also an heteroatom, typically P, As, Si, Ge. In other words POM are metal oxides that may contain hundreds of atoms in the same cluster: they can reach a very high nuclearity and may differ from each other through a wide variety of shapes, size and composition. The most important POM structures are the Keggin-type and the Dawson-type; not always a priori the POM structure could be determined, because it depends on the preparation method. Characterizations and study of POM properties started at the beginning of the last century, mainly by spectroscopic (UV-Vis, IR, Raman), electrochemical and NMR analysis [176, 177]. The application of POM in both homogeneous and heterogeneous catalysis takes advantage of the easy electrons exchange of these materials, that occurs without an overall modification or decomposition of the chemical structure [178, 179]. Several examples are reported in scientific literature: as acid catalysts for dehydration reactions [171, 180], as redox "green" catalyst in organic-solvent-free systems [181, 182], as photosensitive materials acting as primer for radical polymerization reactions [183].

Thanks to their peculiar properties, POM have shown interesting applications also in medical and biological field as anticancer, antiviral and antibacterial [184].

Usually the synthesis of POM takes place in aqueous medium, but it could be realized also in non-aqueous medium or at solid state [185, 186]. The synthesis consists in the protonation of the oxometalates anion, giving the condensation of the tetrahedral structures into a more complex polyanionic structure: the synthesis is regulated by a proper choice of the reaction conditions, namely pH, temperature and concentration of

the reactants. Depending on the mechanism of the condensation occurred, two classes of compounds could be formed:

1. Isopolyanions (IPA): the condensed units have the same structure and a octahedral polyanion is formed; generally, the number *n* of units condensed iis higher than 6. The reaction could be schematized as reported below:

$$nMO_4^{2-} + 2mH^+ \leftrightarrow MnO_{(4n-m)}^{(2n-m)-} + mH_2O$$

2. Heteropolyanions (HPA): when the condensation of the units occurs around a central metal atom or heteroatom, giving a compound with the general formula $X_sM_nO_m^{y-}$ (X = heteroatom, M = metal of the starting oxomethalate). These clusters are associated with a number of protons (H^+) that balance the negative charge of the HPA, producing heteropolyacids and water molecules which guarantee the cohesion of the crystalline structure. Moreover, it is commonly accepted that the HPA formation follows a kinetic control [187]; their structure is function of X/M ratio, so many types of HPA clusters could be obtained, because of the wide variety of combination of metal, heteroatoms and X/M ratios.

The most recurring structure is the Keggin-type cluster, typically of POM with X/M=1/12 ratio, i.e. an arrangement of twelve metal atoms surrounding a central atom. This structure was first proposed by Pauling [188] and later confirmed by Keggin [189] in XRD experiments on the $PW_{12}O_{40}^{-3}$: the heteroatom is linked to four oxygen atoms, forming a tetrahedral structure, while each metal atom is connected with six oxygen atoms, forming an octahedral. The condensation of three of these units produces a trimetallic M_3O_{13} group (see Figure 2.20); these trimetallic groups are linked together surrounding the central heteroatom and giving the Keggin-type POM structure with the following formula:

$$[(XO)_4M_{12}O_{36}]^{n-}$$

where X = heteroatom (for example P, As, Si, Ge), M = metal of the first transition serie (for example V, Nb, Ta, Mo, W).

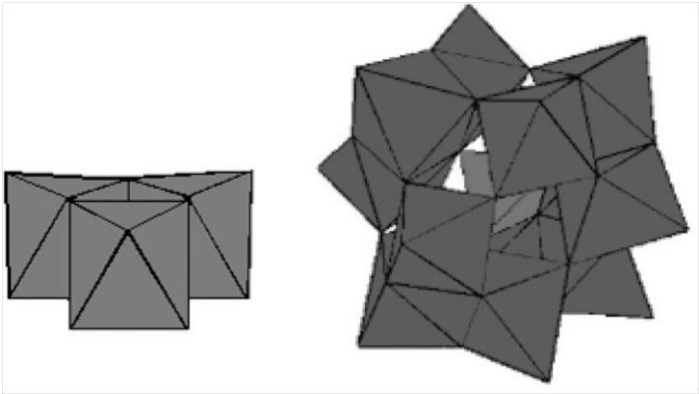

Figure 2.20: Trimetallic group (left) and Keggin-type POM (right) [175]

POM with Keggin-type structure have three symmetry axis, that means that different rotations are allowed and different isomers are generated. Theoretically, five isomers are possible, but only three have been synthesized, isolated and characterized.
Besides Keggin-type, another important primary structure of POM is the Dawson-type, where X/M ratio is 2/18 and the general formula is $X_2M_{18}O_{62}^{n-}$.

In this thesis our interest was focused on the application of Keggin-type POM as catalyst for the dehydration of 1-butanol to butenes, thanks to their acid properties. POM totally-substituted and partially-substituted were applied: in particular in two samples the protons of the heteropolyacids necessary for the charge balance were substituted with an equal number of alkali cations (Cs^+ and K^+). As reported by Corma et al. [190] this substitution modifies the secondary structure (i.e the union of the Keggin units) without altering the primary structure. These clusters are characterized by an increased surface area and a good thermal stability, while the solubility in water becomes lower than the original heteropolyacid. The growth in surface area is due to the formation of a microporous and well-defined structure, which depends on the dimension of the alkali cation utilized in the substitution mechanism. In particular, the microporosity is due to rotation and translation phenomena of HPA: this generates a partial removal of the barrier inside the interstitial holes of the original heteropolyacid and permits the formation of channels between HPA and the cations utilized for the charge balance. These substituted-POMs

show an high catalytic activity for reactions requiring acid functionalities and it is known that they exhibit a peculiar activity in some case higher than other acid catalyst, such as zeolites, sulphated zirconia and Nafion-H [191].

3 Experimental

3.1 1-butanol to maleic anhydride

3.1.1 Reactants

Different types of 1-butanol were used, both chemically sourced (CB, purchased from Aldrich) and bio-based, from different suppliers (BB1, BB2, and BB3: see Table 3.1).

Code	pH	Impurities
Chemical 1-butanol	5.8	**1-propanol, ethanol, 2-butanol, n-butylether,** acrolein, butanoic acid ethyl ester/propanoic acid propyl ester
Bio-1-butanol BB1	5.3	**After Claisen: 1-propanol, 1,1-dibutoxybutane, 2-methyl-1-butanol,** butyraldehyde, acrolein, benzaldehyde, 2-butanol, 2-methyl-1-propanol (isobutanol), propionaldehyde, 3-methyl-1-butanol, butylacetate, butylformate, styrene, $C_{21}H_{15}N$ (tentative identification: 5H-Naphtho[2,3-C]carbazole-5-methyl)
BB1-pur	5.3	**As BB1, but with lower concentration**: 1-propanol, 1,1-dibutoxybutane, butyraldehyde, furan
BB1-superpur	6.1	**1,1-dibutoxybutane, 1-propanol**, **2-butanol, 1-butanol 3-methyl, 1-propanol 2-methyl**, methanol **(all impurities are in lower concentrations than in BB2 – the purity is better than for BB1-pur)** **After Claisen** : Acetone, 1-propanol, butanal, 2-butanol, 1-propanol 2-methyl, 1-butanol-2-methyl, butylacetate, acetone dibutyl acetal, 1,1 dibutoxy butane. **No carbazole**.
BB2	6.3	**Ethylpropionate, butylpropionate**, 2-methyl-1-butanol, butylacetate, ethanol, 1-propanol, butylacetate, 1,3 butanediol
BB3	6.1	***n*-butylether, 1,3 diazine**, **1-propanol, butyrraldehyde, 2-butanol**, **1-butanol 3-methyl, 1,1-dibutoxybutane,** methanol, acetone, 2-propanol 2-methyl, 2-pentanol, 1,3 butanediol **After Claisen**: 1-propanol, butanal, 2-butanol, 2-pentanol, 1-propanol 2-methyl, 1-butanol-2-methyl, 1-butene-2-butoxy, 2-butene-1-butoxy, n-butyleter, butylacetate, 1,1 dibutoxy butane, 1,3-diazine (CAS 000289-95-2). **No carbazole**.

Table 3.1: Chemical impurities and pH present in chemical 1-butanol and in bio-1-butanols used for reactivity experiments.. Main impurities are highlighted in bold.

Some bio-butanol were purified in order to lower the impurity content; the following method was set up: 0.03 g of bleaching earth enriched with activated charcoal was

added to 10 g of BB1; the slurry was stirred for 5 h, at room temperature; then the solid was separated by centrifugation. This "purified" BB is referred to as BB1-pur in Table 3.1. As can be seen, the treatment was only partly successful, since the removal of the more undesired contaminants was not complete. The treatment was repeated for a longer time, and more specifically: 17 g of BB1 were treated with 0.06 g (0.35 wt%) of bleaching earth enriched with activated charcoal, at room temperature for 24 h. The suspension was then centrifuged at 1500 rpm for 15 min; the liquid was separated and then centrifuged again for 15 min, and finally filtered with a filter-syringe (0.20 micron). This sample is referred to as BB2-superpur in Table 3.1. The procedure used was efficient, because the sample was much purer than the fresh one, with remarkably decreased concentrations for all impurities, and no residual amount of heavier by-products (see Table 3.1).

3.1.2 Catalyst preparation

DuPont VPP catalyst

The catalyst was a vanadyl pyrophosphate delivered by DuPont, which showed the best performance in *n*-butane oxidation to MA in a circulating-fluid-bed reactor. Details concerning the characteristics of catalysts were reported in a paper by Hutchings et al. [192].

Synthesis of $VOPO_4 \cdot 2H_2O$

The synthesis of $VOPO_4 \cdot 2H_2O$ (VPD) was prepared suspending the desired amounts of V_2O_5 (99% Sigma Aldrich) and H_3PO_4 (85% Sigma Aldrich) in water, according to the procedure reported in the literature [193]. The phosphoric acid was added in large excess (P/V= 4), since in a stoichiometric amount does not permit a complete dissolution of V_2O_5 and gives an incomplete conversion of vanadium pentoxide.

The equipment used for VPD synthesis is reported in Figure 3.1.

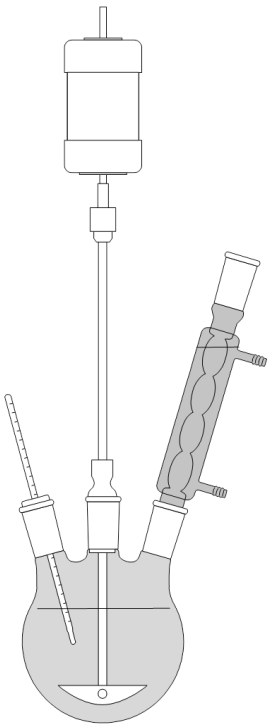

Figure 3.1: Apparatus for lab-scale catalyst synthesis

The mixture was heated at reflux temperature (100°C) for 17 hours, under vigorous stirring: the color changes from dark orange (V_2O_5) to bright yellow ($VOPO_4 \cdot 2H_2O$). After the mixture filtering and washing, the solid obtained is dried for few hours at 100 °C.

The calcination was performed over the catalyst (pellet 30-40 mesh) directly inside the lab-scale reactor at from room temperature up to 440°C; then in isothermal step at 440°C for 24 h**.**

3.1.3 Lab-scale plant tests

Catalytic tests were carried out in a quartz continuous flow reactor, by using an inlet feed containing 1% 1-butanol in air, with a W/F = 1.33 $g \cdot s \cdot ml^{-1}$. Products were analyzed online by sampling a volume of the outlet gas stream which was injected into a gas chromatograph equipped with two columns: HP-1 for the separation of 1-butanol, C4 hydrocarbons, MA, formaldehyde, acetic acid, and acrylic acid, and Carbosieve SII to analyse O_2, CO, and CO_2.

The catalysts used for the reactivity tests were loaded in the reactor in different ways: DuPont VPP was used is powder (microsphere), VPD and VPD-Nb in pellets 30-40 mesh: for all the tests corindone was utilized as inert filler.

3.1.4 DRIFT Spectroscopy-Mass Spectroscopy

The sample was pre-treated at 450°C in a He flow (10 mL min-1) for 45 min, in order to remove any possible molecules adsorbed on the material. Then the sample was cooled down to the adsorption temperature (140, 300 or 360°C) and 1-butanol was fed at 0.6 μl·min^{-1} until saturation was reached. Subsequently, He was left to flow until weakly adsorbed ethanol was evacuated. In the case of the TPD experiments, the temperature was raised at 10°C min^{-1} up to 400°C). The IR apparatus used was a Bruker Vertex 70 with a Pike DiffusIR cell attachment. Spectra were recorded using a MCT detector after 128 scans and 2 cm^{-1}. resolution. The mass spectrometer was an EcoSys-P from European Spectrometry Systems.

3.2 *n*-Butane to maleic anhydride

3.2.1 Lab-scale plant tests

The reactivity tests were carried out using A or X catalysts, in form of pellets sized in 30-40 meshes. The reactor was filled with an inert material, steatite, in order to avoid side reactions in homogeneous phase. *N*-butane was not fed pure but it was furnished as 10%vol mixed in He. The experiments were conducted either in hydrocarbon lean or rich conditions, i.e 1.7% or 4%, varying the residence time from W/F = 1.33 g·s·ml^{-1} to shorter one. Typically, the catalytic tests were carried out in a temperature range between 340°C and 440°C.

3.2.2 Industrial catalyst for MA from *n*-butane

In the study of the synthesis of MA from *n*-butane industrially-made catalysts were utilized: for confidential agreements they have been renamed “A” and “X”.

The A catalyst has been developed by Lonza for the selective oxidation of *n*-butane to MA in fluidized bed reactors [194]. This is a V/P/O based catalyst, typically produced with the organic route (VPO): the precursor VHP is heated at high temperature (350°C) obtaining a mixture of vanadyl pyrophosphate, amorphous phases and V^{3+} or V^{5+} compounds; then the material is dried through a *spry-drying* method and calcined at 425°C with a mixture of air and steam in fluidized bed calciner.
The thermal treatment described so called hydrothermal was developed in industrial scale by Lonza and allowed the obtainment of a new catalytic system more efficient than the that one prepared with a traditional thermal treatment. This was confirmed by catalytic tests experiments carried out in the same reaction conditions: the A sample showed not only better performances but also more stable during time on stream, giving an global improvement in MA yield. [40]. More in details, the A catalyst shows to be active already in the first hours of its time on stream, without requiring the equilibration period commonly given to the traditional catalysts to obtain a proper chemical modification and stabilization of the catalyst surface. This significant improvement is due to the peculiar conditions of the hydrothermal treatment, where the steam-rich atmosphere and the high pressure favor the formation of an higher crystalline VPP structure, avoiding the development of amorphous phases and of other undesired VPO-based phases. Moreover, this treatment favors the production of low amount of δ-$VOPO_4$, which is known to positively affect the catalytic behavior of VPP [55]. These characteristics are translated in a more efficient catalysts, thanks to the better performances and the shortening of the activation period in the reactive mixture.

Some years later, a new catalytic system was developed, that we have renamed "X". This was synthesized following the same method of preparation and the same hydrothermal treatment as the A one: the innovation was the introduction of Nb as dopant. A controlled amount of Nb is added using $NbCl_5$ as Nb source and leads to a significant improvement of the catalytic performance of the VPP system. Many papers dealing with the role of Nb have been published [116, 119, 120], and the

behavior of X catalyst catalyst agrees with the same consideration reported for Nb-doped VPP.

3.3 General arrangements

Lab-scale plant tests

Catalytic tests were carried out in a continuous-flow fixed bed quartz reactor. The system permits to change different reaction parameters: feed composition, residence time and temperature. The lab-plant is schematized in Figure 3.2 f*or* n-butane/air configuration, and in Figure 3.3 for 1-butanol/ He or air configuration.

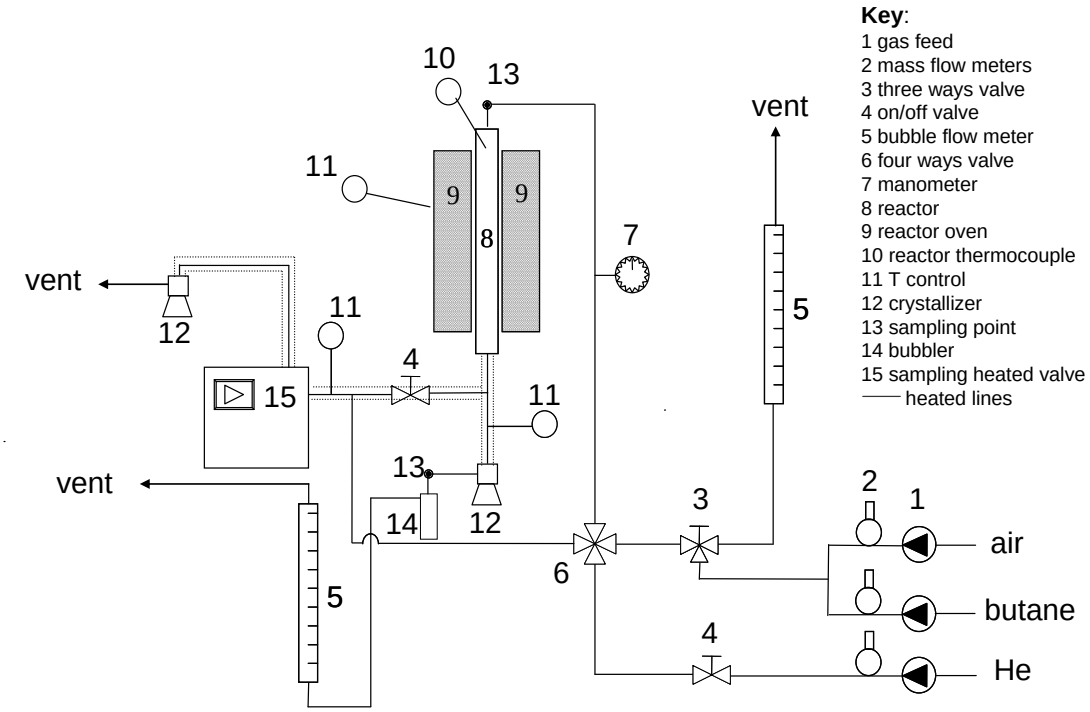

Figure 3.2: Scheme of laboratory scale plant, for *n*-butane catalytic tests configuration

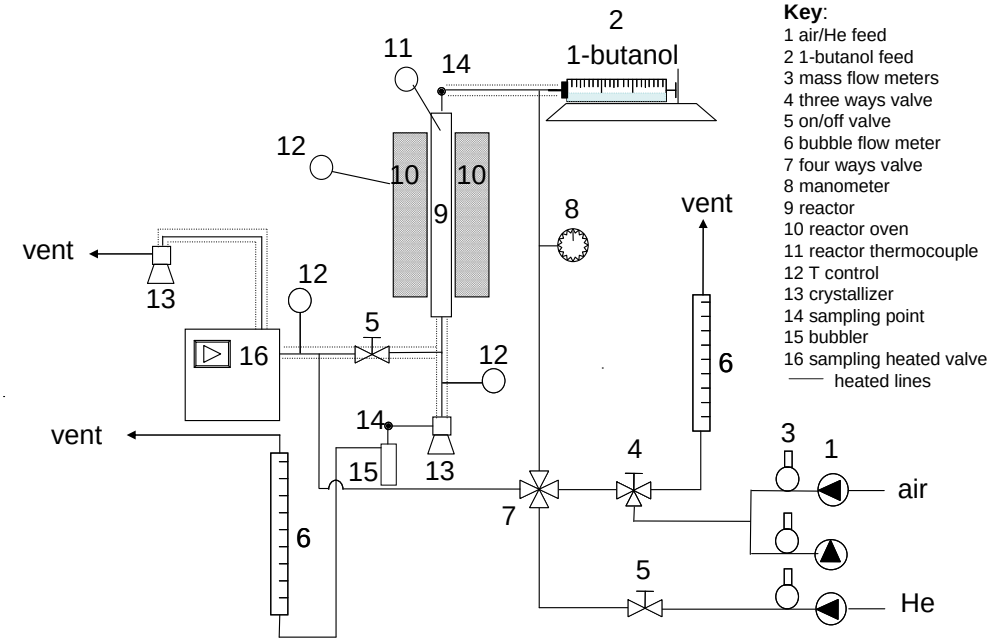

Figure 3.3: Scheme of laboratory scale plant, for 1-butanol catalytic tests configuration

The apparatus could be divided in three main different parts:

1) Feed
2) Reaction
3) Downstream

1) Feed

Gases (*n*-butane, He, air) were fed to the reactor, in separated streams or simultaneously, by three mass-flow meters ((2) in Figure 3.2; (3) in Figure 3.3. 1-butanol is liquid at room temperature and it was fed by a syringe pump ((2) in Figure 3.3), properly calibrated for the desired quantity of liquid flow; it was vaporized in a inlet line heated at 120°C. *n*-butane, air and He flows could be mixed together or kept separated: then they are fed to a three-ways valve (3 or 4) and send either to a bubble flow meter (5 or 6), in order to measure the inlet flow rate, or to the reactor, through a four-ways valve (6 or 7). The switch of this four-ways commutation valve permits two possible configurations: to feed simultaneously either *n*-butane/air to the reactor

and He to gas chromatograph through the by-pass line; the other possible configuration is *n*-butane/air to the gas chromatograph and He to the reactor.

2) Reaction

The fixed bed reactor is a quartz tube, operating at atmospheric pressure. On the top of the reactor (room temperature) a porous septum allows the sampling of the feed inlet. The thermocouple is positioned in the inner part of reactor inside a thin quartz tube at the level of the catalytic bed. The reactor is inserted inside a Lenton oven LFT 12/25/250 with inner diameter 2.5 cm and external diameter 25 cm.

The exit of the reactor emerging outside the oven is wrapped with a heater string kept at 220°C, in order to avoid the crystallization of the products coming out from the reactor.

3) Downstream

Coming out from the reactor, the flow of gas products is split: a part is sent to the on-line analysis in the gas chromatograph by opening the on/off valve (5 or 6) and connected to the FID detector; the other part flows to the vent, passing through a crystallizer and then to a glass bubbler filled with acetone, in order to condense the organic products not yet collected in the crystallizer. From the crystallizer septum, it is possible to sample the incondensable gases and inject them in the gas chromatograph. The total flow coming out from the lab-scale plant could be measured by a bubble flow meter (5 or 6), positioned before to the vent.

Products Analysis

Reactants and products has been analyzed by a Varian CP-3380 gas chromatography, equipped with the following columns and detectors:

1) semicapillar CPSil-5CB column (30m length; i.d. 0.53mm; stationary phase of 100% dimethylpolysiloxane with a thickness of 3.00 μm). By this column are separated maleic anhydride, by-products (acetic acid, acrylic acid and other light compounds e.g. butenes) and *n*-butane (in and out). The correspondent detector is a FID.

2) packed Carbosieve SII column (2m length, stationary phase of active carbons having dimensions of 80-100 mesh). In this column CO, CO_2, H_2O, O_2 and N_2 are separated and detected by a TCD.

The carrier gas used is He. The temperature ramp program of the oven is: 7 minutes at 40°C, then the temperature is increased up to 220°C with rate of 30°C/min, finally isothermal step at 220°C for 10 minutes.
It is worth to note that the semicapillary column and FID detector are connected in on-line analysis: the sampling loop valve (about 350 µl) is maintained at 200°C.
The incondensable products (CO, CO_2, O_2, N_2) have been sampled with a gas syringe (500 µl volume) through the porous septum positioned in the crystallizer or at the top of the reactor; then the sampled gaseous mixture have been injected in the packed column, linked to the TCD.

3.3.1 Data elaboration: conversion, yield and selectivity

By gas chromatograph analyses the percentage values of conversion, yield and selectivity were determined, using the following equations:

$$Conversion = \frac{n°\ mols\ of\ converted\ reactant}{n°\ mols\ of\ fed\ reactant} \times 100$$

$$Yield = \frac{n°\ mols\ of\ product/stoichiometric\ coeff.}{n°\ mols\ of\ fed\ reactant/stoichiometric\ coeff.} \times 100$$

$$Selectivity = \frac{Yield}{Conversion} \times 100$$

$$C\ balance = \frac{\sum Yields}{Conversion} \approx 100$$

3.3.2 Catalyst characterization

Raman spectroscopy

Raman analysis were carried out using a Renishaw Raman System RM1000 instrument, equipped with a Leica DLML confocal microscope, with 5x, 20x and 50x objectives, video camera, CCD detector and laser source Argon ion (514 nm) with power 25 mW. The maximum spatial resolution is 0.5 μm and the spectral resolution is 1 cm^{-1}. For each sample a wide number of spectra have been collected changing the surface position. Generally, the parameters of spectrum acquisition are: 5 accumulations, 10 seconds, 25% of laser power to prevent sample's damage, 50x objective.

In-situ analysis

"*In-situ"* analysis were performed using a commercial Raman cell (Linkam Instruments TS1500). The quantity of sample used for the analysis is about 5-10 mg. The gas flow, fed from the beginning of the experiment, is about 10 ml/min; to get an humid flow, air (or N_2) was fed through a bubbler containing water, the temperature of which was changed (partial pressure of steam from 0.03 to 0.10 bar). Spectra are recorded at room temperature (rt), while increasing temperature (heating rate generally of 100°C/min, except 10°C/min for NP4 and NP2 samples) up to the desired one and during the isotherm period. The laser power used is 25% which permits a good spectrum acquisition without damaging the sample; the acquisition parameters are 10 accumulations, 10 s each one; the objective used is 20x.

X-Ray powder diffraction

The XRD measurements were carried out using a Philips PW 1710 apparatus, with Cu Kα (λ = 1.5406 Å) as radiation source in the range of $5°<2\theta<80°$, with steps of 0.1 grade and acquiring the signal for 2 seconds for each step (phosphates samples) or in the range of $10°<2\theta<50°$, with steps of 0.05 grade and acquiring the signal for 3 seconds (VPP samples). Reflects attribution was done by the Bragg law, using the d value: $2d \, sen\theta = n\lambda$.

Specific surface area (BET single point)

The specific surface area was determined by N_2 adsorption at 77K (the boiling T of nitrogen), with a Sorpty 1750 Instrument (Carlo Erba). The sample was heated at 150°C under vacuum, to eliminate water and other molecules eventually adsorbed on the surface. After this pre-treatment, sample was maintained at 77 K in a liquid nitrogen bath, while the instrument slowly sent gaseous N_2, which was adsorbed on the surface. By BET equation it was possible to calculate the volume of monostrate and finally the sample surface area.

4 Results and discussion

My PhD work was focused on the study of the synthesis of maleic anhydride by means of the catalytic selective oxidation in gas phase of either *n*-butane or a new bio-based reactant, 1-butanol.

Although the selective oxidation of *n*-butane has been one of the most studied topics in catalysis since the 80's, several patents and scientific papers still continue to be published because of both the significant role of MA as a platform molecule and of the difficulty in understanding the reactivity features of the industrial catalyst and the parameters affecting its behavior [115, 195, 196, 197]. My research was aimed at investigating the selective oxidation of *n*-butane to maleic anhydride with both an industrial and an academic perspective at the same time, thanks to the collaboration with the company Polynt SpA.

The second part of my work was focused on the study of a new route for the production of MA, starting from a bio-based reagent, 1-butanol. This research took place within the Seventh Framework Programme of European Union, with the aim of replacing the petroleum-based synthesis of chemicals with alternative routes integrated in the bio-refinery concept.

4.1 Synthesis of maleic anhydride from *n*-butane

The first part of my PhD work was focused on the synthesis of maleic anhydride from *n*-butane in collaboration with Polynt SpA, an important Italian company specialized in the production of organic anhydrides (and their derivatives) and of the industrial catalysts utilized for their production at plant-scale. We carried out catalytic tests in lab-scale reactor, using industrial catalysts delivered by Polynt; the aim was to investigate and understand the catalytic behaviors of the industrial system, and

compare the lab-scale data with those obtained in the industrial plant. In fact, although the lab-scale reactor used was a fixed-bed and the industrial is a fluidized-bed, the study of the catalytic behaviors in a smaller scale is an useful way to find new factors in order to improve the system and to achieve new goals for the industrial process.
We studied mainly two types of vanadayl pyrophosphate catalysts, renamed "A" and "X" for confidential reasons (see *Experimental*); the work was divided in the following parts:

1. Comparison between the catalytic performances of A and X catalysts under either hydrocarbon-lean or hydrocarbon-rich conditions, which are respectively the *n*-butane concentration used in fixed-bed (1.7%) and fluidized-bed (4%).
2. Study of the effect of water over the A catalyst, by means of catalytic tests and *in-situ* Raman analysis.
3. Study of the industrial ageing of the X catalyst, by means of catalytic tests and Raman analysis.

4.1.1 Catalysts characterization

The industrial catalysts studied, A and X, are *bulk*-type, that means totally constituted of active phase, without any support or diluting material. They differ in the composition and in the method of preparation: the A catalyst is mainly made of VPP, while the X one also contains Nb as a dopant. Both systems were industrially synthesized by means of a patented method developed by Lonza [59, 40, 59]: this so called "hydrothermal" route gives catalysts which are already activated, avoiding the need for an equilibration period under reactive mixture.
These catalysts have been characterized by Raman spectroscopy, XRD and BET surface area; the conditions are reported in the *Experimental* section. The Raman analysis will be treated in the following section.

X-ray diffraction analysis

XRD analysis of A and X powder catalysts are reported in Figure 4.1.

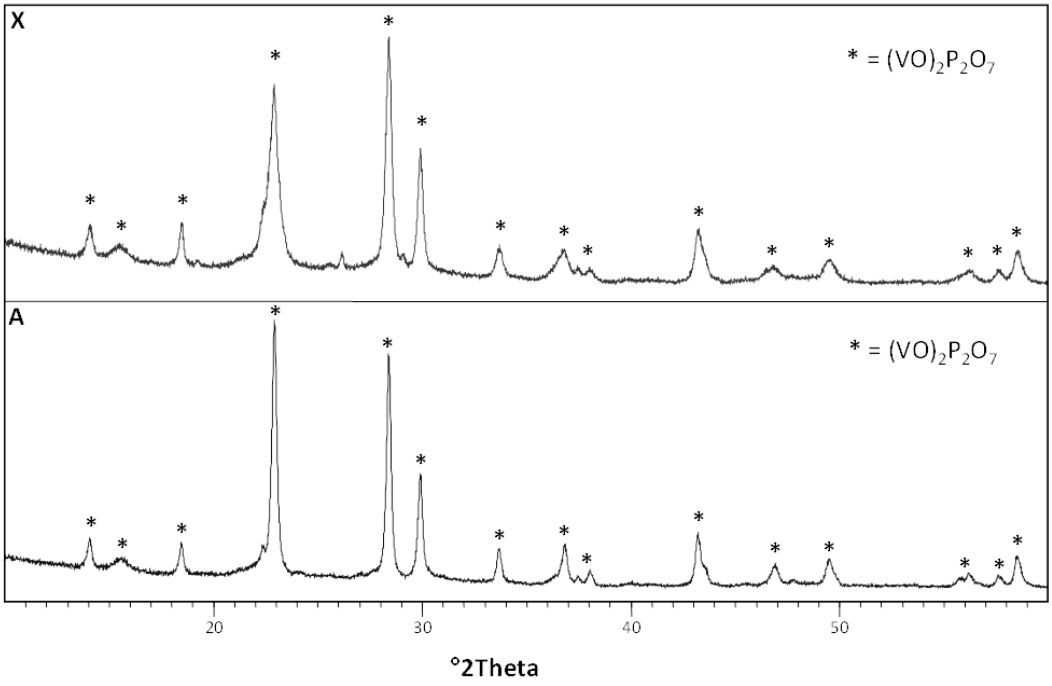

Figure 4.1: XRD diffractograms of A and X catalysts.

It is evident that the diffraction patterns are attributed to $(VO)_2P_2O_7$ crystalline phase: in fact, even if the X catalyst is doped with Nb, its low amount could not be detected. However, the X catalysts appears to be slightly less crystalline than the A, showing broader lines.

BET surface area

The surface area of the catalysts has been measured by the BET method: for the A catalyst it was 21 ± 2 m^2/g, while for the X was 25 ± 2 m^2/g.

4.1.2 The effect of *n*-butane concentration

The first aspect investigated was the different catalytic behavior of the undoped and doped catalysts, under either hydrocarbon-lean or hydrocarbon-rich conditions.

Many hypothesis have been proposed in literature about the role of Nb in VPP catalyst for the selective oxidation of *n*-butane to MA [96, 119], but these studies were only limited to lab-scale samples. Our aim is to find scientific evidences of the dopant effect of Nb also in industrial catalysts.

Catalytic tests were carried out in lab-scale reactor, using the same configuration for both systems: the catalyst was loaded in pellet sized 30-40 mesh, using steatite as inert filler for the void space. Identical were also the reaction conditions: 0.8 g of catalyst, contact time W/F = 1,33 g·s/ml, 36 ml/min as total flow. The experiments were conducted in function of temperature, between 340°C and 420°C, which is the typical range utilized at plant-scale. Two feed compositions were chosen: 1.7% *n*-butane in air, that is the hydrocarbon-lean condition, normally utilized for fixed-bed configuration, and 4% *n*-butane in air, that is the hydrocarbon-rich condition, normally utilized for fluidized-bed configuration. The experimental results are reported in Figure 4.2 and in Figure 4.3.

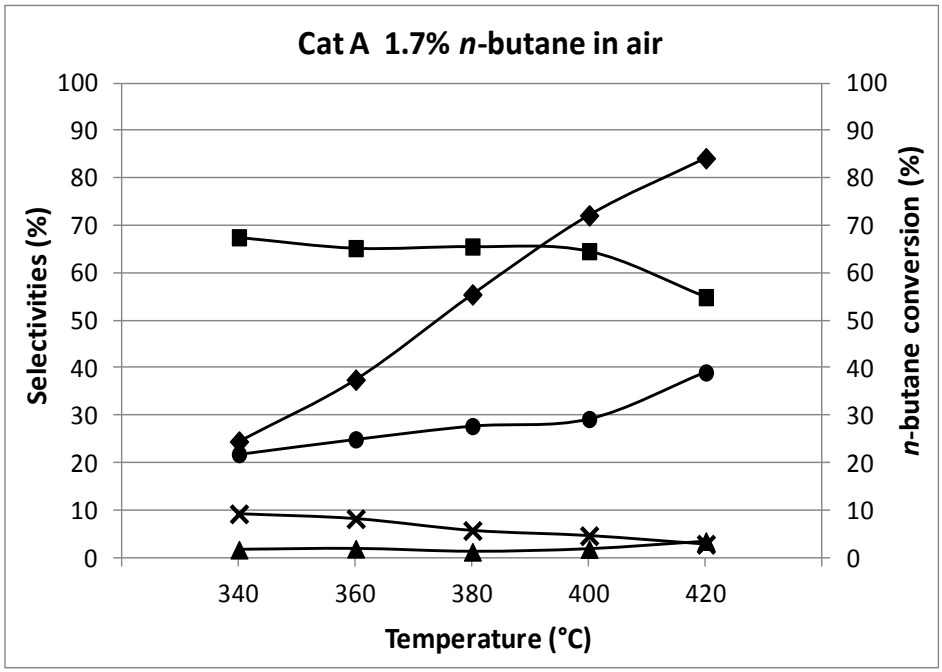

Figure 4.2: Catalytic behavior of A catalyst in the selective oxidation of *n*-butane to MA in hydrocarbon-lean condition as function of the temperature. Conditions: feed 1.7 mol% *n*-butane, 20% O_2, remaining: N_2; W/F 1.33 g·s·mL^{-1} Symbols: *n*-butane conversion (◆); selectivity in MA (■), CO_x (●), acids (acrylic and acetic) (✕), light (▲).

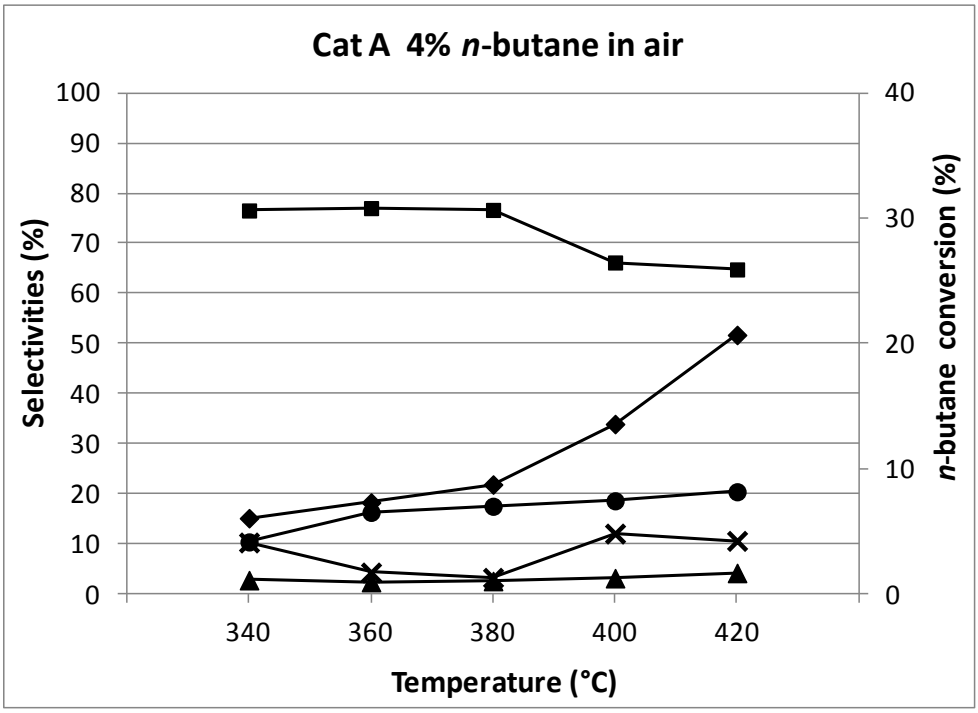

Figure 4.3: Catalytic behavior of A catalyst in the selective oxidation of *n*-butane to MA in hydrocarbon-rich condition as function of the temperature. Conditions: feed 4 mol% *n*-butane, 20% O_2, remaining: N_2; W/F 1.33 g·s·mL^{-1} Symbols: *n*-butane conversion (◆); selectivity in MA (■), CO_x (●), acids (acrylic and acetic) (✕), light (▲).

In general, in both conditions similar trends are shown: the conversion of *n*-butane and the selectivity to COx both increase with temperature, while the selectivity to MA decreases with temperature. However, the values of conversion and selectivity show a significant difference in the two conditions, in particular a drop in activity, passing from 80% to 20% of conversion shown at 420°C under hydrocarbon-rich conditions. On the other hand, a higher n-butane concentration favors the selectivity, that becomes slightly higher at low temperature, increasing from 67% to 76% at 340°C. The lower activity shown under n-butane-rich conditions is attributable to both a saturation of the catalyst surface (it is known that a limited number of active sites is available on the surface of the VPP catalyst), and an over-reduction of V, which makes the number of available oxidized V sites lower compared to more oxidizing conditions (those which develop under n-butane-lean conditions).

The same experiments were carried out for the X catalyst, with the aim of investigating the effect of Nb. The catalytic tests in hydrocarbon-lean and rich conditions are reported in Figure 4.4 and in Figure 4.5, respectively.

The Nb-doped catalyst exhibits a similar behavior under *n*-butane lean atmosphere compared to the A catalyst (indeed, a slightly lower selectivity is shown with the X catalyst at 400°C, at ca 70% n-butane conversion). Nevertheless, when the hydrocarbon fed is 4%, the MA selectivity is substantially stable in the entire range of temperature, accompanied by an increasing trend of the conversion.

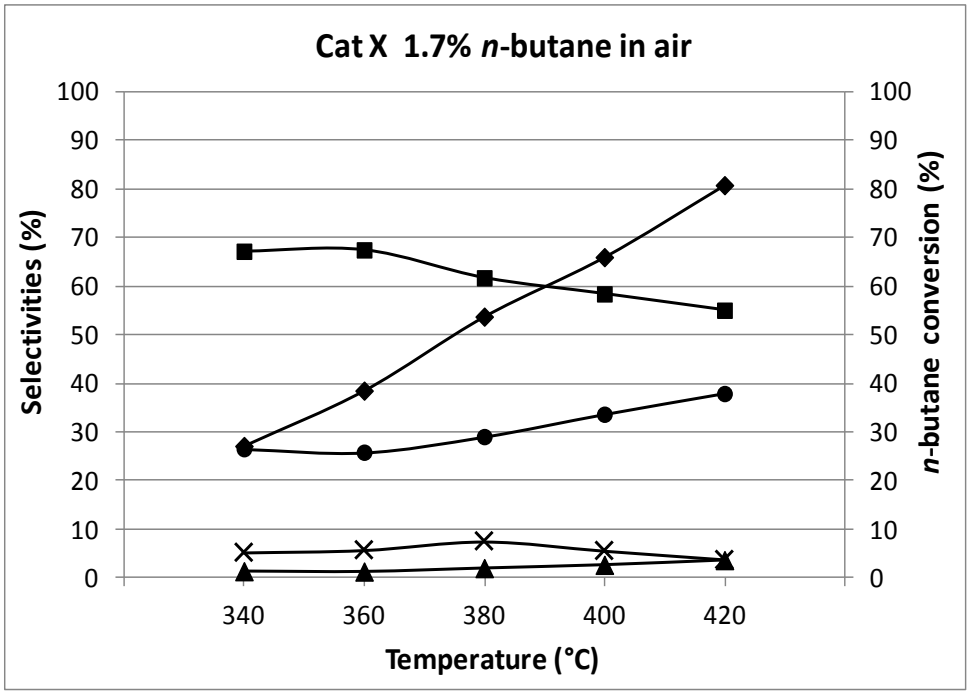

Figure 4.4: Catalytic behavior of X catalyst in the selective oxidation of *n*-butane to MA in hydrocarbon-lean condition as function of the temperature. Conditions: feed 1.7 mol% *n*-butane, 20% O_2, remaining: N_2; W/F 1.33 g·s·mL^{-1} Symbols: *n*-butane conversion (◆); selectivity in MA (■), CO_x (●), acids (acrylic and acetic) (✕), light (▲).

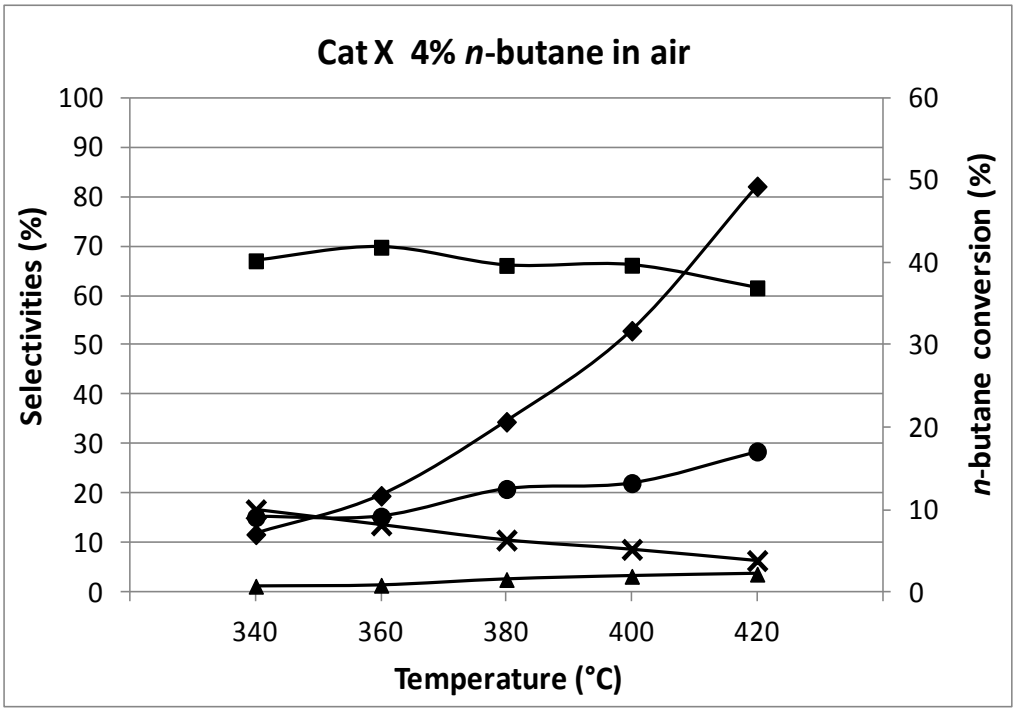

Figure 4.5: Catalytic behavior of X catalyst in the selective oxidation of *n*-butane to MA in hydrocarbon-rich condition as function of the temperature. Conditions: feed 4 mol% *n*-butane, 20% O_2, remaining: N_2; W/F 1.33 g·s·mL^{-1} Symbols: *n*-butane conversion (◆); selectivity in MA (■), CO_x (●), acids (acrylic and acetic) (×), light (▲).

The comparison with the A catalyst highlights that the X catalyst is clearly more active, but the selectivity to MA is lower at 340°C, and quite similar (ca 66%) at 400°C. Therefore, because of the increased conversion at 400°C, the yield to MA obtained (i.e., at a temperature and conversion close to those used industrially), is clearly better with the X doped catalyst than with the A undoped one. This fully agrees with what shown industrially; since industrially usually the reaction temperature is fixed, the Nb-doped VPP exhibits a superior catalytic performance.

These results confirm the industrial performance: the doped-VPP has better catalytic performances than the undoped one, but this gain is evident only at hydrocarbon rich conditions. In fact, if we compare the tests conducted at 1.7% n-butane, the addition of Nb does not give any improvement neither in selectivity nor in activity; therefore, under hydrocarbon-lean conditions, the two catalysts behave very similarly. This can be explained by taking into account that under hydrocarbon-rich conditions the

catalyst surface works with a non-optimal V^{4+}/V^{5+} ratio, with a relatively large concentration of reduced sites compared to oxidized V sites; in fact, it is known that this feature is greatly affected by the gas phase environment [86]. Under these circumstances, the Nb dopant could play its role, by favoring the oxidation of V^{4+} to V^{5+} thus allowing for a more favorable V^{4+}/V^{5+} ratio even under highly reducing conditions [96]. In particular, Nb^{5+} acts by favoring the formation of controlled amounts of δ-$VOPO_4$, the V^{5+} compound which is known to be responsible for the selective formation of MA [55]. Summarizing, when the reaction environment is more oxidizing (namely at high temperature when the conversion is the highest, and at low *n*-butane content in feed), the formation of δ-$VOPO_4$ occurs even in absence of Nb, explaining why A and X catalysts show the same performance. On the other hand, when the system works at 4% *n*-butane, the environment is more reducing and Nb becomes essential in order to allow the in-situ generation of the δ-$VOPO_4$ phase, that is the reason why the X catalyst exhibits its best performances in this condition.
In conclusions, the experiments carried out with the A and X catalysts at low and high *n*-butane concentration have led to a significant result, since it has made possible to demonstrate the role of Nb in affecting the V^{4+}/V^{5+} ratio also in the industrial VPP catalyst.

After the catalytic tests, we carried out some *in-situ* Raman spectra of A and X catalyst with the aim of investigating which are the conditions needed for the formation of the δ-VOPO phase in the two catalysts.

The Raman spectra for the A and X catalysts are reported in Figure 4.6 and Figure 4.7, respectively.

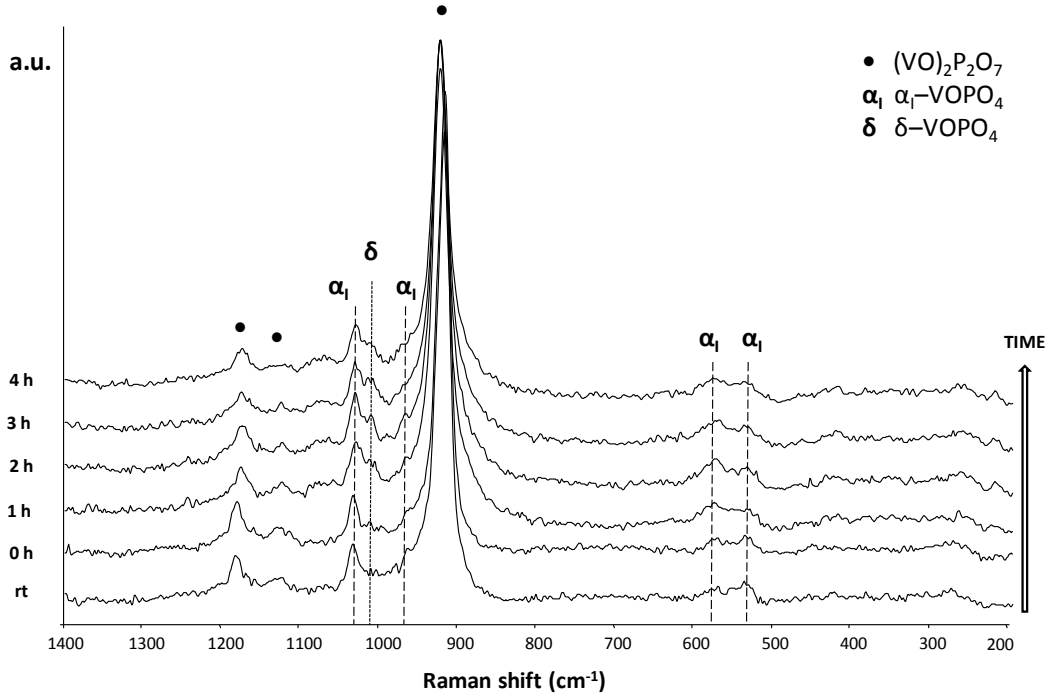

Figure 4.6: *In-situ* Raman spectra of A catalyst collected during time on-stream analysis. Feed: air and steam. Temperature: 400°C.

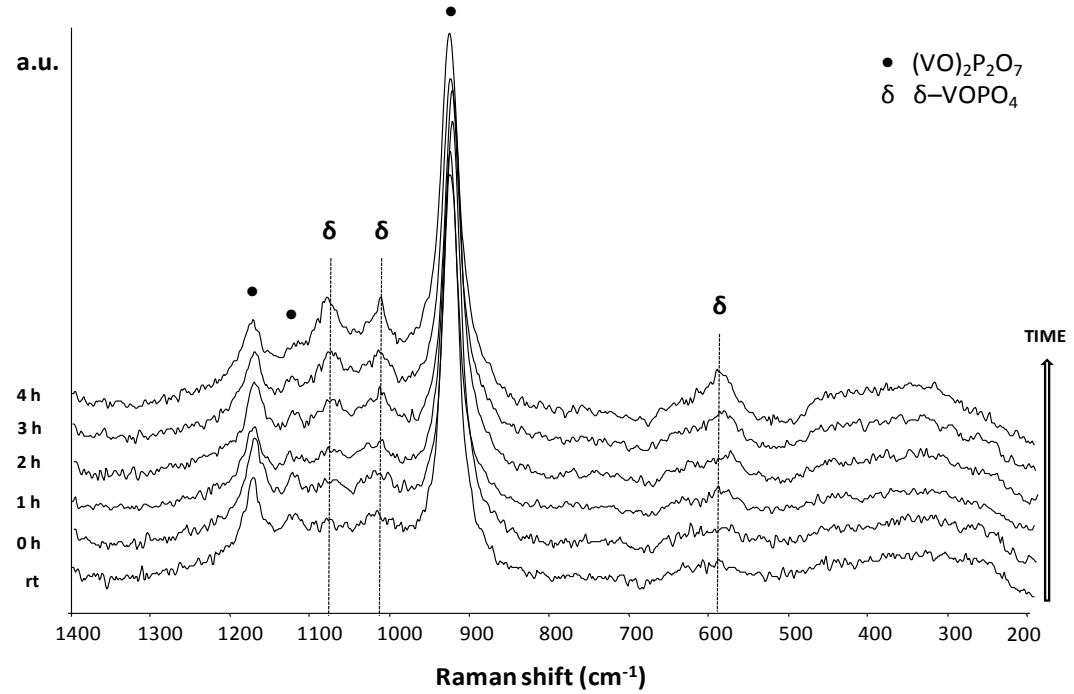

Figure 4.7: *In-situ* Raman spectra of X catalyst collected during time on-stream analysis. Feed: air. Temperature: 400°C.

The Raman analysis shows that the formation of the δ-$VOPO_4$ phase occurs in presence of air (without steam) for the X catalyst, while for the A catalyst it is necessary the co-feeding of steam (without steam there was no formation of δ-$VOPO_4$; spectra not reported). These results confirm our hypothesis dealing with the role of Nb in the formation of the δ-$VOPO_4$ phase: in fact, while in the doped sample the bands attributable to δ-$VOPO_4$ phase increased during time-on-stream, in the case of the A catalyst only a slight growth of these bands could be seen, while being less intense than bands attributable to the unselective α_I-$VOPO_4$ compound.

4.1.3 Raman investigation of A catalyst: the effect of water

The Raman analysis described in the previous paragraph have shown the key role of water in the modification of the catalyst surface, in particular its correlation with the formation of δ-$VOPO_4$ phase. Since the selective oxidation of *n*-butane to MA gives four molecule of water per molecule of *n*-butane, water is an important co-product of the reaction which could alter the composition of the surface phases. V/P/O compounds are known to have the tendency to undergo changes as a consequence of slight variations in either temperature or composition of the atmosphere in the reaction condition [65, 115]: for this reason the variation of steam partial pressure was investigated by many authors, in particular it was examined in correlation with the P/V ratio [104] and the surface acidity [192]. It is clear that the steam partial pressure increases in parallel with the conversion of *n*-butane and should enhance the hydrolysis phenomena. Caldarelli et al. [198] reported some reactivity tests carried out by co-feeding 10% of inlet steam using zirconia supported vanadyl pyrophosphate catalysts with different P/V ratio, 1.1 and 1.5: in both cases the addition of steam led to a decrease in the selectivity to CO_x and an increase in the selectivity to maleic acid, being MA hydrolyzed to its acid. Nevertheless, scientific literature reports that water could also negatively affects the VPP catalyst, because when a relatively high water partial pressure is present, the hydrolysis of the active phase could occur [199, 200, 201]. In particular, water could dissociatively adsorb breaking V-O-V, V-O-P or P-O-P bonds and form V-OH and/or P-OH groups [202]: when the hydrolysis of V-O-P

occurs, isolated or oligomerized VO_x species are generated (containing either V^{4+} or V^{5+}) surrounded by phosphate groups [VO_x + $(PO_4)_n$]. These oxidized phases rich in V^{5+} are more active than VPP but at the same time they favor the consecutive reactions of combustion, causing a drop in MA selectivity. Other scientific papers dealing with the effect of steam have been reported: for example steam could have a reversible blocking effect, responsible of a decrease in activity and a simultaneous increase in selectivity to MA [203, 204]; on the other hand, the hydrolysis of the active phase could evolve with the formation of an amorphous and thin layer of V_xO_y which gives an oxygen-enrichment of the VPP surface [199, 200, 201],

Our aim was to investigate the effect of steam over an industrial VPP catalyst, both in terms of catalytic performances and surface modification; in particular, we investigated the effect of water at intermediate temperature (360°C) using the A catalyst in hydrocarbon-lean conditions (1.7% *n*-butane, W/F 1.33 g·s/ml, catalyst in pellets 30-40 mesh, steatite as inert filler). The results obtained in the catalytic tests with and without the co-feeding of steam are reported in Figure 4.8.

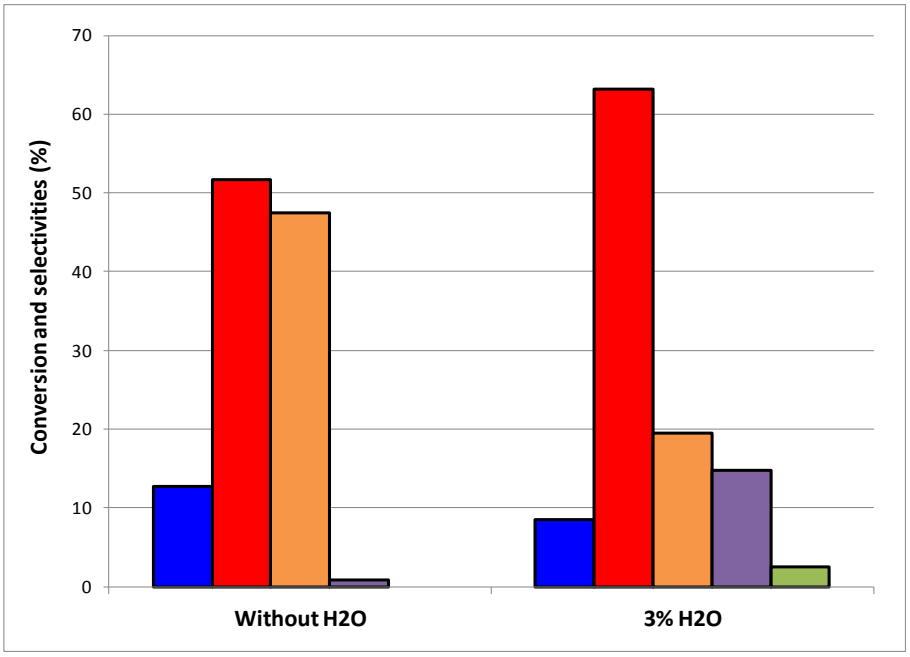

Figure 4.8: Results of reactivity experiments with and without the steam co-feeding over the A catalyst. Conditions: feed 1.7 mol% *n*-butane in air (17 % O_2), remaining: N_2 and He; temperature 360°C. Symbols *n*-butane conversion (■); selectivity to MA (■), CO_x (■), acids (acrylic and acetic) (■), light (■).

As shown in Figure 4.8, the steam co-feeding has a positive effect on the catalytic behavior of the A catalyst: in fact, while it gives a slight decrease in n-butane conversion, a significant improvement in terms of selectivity occurs, since COx are reduced from 47% down to 19% and MA increases from 52% to 63%. In order to understand the modifications occurred, we carried out in-situ Raman experiments reproducing the effect of steam over the catalyst surface: we fed a mixture of air and steam over the A catalyst at 360°C and we collected spectra in function of time-on stream. Raman spectra are reported in Figure 4.9.

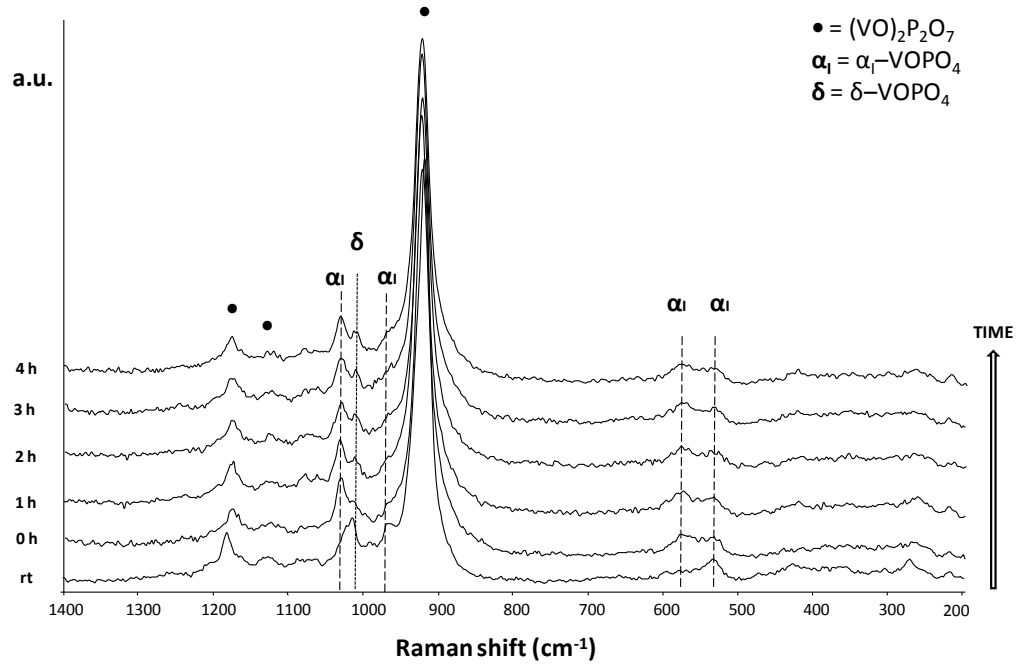

Figure 4.9: *In-situ* Raman spectra of A catalyst collected during time on-stream analysis. Feed: air and steam. Temperature: 360°C

In-situ Raman experiments show that the co-feeding of water favors the formation of δ-$VOPO_4$ phase, whose relative amount increases during time. As previously reported, δ-$VOPO_4$ phase is poorly active but very selective to MA and this agrees with the catalytic results: in fact, 3% of steam led to a slight decrease in *n*-butane conversion and an improvement in selectivity to MA. This result allows us to state that a proper partial pressure of steam fed over an industrial undoped vanadyl

pyrophosphate catalyst could favor the formation of limited and isolated δ-$VOPO_4$, enhancing the catalytic performances of the system.

4.1.4 Study of the ageing of industrial VPP catalyst

Since the industrial VPP catalyst is widely used in several technologies, one key point to address is the mechanism of its ageing and regeneration. The first point to be considered is the nature of the VPO phases that may coexist with VPP: different crystalline, polymorphic, oxidized, reduced and hydrated phases have been observed and studied [76, 77, 79, 80]. The ageing of the catalyst is strictly related to the reactivity of these phases, since modifications occurring on the catalyst surface and in the bulk greatly affect its behavior. First of all, the equilibrium shape of VPP is not platy but mostly prismatic and as a consequence of this, one possible mechanism of ageing involving the structure is the progressive increase of thickness of the VPP crystals, that makes the VPP more prismatic along the time of reaction [80, 205]. As a consequence, a decrease of the selective (100) face exposure occurs with a decrease of MA selectivity. Another ageing mechanism involves the over-reduction of vanadium sites, leading to the local formation of V^{3+} species: it is known that these sites are formed as a result of the strongly reducing reaction conditions, especially at high $C4/O_2$ ratio [126]. V^{3+} species may have a positive effect in some cases, but could also evolve towards the formation of detrimental compounds such as VPO_4, $V(PO_3)_3$ and $V_4(P_2O_7)_3$.

Dealing with industrial VPP, a frequent cause for ageing is the presence of an excess of phosphorus: even if P is fundamental to keep an optimal compromise between activity and selectivity, preventing the over-oxidation of vanadium [16, 63], phosphorus enrichment on the surface could lead to the formation of $VO(PO_3)_2$ which is detrimental for the catalytic activity [65]. On the other hand, also a loss of P could happen, a phenomenon particularly relevant in industrial plants, which could lead to a worsening of performance; this explains why P is added as a make-up in the inlet feed. In particular, the loss of P occurs upon the reoxidation of VPP: the pyrophosphate group [P_2O_7] gives rise to two phosphate group [PO_4], producing

[VO_x] species [104]. In this process a key role is played by water: in fact, the formation of four molecules of water per MA molecule (not accounting those accompanying the formation of CO and CO_2) leads to a substantial hydration of the surface. This means that when $VOPO_4$ is already present, it will transform into hydrated phases $VOPO_4 \cdot nH_2O$ if the reaction temperature is below 350°C; on the other hand, too much water will produce the segregation of phosphorus, forming strong phosphoric acid sites and [VO_x] species. These oxidized phases rich in V^{5+} are more active than VPP and give an increment in the conversion of *n*-butane; otherwise, at the same time they favor the consecutive reactions of combustion, causing a drop in MA selectivity.

Another way of ageing is related to the adsorption of products and reactants during the reaction: this phenomenon could cause the deactivation of the catalyst, since some carbon deposits could occupy the active sites.

Despite what we have just reported about ageing, VPP industrial catalyst is considered one of the most long-running bulk catalyst [40]. Otherwise, several regeneration treatments of VPO catalyst have been patented using different reagents, consisting in a reduction treatment with *n*-butane [206], H_2, CO, CH_4 or H_2S [207], sulfur oxides [208] or H_2O [209]; in particular, the treatment with *n*-butane patented by Lonza [206] has the aim of restoring the average valence state of less than 4+. The mechanism of deactivation during long-term runs, i. e. for an industrial catalyst, is probably more complex than being related only to P loss. In fact, various aspects are involved in the regeneration process:

1. Desorption of adsorbed organic species formed during reaction, which are responsible of the inhibition of the active sites [63].
2. Surface reconstruction of the active phase.

In this field, our work was focused on the study of the evolution of a VPP industrial catalyst (sample M) during a long-term run (i. e. some years of run in a fixed-bed industrial-scale reactor) with the aim of investigating the deactivation factors affecting both the catalytic activity and the catalyst surface modifications.

Catalytic tests in lab-scale reactor

First, the catalyst ageing was monitored by means of catalytic tests in lab-scale reactor as function of the temperature, in the usual fixed-bed conditions: 1.7%mol *n*-butane, 17%mol O_2, contact time W/F 1,33 g·s/ml, total flow 36 ml/min, 0.8 g of catalyst in pellets sized 30-40 mesh, steatite as inert filler. We chose different catalyst samples as representative of the increasing age of the catalyst: to simplify, we have renamed them with increasing numbers, corresponding to the period elapsed in the reactor. The results of catalytic tests are summarized in Figure 4.10 and Figure 4.11.

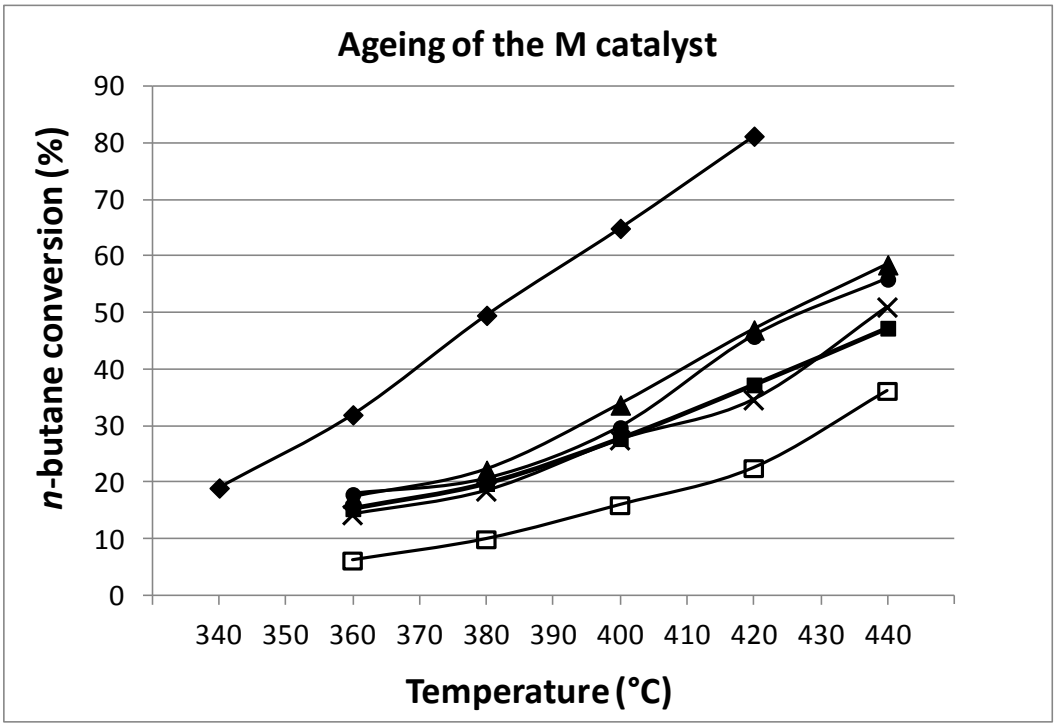

Figure 4.10: Ageing of different samples of M catalyst in the selective oxidation of *n*-butane to MA: conversion of *n*-butane as function of the temperature Conditions: feed 1.7 mol% *n*-butane, 20% O_2, remaining: N_2. Age of the catalyst: fresh (◆); 4 years (▲), 5 years (●), 6 years (✕), 7 years (■), 8 years (□).

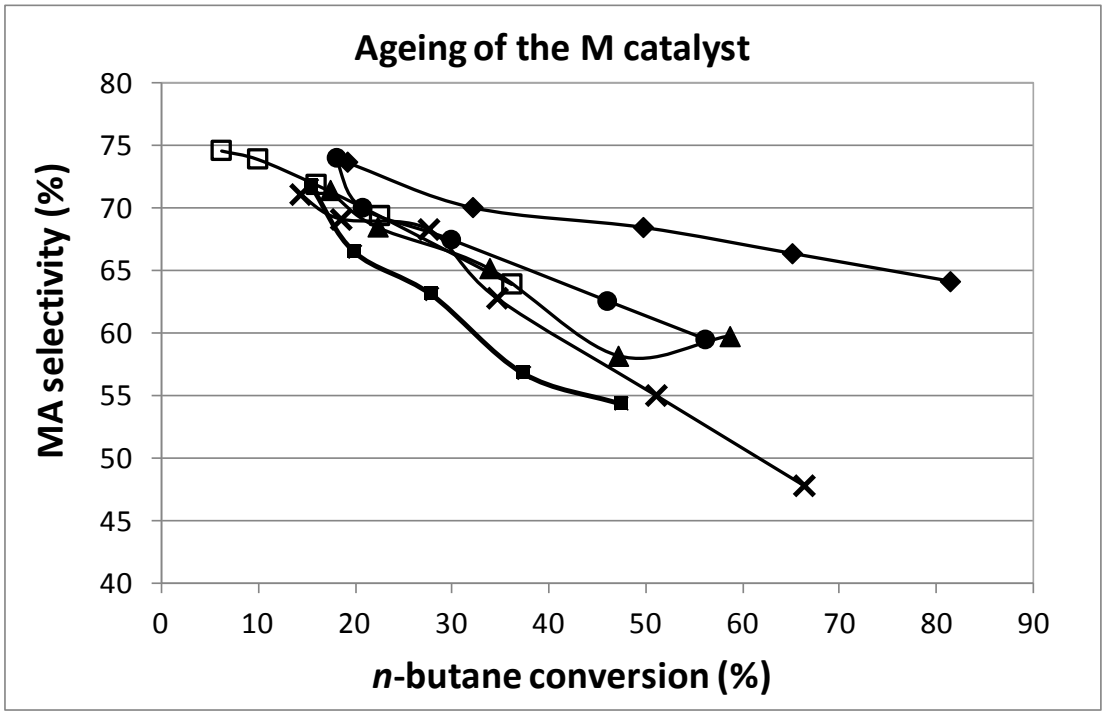

Figure 4.11: Ageing of different samples of M catalyst in the selective oxidation of *n*-butane to MA. MA selectivity *versus* *n*-butane conversion. Conditions: feed 1.7 mol% *n*-butane, 20% O_2, remaining: N_2. Age of the catalyst: fresh (◆); 4 years (▲), 5 years (●), 6 years (✕), 7 years (■), 8 years (□).

The results reported in Figure 4.10 and Figure 4.11 clearly show the deactivation trend of the industrial catalyst after 8 years of work. The fresh catalyst gives the highest values of *n*-butane conversion in the entire range of temperature examined and the highest MA selectivity, leading to the best catalytic performance in terms of both activity and selectivity. The worsening due the ageing is represented by a significant drop in activity, since the conversion of *n*-butane passes from 80% at 420°C for the fresh catalyst, to less than 40% at 440°C for the 8-years old catalyst. Worth of note, the worsening of the catalytic performance is more pronounced in the second half of catalyst life, as shown by the low values of conversion measured for the "oldest" samples. Nevertheless, the ageing of the catalyst is not simply a gradual reduction of the catalytic performance due to long-time runs, but it has to be investigated also in terms of surface modifications occurred.

Characterization by Raman spectroscopy

It is known from scientific literature that the evolution of the vanadyl pyrophosphate catalyst during reaction is affected by the P/V ratio [16] and by the reaction condition, namely the hydrocarbon/O_2 ratio [86]. For this reason, one of the possible causes for catalyst ageing is the formation of VPO phases which worsen the activity and the selectivity. Therefore, in order to understand the catalyst evolution, we analyzed the different samples by Raman spectroscopy, identifying the VPO phases present on the catalyst surface. The spectra are reported in the following figures (Figure 4.12).

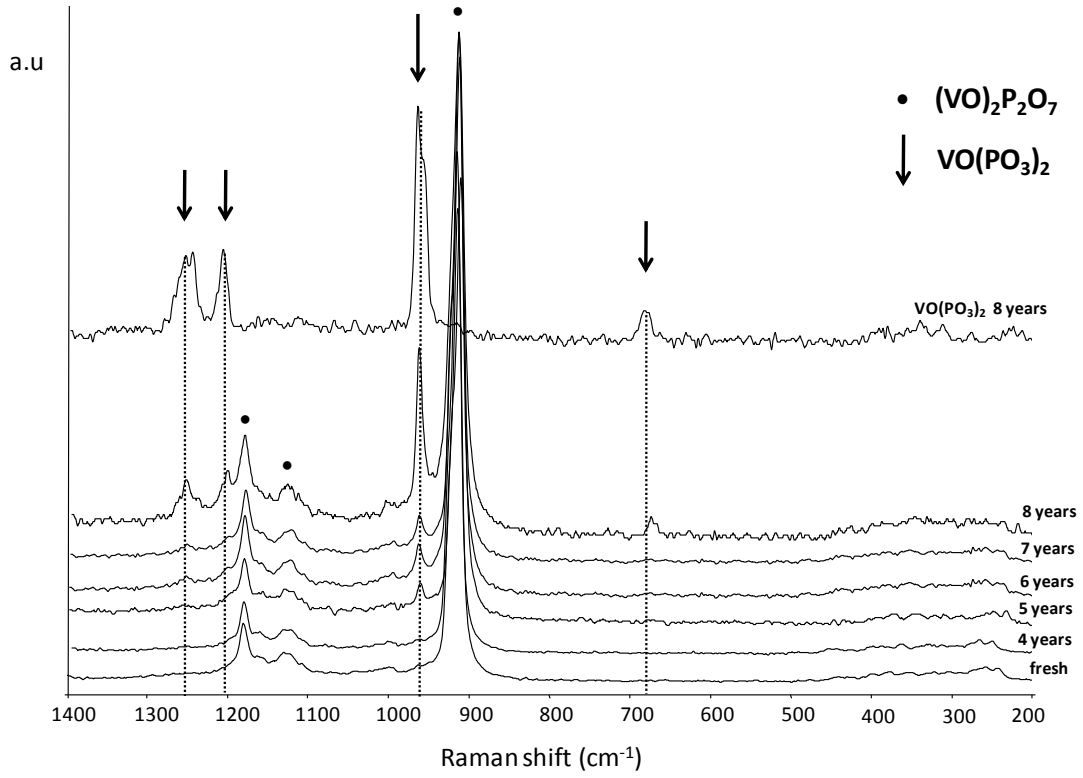

Figure 4.12: Raman spectra of the industrial catalyst, collected for studying the effect of ageing; the sample are named with their age. Spectra collected over grey and pale-blue particles.

It is shown that the fresh catalyst only contains vanadyl pyrophosphate, while the progressive ageing leads to the formation of vanadyl metaphophate $VO(PO_3)_2$, as demonstrated by the increasing relative intensity of its characteristics bands at 692, 957, 1216 and 1255 cm^{-1}. Worth of note, the spectra were collected over grey and pale-blue particles: in particular, over the pale-blue particles the formation of the

metaphosphate was so relevant to be detected also as an isolated phase, as shown in the "8-years" sample. Since the $VO(PO_3)_2$ phase is characterized by a P/V ratio twice as much that one of the VPP, this is a clear indication that ageing occurs through an excessive phosphorus surface enrichment, that could lead to the segregation of the metaphosphate and cause the drop of the catalyst performance. As already mentioned, the P/V ratio greatly affects the catalyst behavior and even if a slight excess of phosphorus is essential to reach the optimal performance, a too high P/V ratio has a negative effect and reduces the catalyst re-oxidation rate [47, 65, 76]. In fact, when the phosphorus content increases, it is more difficult to keep the vanadium in its higher oxidation state, so as a consequence the selectivity to MA decreases. In particular, the scientific literature reports that $VO(PO_3)_2$ can be easily formed when the P/V ratio is in the range between 1.6 – 2.0 [76] and that this compound is inactive in *n*-butane oxidation [210]. Even if its action could prevent the oxidation of the V^{4+} over the selective (100) plane when the P/V ratio is in slight excess [211], on the other hand $VO(PO_3)_2$ has an important detrimental effect on the VPP catalyst when it is present in high amount; therefore, we can explain the drop in activity shown during ageing with the formation of the inactive $VO(PO_3)_2$.

Raman investigation was continued over the oldest sample, namely over particles showing different colors and particular aspects: the most significant spectra are reported in Figure 4.13, Figure 4.14 and Figure 4.15.

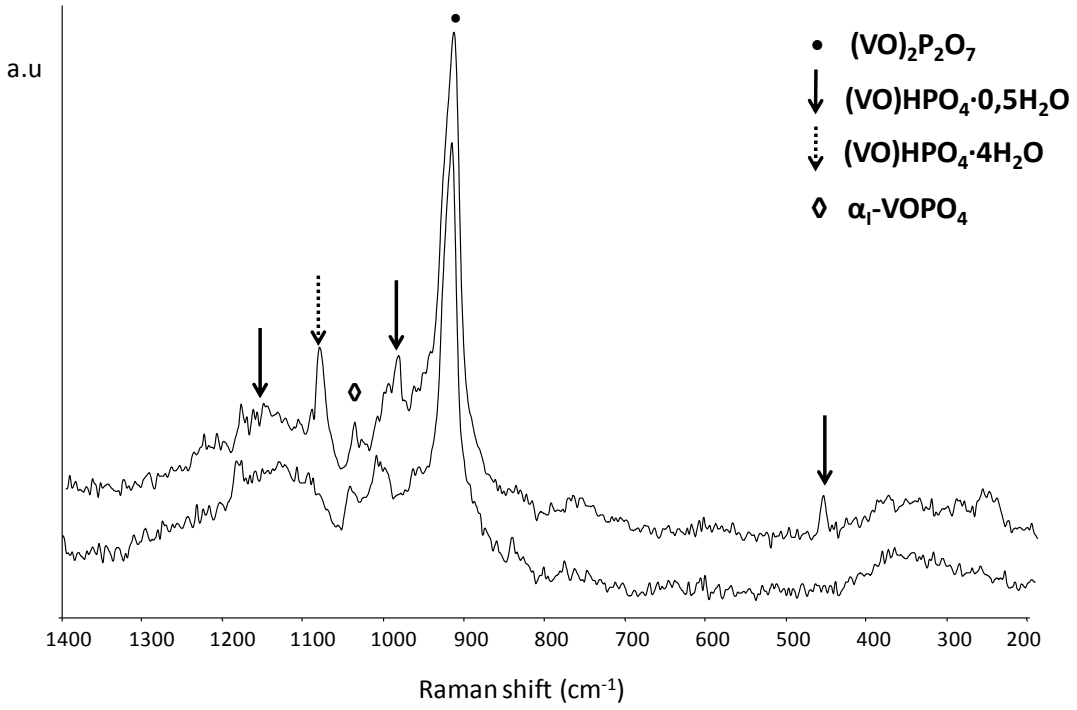

Figure 4.13: Raman spectra of the "8-years" industrial catalyst collected over brown particles.

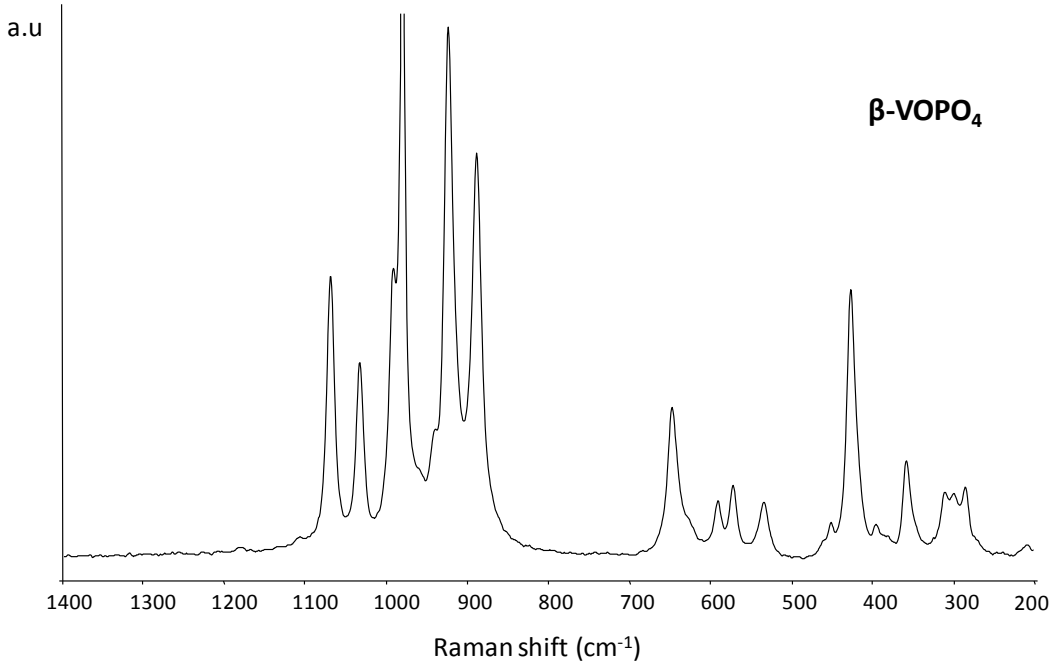

Figure 4.14: Raman spectra of the "8-years" industrial catalyst collected over yellow particles.

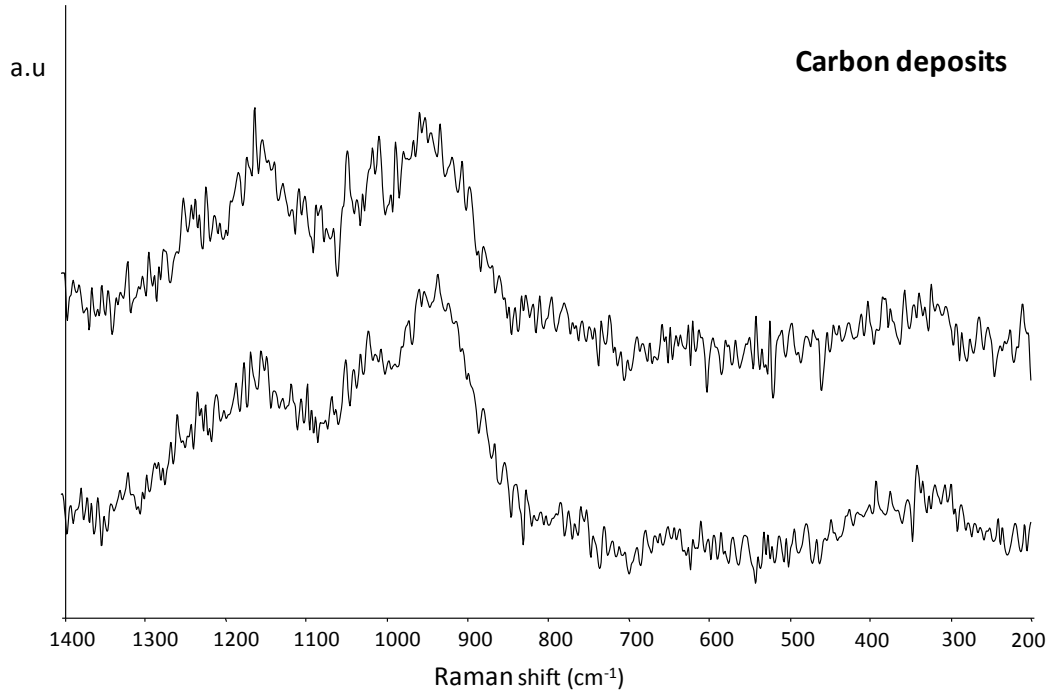

Figure 4.15: Raman spectra of the "8-years" industrial catalyst collected over black particles.

Raman analysis demonstrate that the ageing process is not only due to the formation of the vanadyl metaphosphate, but it is a more complex process in which other compounds are involved, since hydrated phases ($VOHPO_4 \cdot nH_2O$), β-$VOPO_4$ and coke deposits have been detected. In Figure 4.13 Raman spectra have evidenced the presence of the catalyst precursor $VOHPO_4 \cdot 0.5H_2O$ and of the vanadyl hydrogenphosphate tetrahydrated $VOHPO_4 \cdot 4H_2O$ together with the VPP phase. This indicates that, even if VPP still represents the main VPO phase, the catalyst surface has suffered a strong process of hydration. Reminding that the reaction produces four molecules of water per molecule of *n*-butane, the steam co-produced has an important effect on the surface modification of VPP occurring during long-time permanence in the reactor, since it could lead to the hydration of the active phase, with the formation of VHP and even of more hydrated phases, such as $VOHPO_4 \cdot 4H_2O$ [65, 212]. We can hypothesize that the progressive ageing of the catalyst has compromised the desorption ability of the material, being this hypothesis confirmed also by the presence of coke deposits (Figure 4.15). Moreover, the Raman spectrum reported in Figure 4.14 shows that the ageing is accompanied also by the formation of the

oxidized phase β-$VOPO_4$. In theory, the orthophosphate $VOPO_4$ compounds are formed after the thermal treatment of the precursor and they could be transformed to VPP by the reactive mixture during the activation period. However, the different $VOPO_4$ compounds have a different attitude to be reduced to VPP, depending on their morphology and structures [80]. Differently from the other $VOPO_4$ phases, the formation of β-$VOPO_4$ occurs at higher temperature and through a consecutive reaction scheme:

$$\delta\text{-}VOPO_4 \rightarrow \gamma\text{-}VOPO_4 \rightarrow \beta\text{-}VOPO_4$$

δ-$VOPO_4$ and γ-$VOPO_4$ are obtained by dehydration of the precursor respectively at 450°C in air and 680°C in O_2 and γ-$VOPO_4$ is transformed into β-$VOPO_4$ at 780°C [205]. Moreover, also α_I-$VOPO_4$ could be transformed to β-$VOPO_4$ at the high temperatures typically met in the hot-spots zones of fixed-bed reactors [19]. In general, the presence of β-$VOPO_4$ is frequent in used catalysts that have become inactive after long-time runs: in fact, one the reason of the loss of the catalytic performance is due to the β-$VOPO_4$ phase, the presence of which is known to reduce both the activity and the selectivity. Moreover, because of its greater stability at high temperature compared with the other $VOPO_4$ forms, once generated it cannot evolve to any other compound [80].

Lastly, over the surface of the "8-years" catalyst the presence of carbon deposits has been detected (Figure 4.15). More in details, the D4 band was detected at 1200 cm^{-1}, that is due to the A_{1g} symmetry stretching of the amorphous carbon: in particular this signal is correlated to the stretching of C sp^2 and sp^3 of disordered graphitic structures [213, 214].

We suppose the carbon deposits are generated as a consequence of a strong and irreversible adsorption of the organic compounds on the catalyst surface, being the desorption process compromised. This phenomenon generates a covering layer over the catalyst surface that blocks the active sites, as demonstrated by the signals of the VPP bands that could not be detected any more.

The formation of coke over solid catalysts is one of the most frequent causes of catalyst deactivation in industrial processes using acid catalysts, for example zeolites

in FCC, Pt/Al_2O_3 in reforming, Pt/zeolite or NiMoS/zeolite in hydroisomerization and hydrocracking processes. The deactivation is caused by the poisoning of the active sites through the blockage of their pores: the organic molecules are retained on the catalyst surface because of their strong adsorption and their low volatility [215, 216]. The mechanism of deactivation depends on the reaction temperature and on the nature of the reactants: in particular, from *n*-alkane (like *n*-butane) there is generally no coke formation at low temperature (<150°C), but it happens at higher temperatures (>400°C). Since VPP is a bifunctional catalyst and possesses both acid and redox, the acid sites could catalyze the condensation and rearrangement of the unsaturated species, in our case the intermediates molecules involved in the scheme of reaction from *n*-butane to MA, i.e., butenes and butadiene [16, 19]. If we remind that one of the consequences of the ageing is the phosphorus-enrichment occurring on the catalyst surface, this means that an increased acidity is localized on the surface and it could favor the condensation reaction of the organic molecules adsorbed.

In conclusion, the ageing of the industrial vanadyl pyrophosphate catalyst leads to a progressive worsening of the overall catalytic performances due to a complex process characterized by a combination of effects:

1. Phosphorus-enrichment, represented by the formation of $VO(PO_3)_2$, an unselective and detrimental phase.
2. Formation of unselective V^{5+} phase, namely β-$VOPO_4$.
3. Modification of the acidity of the material and worsening of the desorption properties, as shown by the formation of hydrated phases ($VOHPO_4 \cdot nH_2O$) and of carbon deposits.
4. Strong adsorption of the organic products of reaction, that causes the formation of coke and the blockage of the active sites.

4.2 Synthesis of maleic anhydride from 1-butanol

4.2.1 Dehydration of 1-butanol

The synthesis of maleic anhydride from 1-butanol can be schematized in two steps:

1. Dehydration of 1-butanol to butenes
2. Selective oxidation of butenes to maleic anhydride

These reactions need catalytic systems with different properties, in particular acidity for the dehydration and redox property for the selective oxidation. At the beginning of the research, the first step of dehydration of 1-butanol to butenes (1-butene, 2-butenes *cis* and *trans*) was studied, with the aim of investigating and improve the efficiency of this step (Figure 4.16). Solid catalysts with acid properties like Keggin-type polyoxometalates, vanadyl pyrophosphate (VPP) and vanadyl phosphate dihydrated ($VOPO_4 \cdot 2H_2O$) were chosen; they were tested feeding 1% 1-butanol in He, in gas phase lab-scale reactor, with residence time of 1.33 g·s/ml.

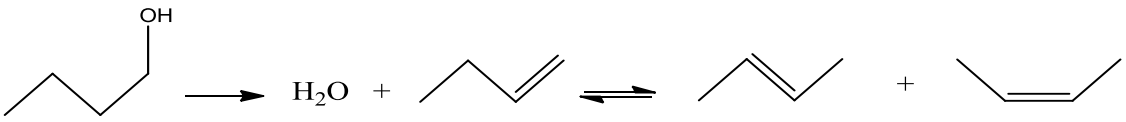

Figure 4.16: Scheme of dehydration of 1-butanol to 1-butene and its isomerization to *cis* and *trans* 2-butenes.

4.2.1.1 Reactivity tests with supported Keggin-type polioxometalates catalysts

The catalysts studied are made of 30%wt. of Keggin-type polyoxometalate (active phase) supported on CARi-ACT Q15 (silica gel, 70%wt.); in the list below the composition of the active phases is reported:

1. $Cs_2HPW_{12}O_{40}$;
2. $Cs_3PW_{12}O_{40}$;

3. $K_3HSiW_{12}O_{40}$;
4. $K_4SiW_{12}O_{40}$.

Catalysts were delivered by the team UCCS (Dr Benjamin Katryniok, Prof. Sebastien Paul and Prof. Franck Dumeignil), Unité de Catalyse et de Chimie du Solide UMR CNRS, Equipe VALBIO, University of Lille and École Centrale de Lille, within the framework of the European Project EuroBioRef.

Catalytic tests were carrried out using the following conditions: 0.8 g of catalyst sized in pellet 30-40 mesh, diluted with an inert filler (steatite); contact time 1.3 s and inlet feed composition 1% 1-butanol in He, the latter with a flow rate of 36 ml/min.
It is worth noting that in completely salified polyoxometalates, like cat. $Cs_3PW_{12}O_{40}$and cat. $K_4SiW_{12}O_{40}$, no acidity should be present, because of the lack of protons in the structure; nevertheless, even if in the method of preparation a suitable amount of alkaline cation is added to compensate for the negative charge of the *cluster*, some traces of the previous non-substituted heteropolyacid still remain.

First of all, we carried out a blank experiments in order to study the reactivity of 1-butanol in gas phase in presence of an inert solid, used as filler, without any catalyst. The aim is to investigate if the filler has some effect on the reactivity of 1-butanol; the experiment was conducted under the same conditions and reactor configurations used for the catalytic test, but without catalyst. The results of the blank test are reported in Figure 4.17.

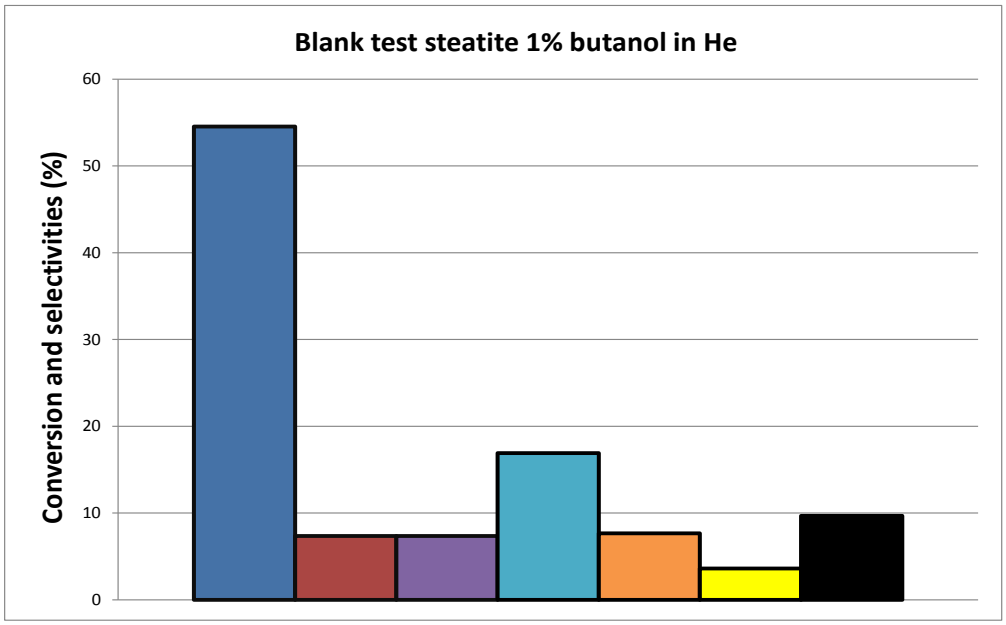

Figure 4.17: Blank test, 1% of butanol in He at 250°C over steatite. Symbols: 1-butanol conversion (■); selectivities in butyraldehyde (■),1,4- butadiene (■), 1-butene (■), 2-buteni (■), isobutanol (■), *n*-butyl ether (■).

Analyzing the results reported, we can state that 1-butanol is a very reactive molecule, being converted only by thermal effect even in absence of an acid catalyst. Nevertheless, its transformation is not selective, because together with the dehydration products (butenes), also isomerization (isobutanol), condensation (*n*-butyl ether) and selective dehydrogenation (butyraldehyde) products are formed. Another blank test was carried out at a lower temperature (150°C): the same 1-butanol conversion was achieved, but *n*-butyl ether and isobutanol also formed. Therefore, in order to enhance 1-butanol conversion and to improve its selectivity to butenes for the two-steps synthesis of maleic anhydride, an acid catalyst has to be added in the process.

First of all we tested the catalytic performances of the four supported-polyoxometalate samples in the reaction of 1-butanol dehydration in function of time on stream, at a constant temperature. The conditions chosen were: temperature of 250°C, contact time 1.3 g·s/ml, feed composition 1% 1-butanol in He (flow rate of 36 ml/min and 0.8 g of catalyst in 30-40 mesh pellets. In Figure 4.18, Figure 4.19 and Figure 4.20 the

results of the catalytic tests for $Cs_2HPW_{12}O_{40}$, $Cs_3PW_{12}O_{40}$ and $K_3HSiW_{12}O_{40}$ are reported.

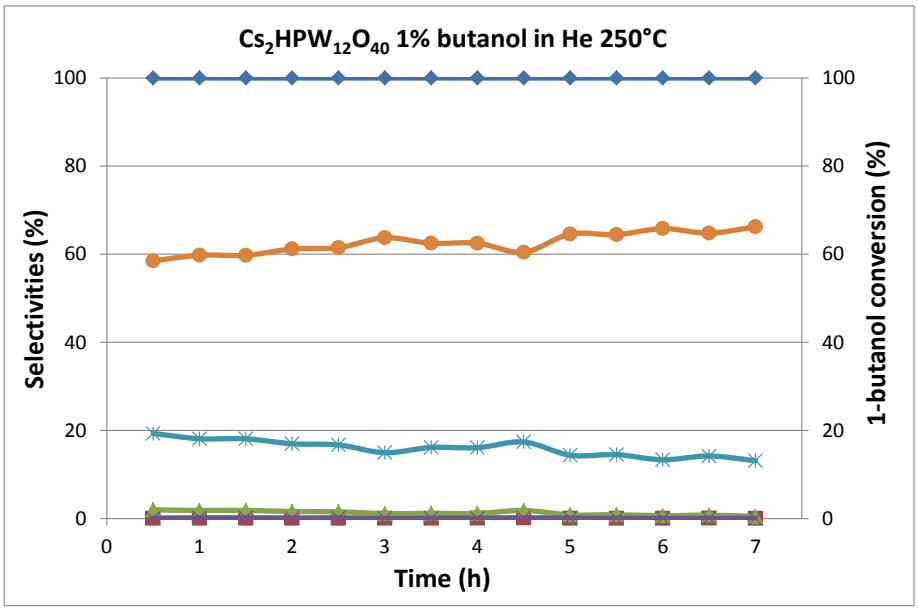

Figure 4.18: Reactivity of $Cs_2HPW_{12}O_{40}$ catalyst in function of time on stream at 250°C. Symbols: 1-butanol conversion (◆), selectivities in 1-butene (*), 2-buteni (●), butyraldehyde (■), 1,4-butadiene (×), light (▲).

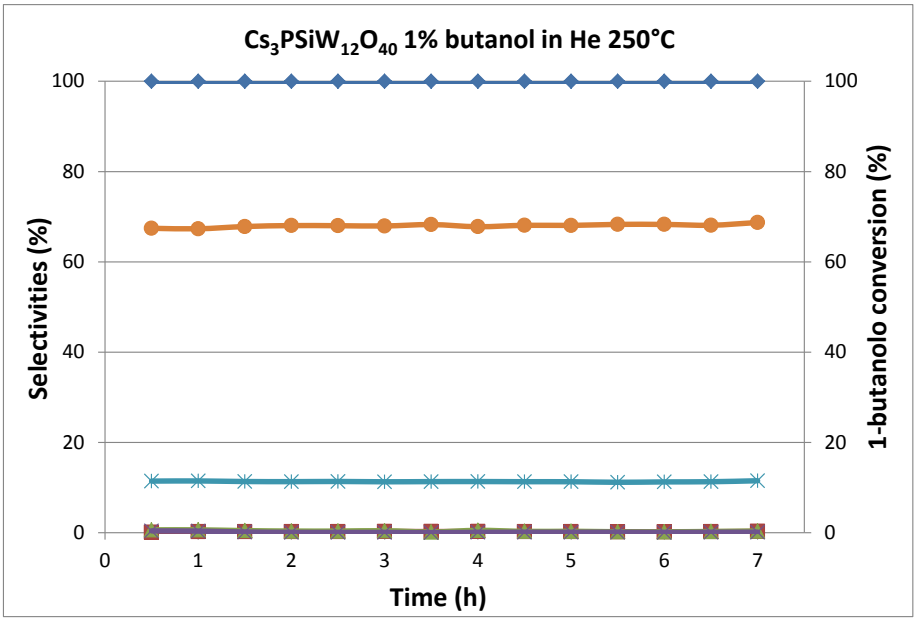

Figure 4.19: Reactivity of $Cs_3PW_{12}O_{40}$ in function of time on stream at 250°C. Symbols: 1-butanol conversion (◆), selectivities in 1-butene (*), 2-buteni (●), butyraldehyde (■), 1,4-butadiene (×), light (▲).

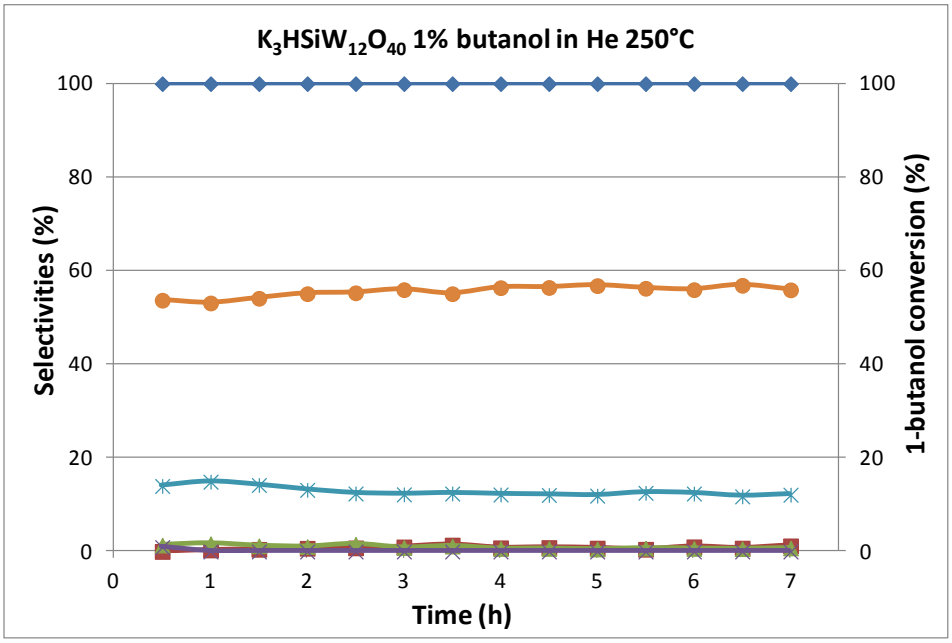

Figure 4.20: Reactivity of $K_3HSiW_{12}O_{40}$ in function of time on stream at 250°C. Symbols: 1-butanol conversion (◆), selectivities in 1-butene (*), 2-buteni (●), butyraldehyde (■), 1,4-butadiene (×), light (▲).

The behavior of the 3 samples examined is very similar; at 250°C, all of them convert completely 1-butanol, with almost total selectivity to 1-butene and 2-butenes. There are very small amounts of butyraldehyde and of an identified compound (maybe a light hydrocarbon). Minor differences between the three samples concern the selectivity to each of the butenes. In particular, the catalytic behavior of sample $Cs_3PW_{12}O_{40}$ is identical to that obtained with the silica-alumina catalyst tested in the past; all samples (and the silica-alumina as well) however show a different behavior compared to alumina. The ratio between the two butenes isomers is close to the thermodynamic one [217]; this means that the isomerisation of the double bond in the primary product of dehydration (1-butene) to yield 2-butenes is very quick.

Finally the results of the experiment with the $K_4SiW_{12}O_{40}$ catalyst is reported in Figure 4.21. As shown in the graph, it was the least active catalyst because even at 250°C it did not reach complete conversion, and also gave the lowest C balance with more than 20% yield to missing C (1-butene yield 27%, 2-butenes yield 47%). Despite all this, the conversion was stable during the experiment time (as it was for

the other samples, also, but in that case conversion was total); this indicates that the formation of coke did not affect so much the active sites for 1-butanol dehydration. Moreover, the catalyst showed a lower selectivity to 2-butenes, which also confirms that the catalyst was less active, because at 250°C it did not reach equilibrium for olefins isomerization; an alternative explanation is the selective poisoning of sites for isomerization.

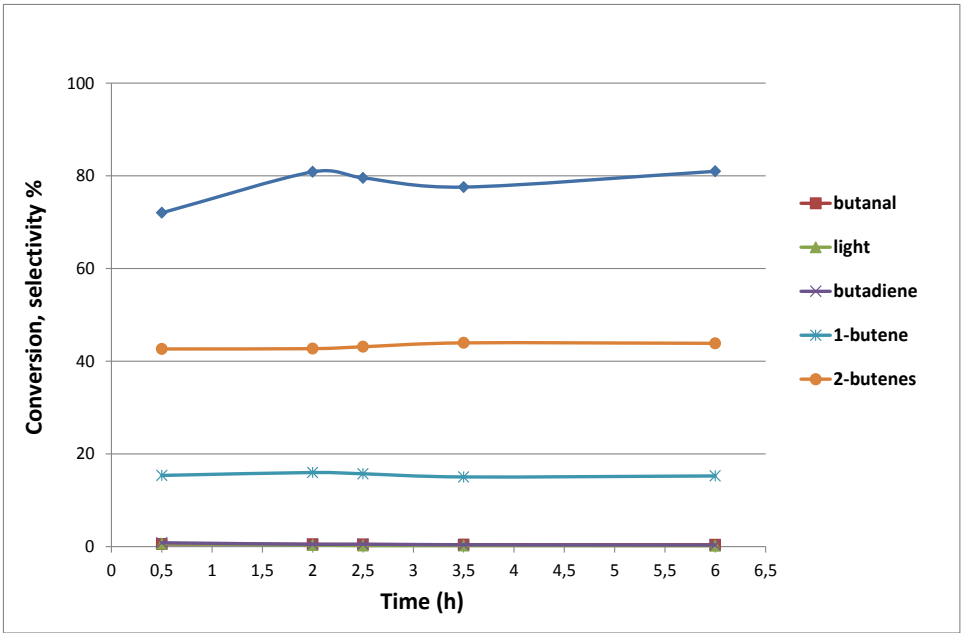

Figure 4.21: Reactivity of $K_4SiW_{12}O_{40}$ in function of time on stream at 250°C Symbols: 1-butanol conversion (◆), selectivities in 1-butene (*), 2-buteni (●), butyraldehyde (■), 1,4-butadiene (×), light (▲).

Afterwards, we tested the performance of the four samples in the dehydration of 1-butanol in function of temperature, in order to evaluate any possible differences in catalytic performances. The conditions chosen for 1-butanol dehydration were: feed composition 1% 1-butanol in He (flow rate 36 ml/min), range of temperature variable from 130 to 310°C, depending on 1-butanol conversion obtained with the catalyst tested, contact time 1.3 s, 0.8 g of catalyst formed in pellets sized 30-40 mesh. First we started tests at 310°C, then we decreased the temperature until 1-butanol conversion was lower than 99% and finally we increased temperature until the conversion was total. In Figure 4.22, Figure 4.23, Figure 4.24 and Figure 4.25 the

results of the catalytic tests in terms of conversion of 1-butanol and yield to the products are reported.

In order to carry out the experiments in function of temperature, we had to regenerate the catalyst because they had been already used for time-on stream tests. The procedure adopted for regeneration was a treatment in flowing air at 350°C for 25 h (air flow rate 36 ml/min for 0.3 g catalyst) in the glass reactor of the lab plant.

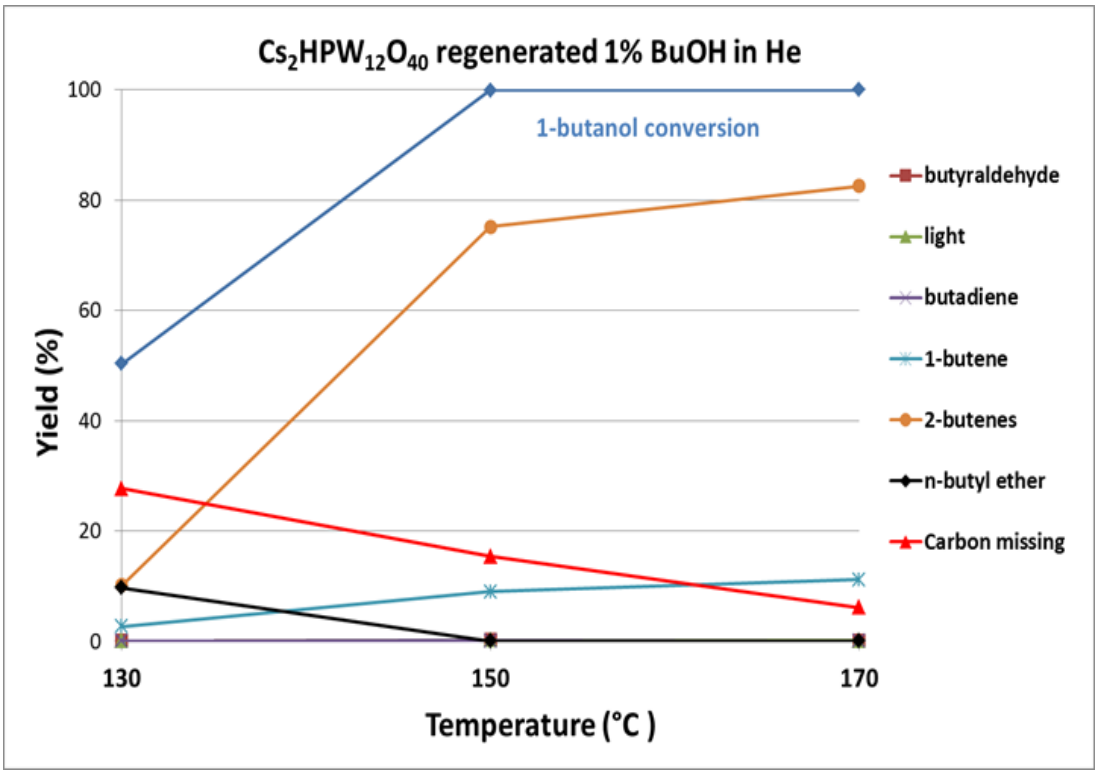

Figure 4.22: Catalytic test of $Cs_2HPW_{12}O_{40}$ in function of temperature.

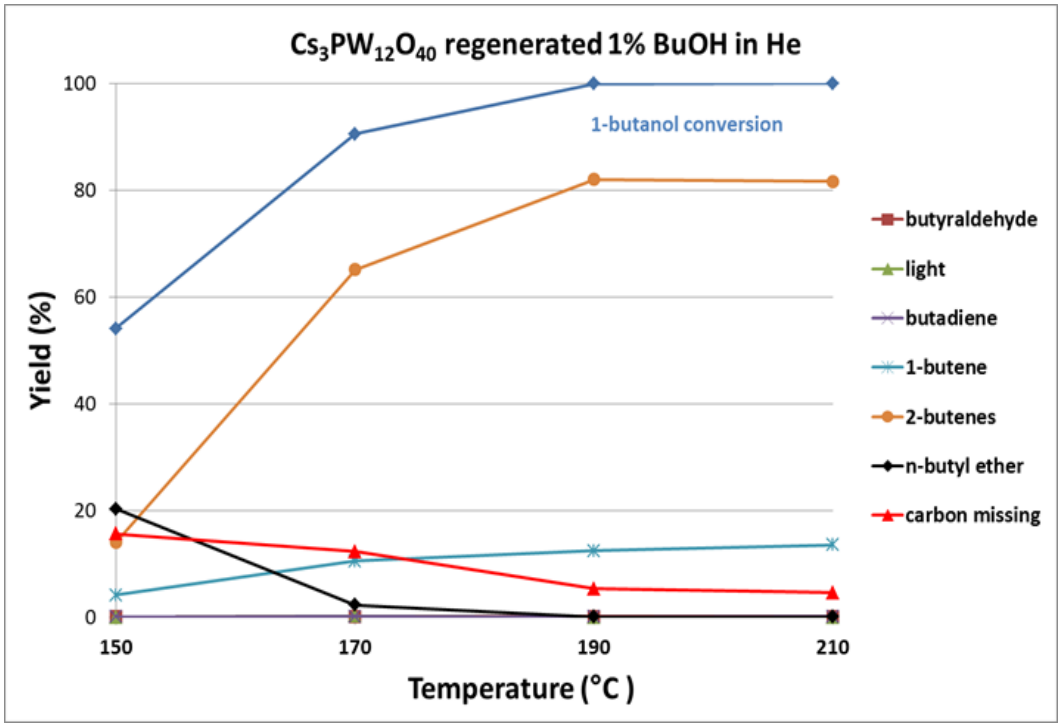

Figure 4.23: Catalytic test of $Cs_3PW_{12}O_{40}$ in function of temperature.

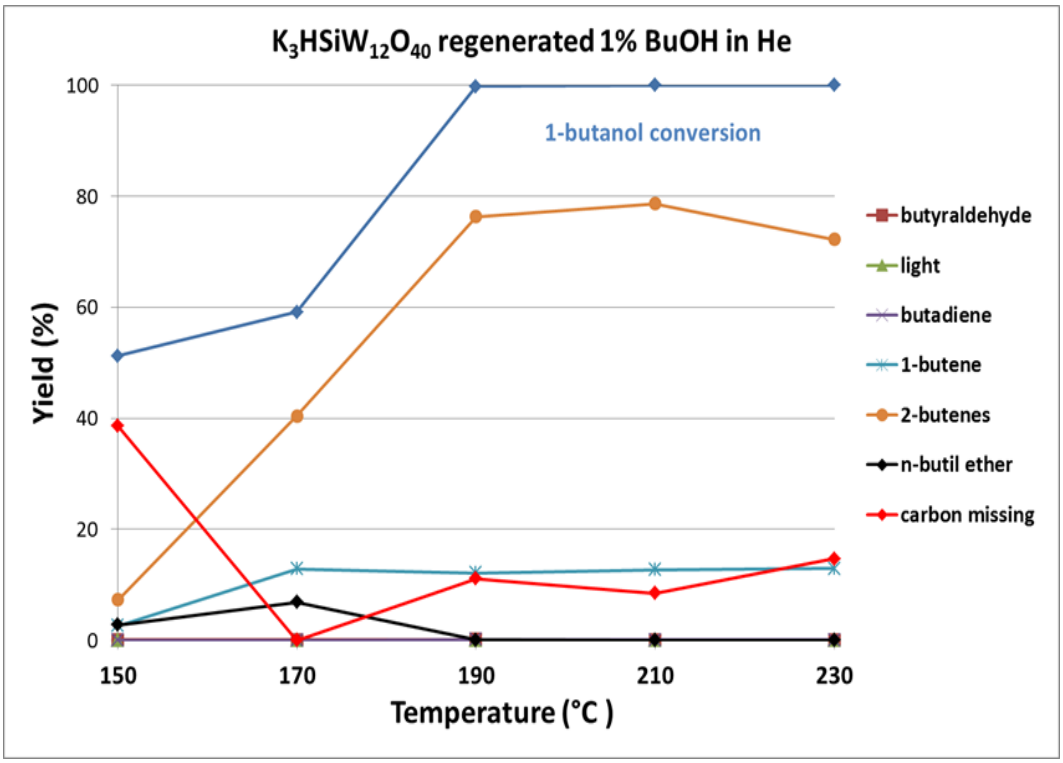

Figure 4.24: Catalytic test of $K_3HSiW_{12}O_{40}$ in function of temperature.

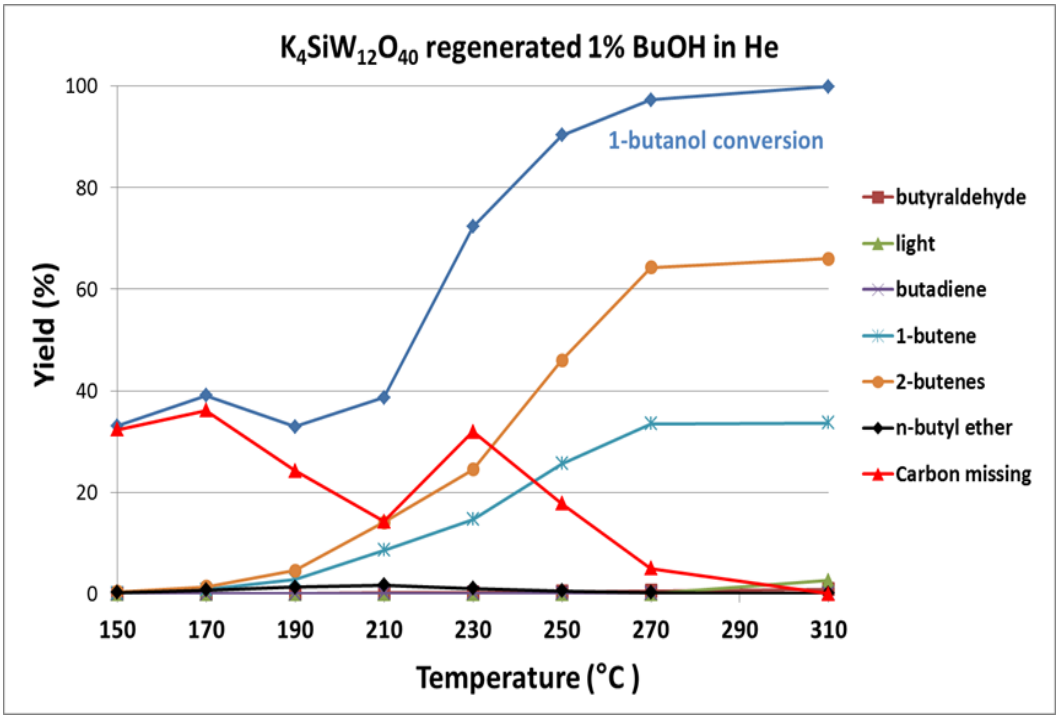

Figure 4.25: Catalytic test of $K_4SiW_{12}O_{40}$ in function of temperature.

It is possible to comment as follows:

1. The four samples examined show important differences in terms of activity: in general, catalysts with Cs and P were more active than those with K and W. With $Cs_2HPW_{12}O_{40}$ total conversion of 1-butanol was shown at 170°C; this was the most active sample. If we compare $Cs_2HPW_{12}O_{40}$ with $Cs_3PW_{12}O_{40}$, and $K_3HSiW_{12}O_{40}$ with $K_4SiW_{12}O_{40}$, we notice that in both cases an increased acidity (due to the presence of protons) led to higher activity at low temperatures. Nevertheless, it is amazing that even with samples which do not hold protons, still remarkable conversions were achieved at moderate temperatures. Worth of note, blank experiments with the empty reactors gave negligible 1-butanol conversion in this temperature range.

2. For all catalysts, the dehydration of 1-butanol led to the same products, and the highest selectivity was shown for 1-butene and 2-butenes *cis* and *trans*. We identified also the presence of small amounts of *n*-butyl ether: the formation of this compound occurred in particular at low temperature, and this behavior

was observed with all samples. Moreover, there were very small amounts of butyraldehyde and butadiene. These results agree with works in literature [171, 218, 219], in particular it is known that $Cs_2HPW_{12}O_{40}$ catalyst for dehydration of ethanol leads to the related olefin (ethylene), aldehyde (acetaldehyde) and ether (diethyl ether).

3. Together with yields values, the "yield to missing carbon" is also plotted, that is the % lack in C balance. We think that this lack of C is due to a strong adsorption of organic compounds occurring at low temperatures, whereas at high temperature this was due to the formation of coke. In fact, all spent catalysts were black after the reactivity test because of the formation of coke on the surface. Therefore, the optimal temperature range may be between 170 and 200°C (in function of the catalyst type); lower temperatures lead to poor C balance because of alcohol "irreversible" adsorption, higher temperatures because of coke accumulation. Usually, in the intermediate range, the C balance is as high as 85-90%, which means that 10% of the converted 1-butanol is missing; this value is not far from the experimental error.

In order to confirm the alcohol adsorption at low temperature, a desorption test with catalyst $K_3HSiW_{12}O_{40}$ was carried out. After one day of reaction (dehydration of 1-butanol, 1% 1-butanol in He – flow rate 36 ml/min – at 170 °C), we stopped the feed and we kept the sample in flow of He still at 170°C, monitoring the evolution of organics. We plotted the number of C moles in function of the desorption time: Figure 4.26 shows that after 20 hours there were still organic compounds leaving the catalyst surface, namely 2-butenes, 1-butene and 1-butanol.

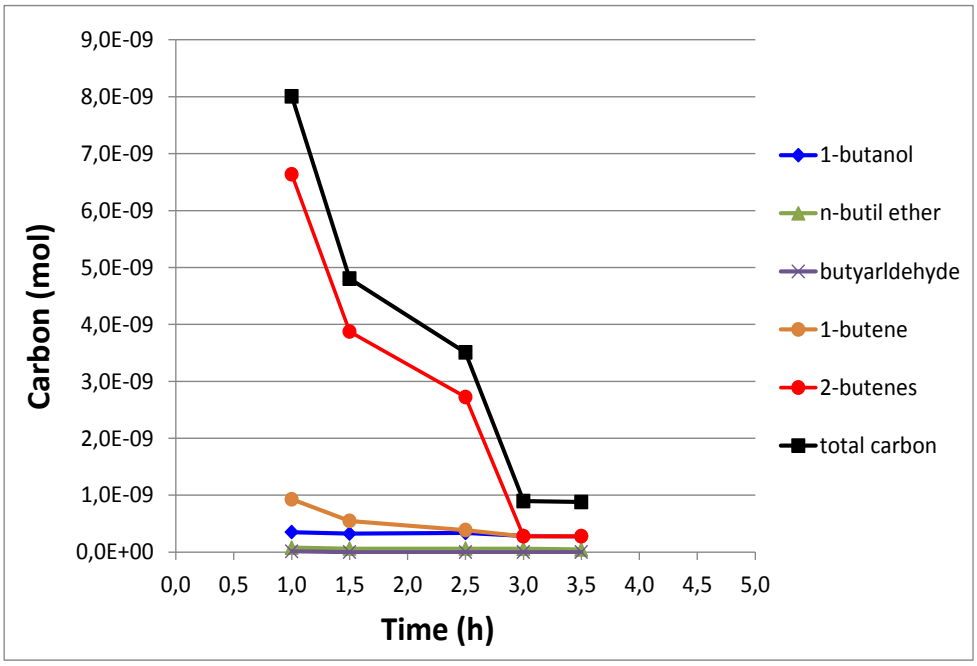

Figure 4.26: Absolute quantity of organic compounds desorbed during the $K_3HSiW_{12}O_{40}$ catalyst "cleaning" with He, at 170°C.

In particular, the value of carbon missing is greatly affected by temperature: it is more relevant at low temperature, when 1-butanol conversion is relatively low, and at high temperature, when the conversion is total.

In conclusions, the catalytic activity of the four polyoxometalates in the dehydration of 1-butanol is strictly correlated with their acid strength: as reported in literature [171], POM acidity could be determined by the deprotonation energy, representing the cluster attitude as H^+ donor. This energy, and consequently both the activity and the selectivity, depends on the structure composition of the catalytic system: variation on it could lead to important modification of the acidity without alteration of the crystalline structure, being the latter a peculiar distinctive trait of Keggin-type POM.

An important key point of POM behavior is the nature of the central atom: a decrease in the oxidation state leads to an increase on the number of protons necessary for the overall charge balance of the structure and a consequent rise of the anionic charge. This phenomenon produces an increase on the deprotonation energy and a reduction of the acid power, resulting in a softening of the catalytic activity. This agree with the

results obtained in the catalytic tests, where the samples with P^{5+} as central atom (cat.Cs_2H and Cs_3) showed to be more active than samples containing Si^{4+} (cat.K_3H and K_4).

On the opposite, the substitution of H^+ with alkaline cations (Cs^+ and K^+) caused a modification on the secondary structure of the POM and an increase of the surface area, due to a growth of the dimensions. However, this substitution produces a reduction of the acid strength, because of the introduction of alkaline cations, having a lower electronegativity than the protons. Moreover, it increases the electrons density of the external shell of POM and consequently an higher deprotonation energy has to be reached to catalyze the dehydration reaction: this produces a loss of the activity. These remarks could explain the differences observed in the experiments performed with the four POM samples: catalyst less substituted (cat. Cs_2H and K_3H) are more active than their corresponding totally substituted (cat. Cs_3 and K_4). Furthermore, catalysts which are nominally completely substituted still show acid characteristics, as demonstrated in the previous experiments. Scientific literature confirms these properties taking into account the method of preparation of the materials [182, 183]: actually, the POM synthetized as precipitate is a mixture containing some traces of the original non-substituted POM ($H_3PW_{12}O_{40}$ and $H_4SiW_{12}O_{40}$ respectively) in amount depending on the condition of the preparation (reactant amount, calcination temperature, precipitation method and activation treatment) and this allows cat. Cs_2H and K_3H to exhibit acid properties.

The nature of the products obtained in the reactivity tests of 1-butanol agrees with the studies reported in scientific literature concerning the dehydration of ethanol catalyzed by POM [184]: the products are respectively its olefin (ethylene), aldehyde (acetaldehyde) and ether (diethyl ether). This is due to the mechanism of alcohols dehydration, which expects two competitive routes:

1. Intramolecular route: it leads to the formation of the olefin, through decomposition of the alcohol adsorbed on the catalyst surface; it is the favorite route, especially at high temperature;

2. Intermolecular route: it leads to the formation of the ether, through the reaction between a physisorbed molecule of alcohol and a chemisorbed one; this pathway is preferred at low temperature.

In addition to these principal routes, other collateral reaction could occur at high temperature, generating aldehyde and coke.

4.2.2 Reactivity tests with $VOPO_4 \cdot 2H_2O$ catalysts

Vanadyl phosphate dihydrated ($VOPO_4 \cdot 2H_2O$) is a V^{5+} phase commonly used for the so-called VPD route, which is one of the methods of preparation utilized for the synthesis of the precursor $VOHPO_4 \cdot 0{,}5H_2O$ [220]. This preparation is a "two-step" route, since in the first step the formation of the phase $VOPO_4 \cdot 2H_2O$ (VPD) occurs, while in the second one the VPD is reduced by the addition of an alcohol or a mixture of alcohols to finally obtain the precursor $VOHPO_4 \cdot 0{,}5H_2O$ [29, 221, 222, 223]. Since the trasformation of the precursor to the active phase is topotactic in the traditional synthesis in the organic medium [29], also in the VPD route the dehydration to VHP takes place retaining its microstucture and for this reason the control of the preparation of $VOPO_4 \cdot 2H_2O$ is essential to fine-tune the morphology of the active phase [224, 193].

Vanadyl phosphate dihydrated has a layered structure composed of repeated octahedral [VO_6] and tetrahedral $[PO_4]^{3-}$ units arranged in the same tetragonal crystal group of the α_I and α_{II} $-VOPO_4$ phase, with tha addition of two crystallization water molecules [193, 225, 226]. One of the charachteritics of VPD is that in general all of the $VOPO_4$ phases could convert more or less easily to VPD after an hydration treatment; the $VOPO_4$ phase that more exhibits this attitude is α_I–$VOPO_4$ [227].

Concerning the dehydration of 1-butanol, VPD was suggested as possible catalyst for the reaction since V/P/O based catalysts are known to have acid properties [90, 91, 92].

First of all we carried out a blank experiment in order to study the reactivity of 1-butanol in gas phase as function of temperature in absence of the inert filler and without any catalyst. The blank tests were carried either in inert or oxidizing environment respectively, feeding 1% butanol in He or in air. In both cases the conversion of 1-butanol was negligible, since the average value obtained was 5%.

After the blank tests the reactivity of $VOPO_4 \cdot 2H_2O$ was investigated feeding 1% 1-butanol in He with residence time W/F=1.33 $g \cdot s \cdot ml^{-1}$: Figure 4.27 reports the results obtained while varying the reaction temperature.

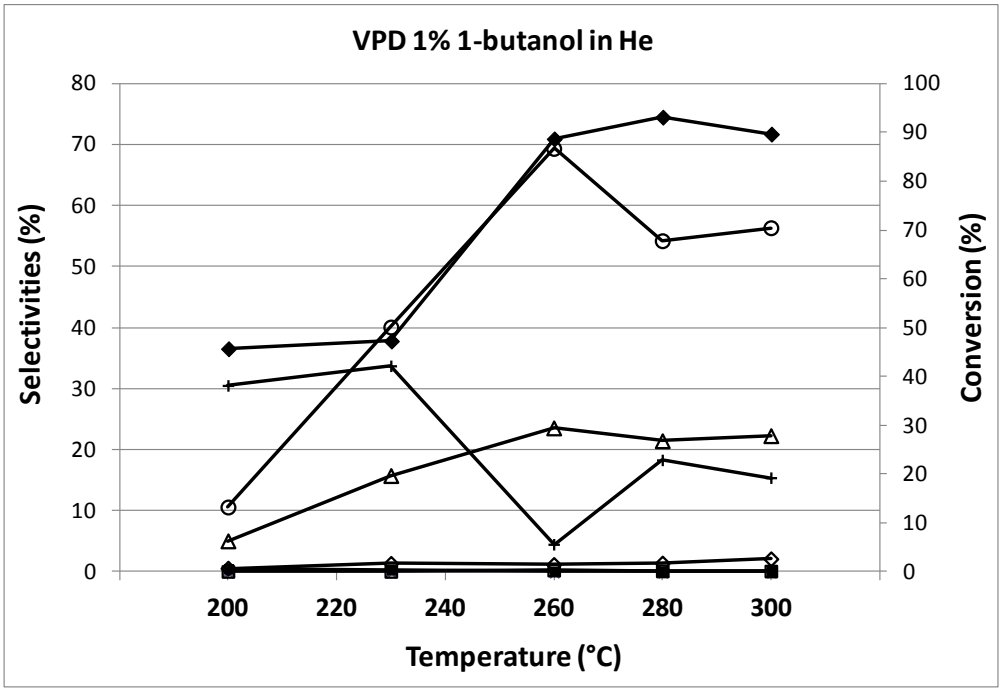

Figure 4.27: Catalytic behaviour of VPD catalyst in 1-butanol dehydration as a function of temperature. Conditions: feed 1 mol% 1-butanol in He, W/F 1.33 g·s· mL^{-1}. Symbols: 1-butanol conversion (◆). Selectivity to 1-butene (△), 2-butenes (O), *n*-butyl ether, (◇) butyraldehyde (■), lack to carbon balance (+).

Comparing the results with the performances obtained with Keggin polyoxometalates, we can observed that $VOPO_4 \cdot 2H_2O$ is less active than POM catalysts, since the total conversion of 1-butanol could not be reached even at 300°C. Moreover, the lack to carbon balance indicated that the adsorbtion of 1-butanol over the catalyst surface occurred at low temperature (30% at 200-220°C); also at high temperature the balance was not total, since probably some coke was formed, as demonstrated by the carbon missing between 20 and 25% at 280 and 300°C. Although the performance of VPD catalyst in the dehydration of 1-butanol was at least worse than that one obtained with POM, we decided to investigate the performances of the catalyst in a different environment, in order to test if $VOPO_4 \cdot 2H_2O$ could compensate for its lower activity with an higher operational flexibility.

Since the aim of our study is the synthesis of MA starting from 1-butanol, we have the keep in mind the possibility to carry out the process in the "one-reactor" configuration, arranged with two separated catalytic beds (the first is the acid catalyst

for 1-butanol dehydration and the second is the redox one, for the oxidation of butenes to MA). Since in this configuration 1-butanol has to be fed together with air, the acid catalyst has to be able to perform the dehydration reaction in oxidizing condition, that mean in presence of air. For this reason, we investigated the reactivity of $VOPO_4 \cdot 2H_2O$ feeding 1% 1-butanol in air with residence time W/F=1.33 $g \cdot s \cdot ml^{-1}$: Figure 4.28 reports the results obtained while varying the reaction temperature.

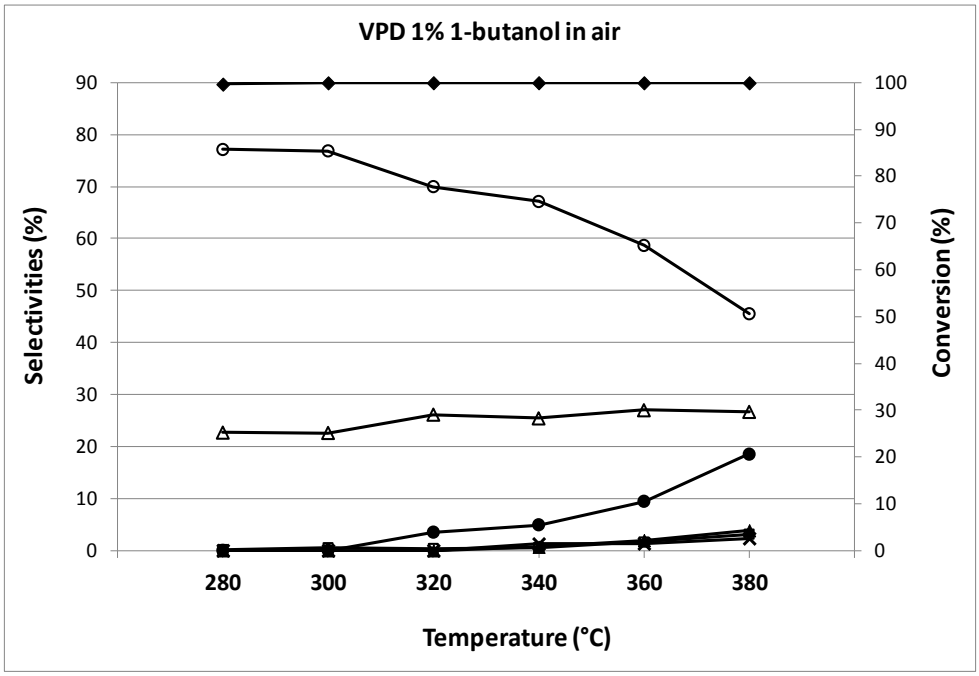

Figure 4.28: Catalytic behavior of VPD catalyst in 1-butanol dehydration as a function of temperature. Conditions: feed 1 mol% 1-butanol, 20% O_2, remaining: N_2; W/F 1.33 $g \cdot s \cdot mL^{-1}$. Symbols: 1-butanol conversion (◆). Selectivity to 1-butene (△), 2-butenes (○), CO (▲), CO_2 (●), furan (□) and "lights" (✕).

$VOPO_4 \cdot 2H_2O$ catalyst showed a different behavior in presence of air: total conversion was reached in the entire range of temperature (280-380 °C) and an high selectivity to 1-butene and 2-butenes was shown, accompanied by a limited formation of oxidative products (CO_x). Even if on increasing the temperature the selectivity to 2-butenes becomes lower, the VPD catalysts gives surprising performances at 300°C: in fact, the total conversion of 1-butanol was accompanied by a total selectivity to butenes; moreover, contrary to what shown with the POM catalysts studied before, with VPD

the carbon balance was close to 100%. For these reasons, VPD catalyst could be considered as a interesting candidate for the 1-butanol dehydration in presence of air in the "one-reactor" configuration.

In order to deeply investigate the behavior of VPD in an inert environment, we carried out two reactivity tests as function of time-on stream at two temperatures, 260 °C and 320°C. The results are shown in Figure 4.29 and Figure 4.30.

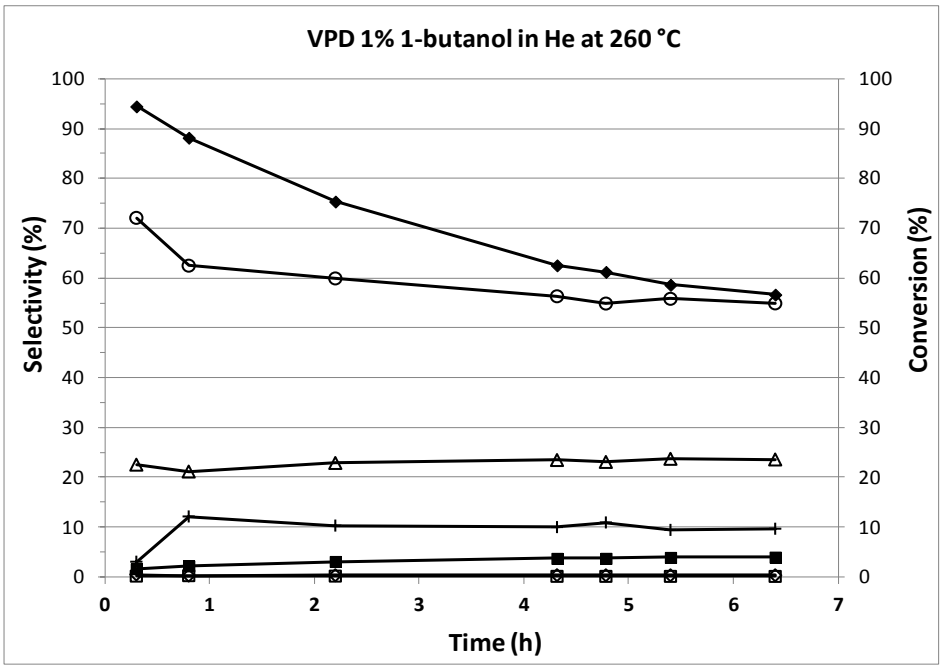

Figure 4.29: Catalytic behavior of VPD catalyst in 1-butanol dehydration as a function of time-on stream. Conditions: feed 1 mol% 1-butanol, 20% O_2, remaining: N_2; W/F 1.33 g·s· mL^{-1}. Temperature: 260°C. Symbols: 1-butanol conversion (◆). Selectivity to 1-butene (△), 2-butenes (○), *n*-butyl ether, (◇) butyraldehyde (■) and furan (□); carbon missing (+).

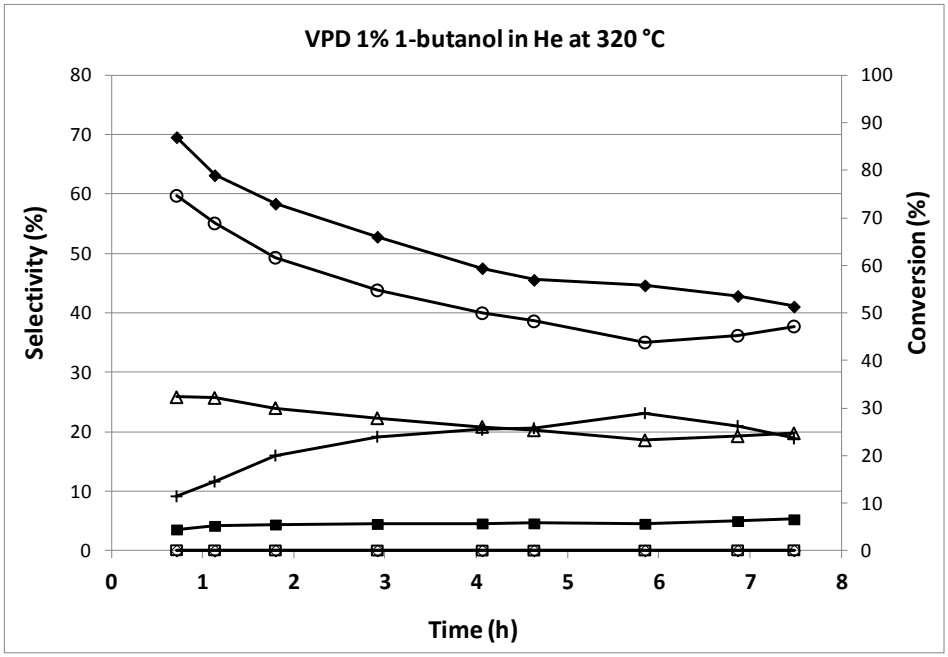

Figure 4.30: Catalytic behavior of VPD catalyst in 1-butanol dehydration as a function of time-on stream. Conditions: feed 1 mol% 1-butanol in He; W/F 1.33 g·s· mL^{-1}. Temperature: 320°C. Symbols: 1-butanol conversion (◆). Selectivity to 1-butene (△), 2-butenes (○), *n*-butyl ether, (◇). butyraldehyde (■) and furan (□); carbon missing (+).

The reactivity tests reported in Figure 4.29 and Figure 4.30 have shown that in both cases the conversion of 1-butanol progressively decreases during the reaction time: in fact, while in the first hour of reaction the catalyst gives a conversion between 80 and 90%, after seven hours the conversion dropped down to 50-55%. This means that a process of deactivation was occurring and led to a worsening of the catalytic performances. Despite the VPD catalyst have exhibited a good behavior in presence of air, this behavior was not followed in He, since the material deactivated very fast after few hours of reaction, at both high and low temperature: for this reason our interest to VPD was focused on its utilization in oxidizing environment.

The study on $VOPO_4 \cdot 2H_2O$ catalyst in the dehydration of 1-butanol was continued testing its behavior in air as function of time-on stream at 260°C. The graph of the catalytic test is reported in Figure 4.31.

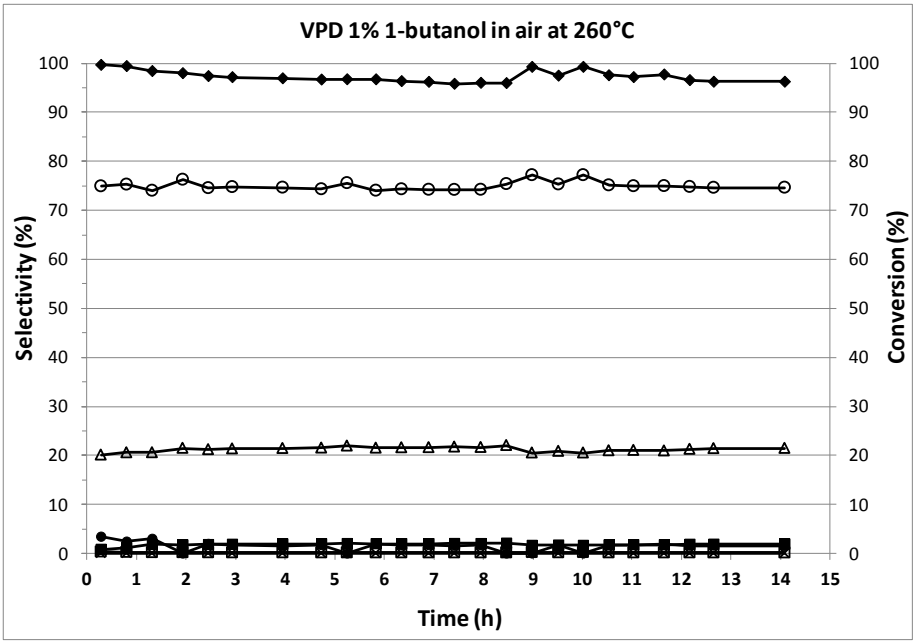

Figure 4.31: Catalytic behavior of VPD catalyst in 1-butanol dehydration as a function of time-on stream. Conditions: feed 1 mol% 1-butanol in He_2; W/F 1.33 g·s· mL^{-1}. Temperature: 260°C. Symbols: 1-butanol conversion (◆). Selectivity to CO_2 (●), acetic acid (✕), 1-butene (△), 2-butenes (○), *n*-butyl ether, (◇) butyraldehyde (■) and furan (□).

The experiments have shown that VPD catalyst exhibited an interesting catalytic performance also during time:

- at 260°C in air the conversion was almost total (always higher than 96%);
- despite the oxidizing condition, the catalyst gave essentially only the product derived from the dehydration of 1-butanol, i. e. 1-butene and 2-butenes; in fact, the carbon oxides and other oxidative products, such as butyraldehyde and furan, were produced with selectivity lower than 3%.
- the catalyst kept stable performances while increasing the time of reaction; in particular, on the contrary of its behavior revealed in He, the deactivation did not occur (the value of conversion did not decrease) and the selectivity to butenes did not drop.

In conclusion, the reactivity tests have demonstrated that the $VOPO_4 \cdot 2H_2O$ is a promising catalyst for the dehydration of 1-butanol to 1-butene and 2-butenes in

presence of air: in fact, not only the system is highly active and selective to butenes but also it gives the products with stable perfomance during time. For this reason, it could be considered a good candidate for the first bed in the "one-reactor" configuration for the synthesis of maleic anhydride starting from 1-butanol.

4.2.3 Characterization of $VOPO_4 \cdot 2H_2O$ catalysts

$VOPO_4 \cdot 2H_2O$ catalyst was characterized by means of Raman spectroscopy and XRD: Figure 4.32 shows the most significant spectra collected on the fresh catalyst.

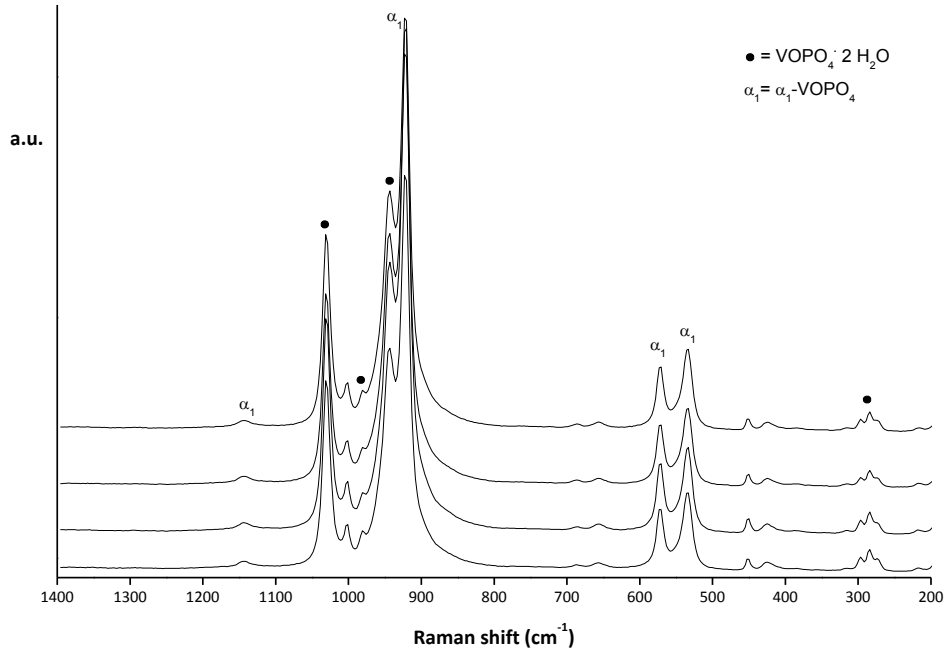

Figure 4.32: Raman spectra of fresh $VOPO_4 \cdot 2H_2O$ catalyst.

The Raman analysis have confirmed that $VOPO_4 \cdot 2H_2O$ is the main phase, as demonstrated by the bands detected at 1038, 985, 954, 543, 280 cm^{-1}. Otherwise, also some traces of αI-VOPO4 were detected, confirming that strong relationship between VOPO4·2H2O and αI-VOPO4: in fact, VPD could be easily transformed to αI-VOPO4, since the latter is the VOPO4 phase which is more quickly hydrated to VPP. The Raman analysis were carried out also on the VPD samples after reaction with 1-butanol either in air or in He: the spectra collected are reported respectively in Figure 4.33 and Figure 4.34.

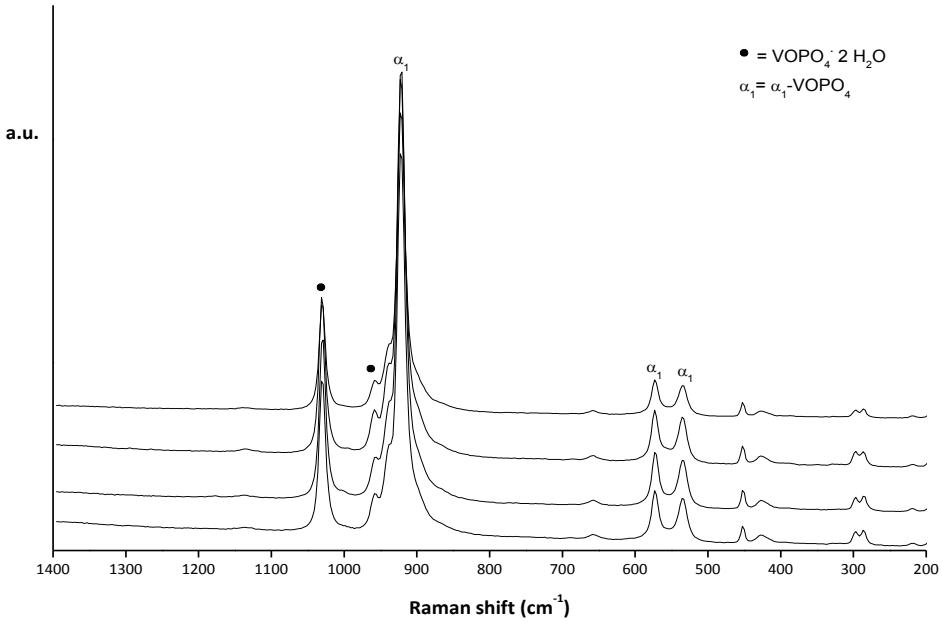

Figure 4.33: Raman spectra of spent $VOPO_4 \cdot 2H_2O$ catalyst after reactivity tests carried out feeding 1% of 1-butanol in air.

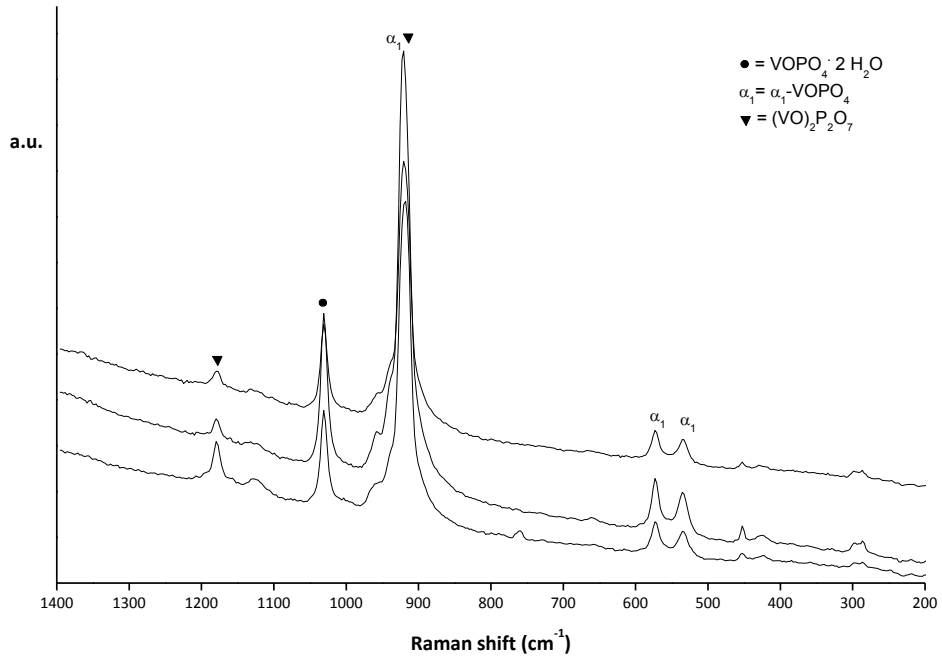

Figure 4.34: Raman spectra of spent $VOPO_4 \cdot 2H_2O$ catalyst after reactivity tests carried out feeding 1% of 1-butanol in He (different positions of analysis).

First of all, the spectra registered over the catalyst after reaction in air have shown that no substantial modifications occurred on the catalyst surface, since $VOPO_4 \cdot 2H_2O$

continued to be the main phase, with some traces of α_I-$VOPO_4$. On the other hand, even if $VOPO_4 \cdot 2H_2O$ and α_I-$VOPO_4$ were still present also in the catalyst after reaction in He, other compounds had formed, as revealed by the bands attributed to $(VO)_2P_2O_7$. The formation of VPP could be explained considering the different gas phase conditions: in fact, in the case of the reaction conducted in air, the environment was oxidizing and preserved the oxidized state of V, as demonstrate by the presence of $VOPO_4$ phases. On the opposite, when VPD was used feeding 1% of 1-butanol in He, the alcohol produced reducing conditions, that led to the formation of a reduced vanadium phase, in this case $(VO)_2P_2O_7$.

In order to confirm differences observed by Raman spectroscopy, we analyzed the VPD sample by means of X-ray diffraction. The diffractograms of the fresh and spent (after reaction) catalyst are reported in Figure 4.35.

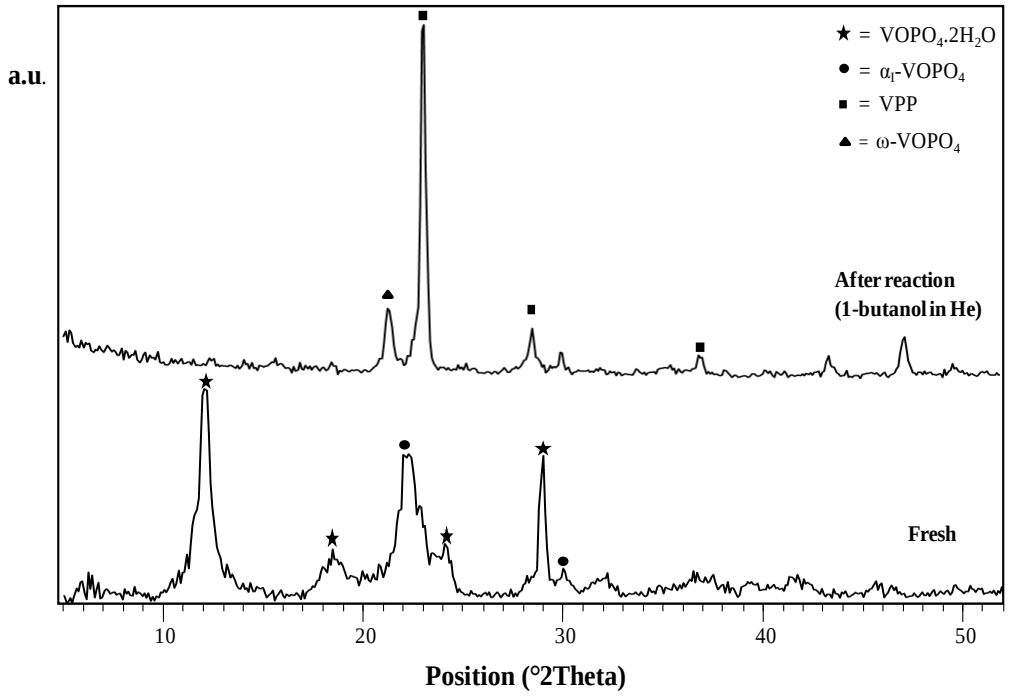

Figure 4.35: XRD diffractograms of fresh and spent (after reaction) VPD catalysts

XRD analysis confirmed what was observed in the Raman spectra: the fresh catalyst was mainly composed by $VOPO_4 \cdot 2H_2O$ and α_I-$VOPO_4$, while in the sample after reaction (in reducing condition) the $(VO)_2P_2O_7$ phase was observed.

4.2.4 Reactivity tests with vanadyl pyrophosphate DuPont catalyst

One of the peculiarity of the vanadyl pyrophosphate catalyst is its multifunctionality: in fact, the presence of strong Brønsted and Lewis acid sites [228, 229] and of redox sites represented by vanadium atoms in different oxidation states [19] has made possible the application of VPP in selective oxidations of several organic molecules, for example the oxidation of methacrolein to methacrylic acid [230], the ammoxidation of propane to acrylonitrile [231], the ammoxidation of picolines [232], the furan synthesis from butadiene [233] and the selective oxidation of decaline and tetrahydrophtalic anhydride [234]. For this reason vanadyl purophosphate furnished by DuPont was suggested also for the dehydration of 1-butanol. First al all, we investigated the reactivity of VPP in 1-butanol dehydration in inert environment, i.e. in presence of He. The results are reported in Figure 4.36.

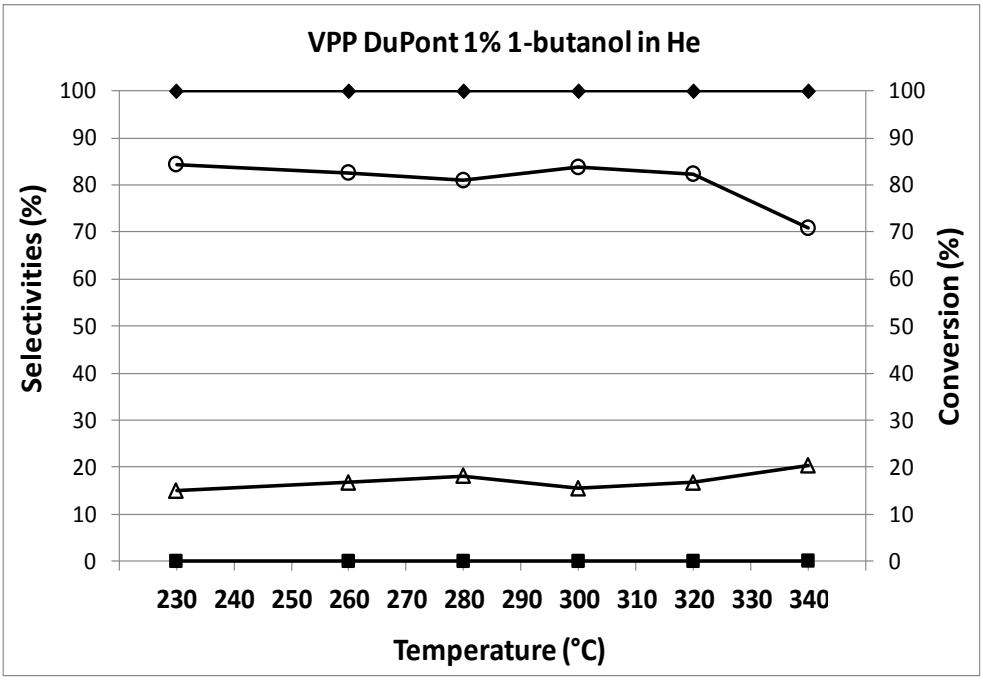

Figure 4.36: Catalytic behaviour of DuPont VPP catalyst in 1-butanol dehydration as a function of temperature. Conditions: feed 1 mol% 1-butanol in He, W/F 1.33 g·s· mL^{-1}. Symbols: 1-butanol conversion (◆). Selectivity to 1-butene (△), 2-butenes (○) and butyraldehyde (■).

The experiments have shown that the catalyst is active and it reaches the total conversion in the entire range of temperature explored; moreover, it is selective to 1-butene and 2-butenes, with minor amount of butyraldehyde. In particular, vanadyl pyrophosphate is more active than VPD (Figure 4.27), as demonstrated by the total conversion of 1-butanol obtained even at low temperature. This is due to its acidity [90, 91], that is probably higher than that one shown by VPD: the acidity of VPP favours the dehydration of 1-butanol, leading to better catalytic performances.

In order to investigate if these performances are stable during time on stream or if deactivation occurs, the reactivity of the catalyst was examined at 260°C as function of the reaction time: the results are reported in Figure 4.37.

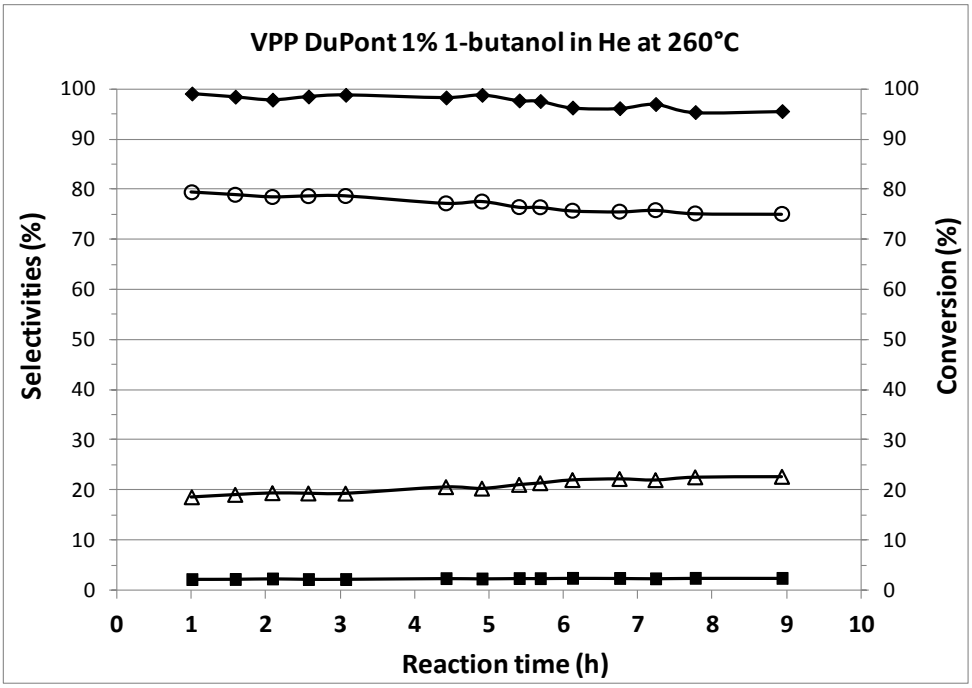

Figure 4.37: Catalytic behaviour of DuPont VPP catalyst in 1-butanol dehydration as a function of reaction time. Conditions: feed 1 mol% 1-butanol in He, W/F 1.33 g·s· mL^{-1}. Temperature: 260°C. Symbols: 1-butanol conversion (◆). Selectivity to 1-butene (△), 2-butenes (○), butyraldehyde (■).

The experiments have confirmed that not only VPP is active but also that it does not deactivate as fast as VPD in the same conditions: in fact, the value of conversion decreased only from 99% to 95% after 9 hours of reactions. Despite this, still the

deactivation shown is non-negligible. This is an interesting result, since vanadyl pyrophosphate catalyst exhibits acid and redox properties, it could be a promising catalyst for the "one-pot" reaction to maleic anhydride from 1-butanol. For this reason we decided to carried out the study of the catalytic behaviour in presence of air, as function of the reaction time at 260°C: the results are reported in Figure 4.38.

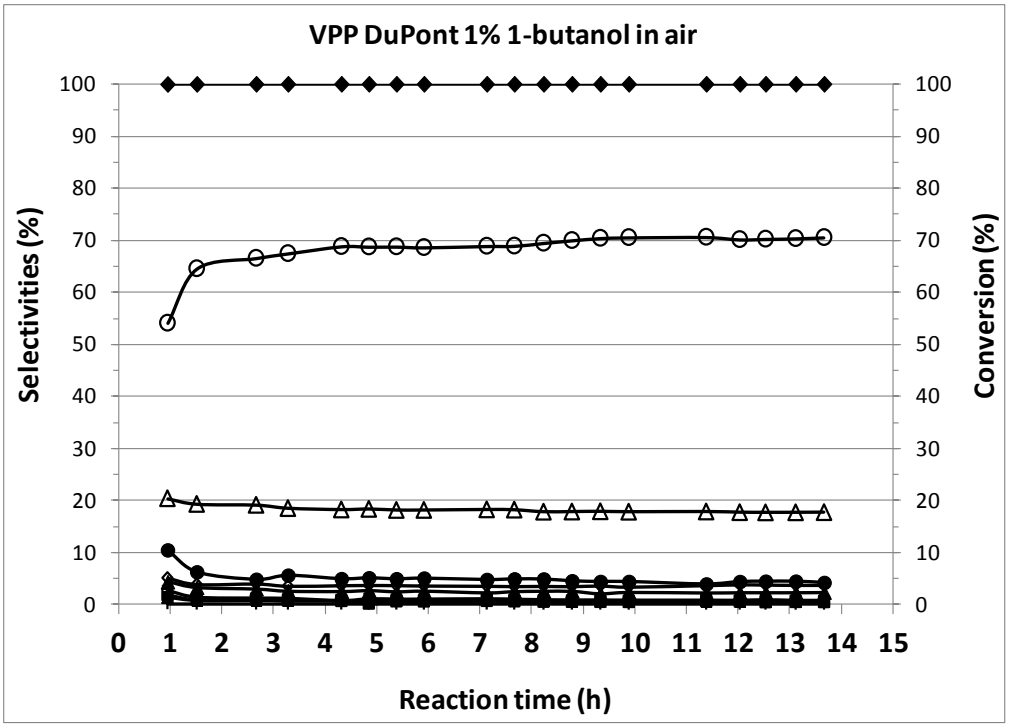

Figure 4.38: Catalytic behaviour of DuPont VPP catalyst in 1-butanol dehydration as a function of reaction time. Conditions: feed 1 mol% 1-butanol in air, W/F 1.33 g·s· mL^{-1}. Temperature: 260°C. Symbols: 1-butanol conversion (◆). Selectivity to CO (▲), CO_2 (●), 1-butene (△), 2-butenes (O), acetic acid + acrylic acid (◇), maleic anhydride (MA) (■), phtalic anhydride (PA) (□), butyraldehyde (✕), furan (+).

Figure 4.38 shows that the catalyst now has a stable catalytic behavior, with no deactivation, as it was for the VPD catalyst under the same reaction conditions. However, it was clearly less selective than the VPD, because of the greater formation of by-products such as butyladehyde and other oxygenated compounds.

Concluding, the best performance, in terms of both catalyst stability and selectivity to butenes, was shown by the VPD catalyst in oxidizing conditions.

4.2.5 1-butanol oxidehydration to MA with vanadyl pyrophosphate DuPont catalyst

The reactivity tests carried out with DuPont vanadyl pyrophosphate in the dehydration of 1-butanol has demonstrated that the material could be used to produced butenes in presence air with interesting results. Since VPP is a multifunctional catalyst, we decided to investigate if it could be utilized also for the "one-pot" configuration to produce directly MA from 1-butanol, i. e. it could catalyze the dehydration of 1-butanol and the selective oxidation of butenes to MA.

4.2.5.1 Thermal reactivity experiments: blank tests

First, we carried out experiments aimed at studying the reactivity of 1-butanol in the gas phase, without any catalyst, both with and without oxygen. Figure 4.39 shows the results obtained in the presence of oxygen; the empty space in the reactor was filled in with inert material (steatite). The range of temperatures chosen for the experiments was that typically used for butene oxidation to MA, that is, between 300°C and 400°C. Under aerobic conditions, with the feed composition used, 1-butanol already converted completely at 370°C.

Figure 4.39 shows the main products obtained, i.e. butenes, butyraldehyde, CO and CO_2; the latter prevailed at 400°C, while olefins were the dominant products at the intermediate temperature of 350°C. However, the overall selectivity to these compounds was largely lower than 100% at 300°C, whereas it was close to 80% at 350, 370, and 400°C. In fact, many other by-products formed, especially at low temperature (these compounds were not quantified individually): formaldehyde (which showed an increasing yield with the rise in temperature), formic acid, acetic acid, acrylic acid, tetrahydrofuran, dihydrofuran, 1-propanol, propionaldehyde, dibutylether, and the butyl esters of formic acid, acetic acid, propionic acid, and butanoic acid; other olefins were propylene, isobutene, and butadiene.

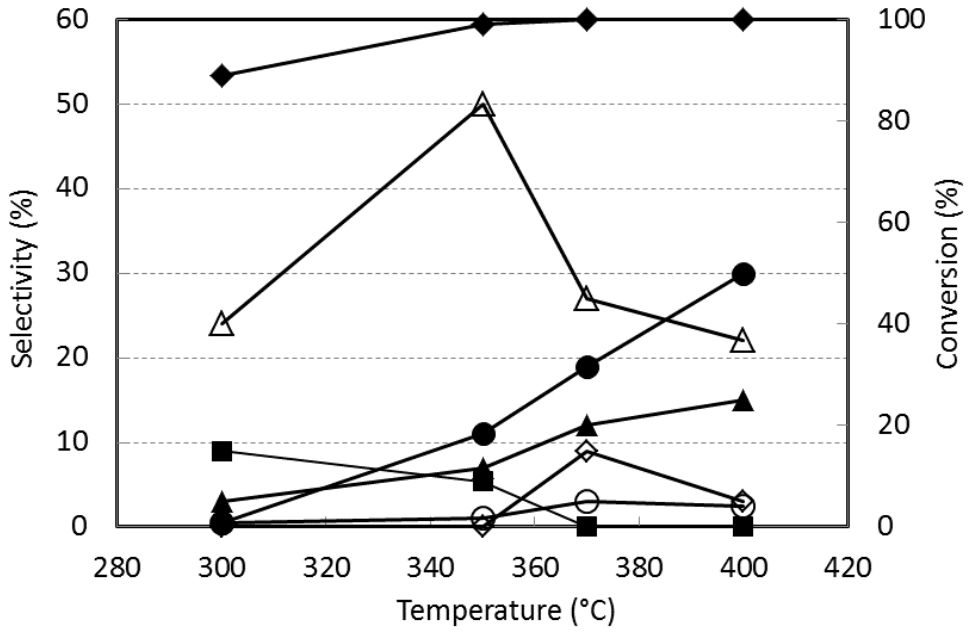

Figure 4.39: Catalytic behaviour of the "inert" (steatite) used in chemical-1-butanol (CB) oxidehydration as a function of temperature. Conditions: feed 1 mol% 1-butanol, 20% O_2, remaining: N_2. Symbols: 1-butanol conversion (◆). Selectivity to butenes (△), butadiene (○), acetic acid + acrylic acid (◇), CO (▲), CO_2 (●), and butyraldehyde (■).

The overall amount of these by-products was considerably lower at T ≥ 350°C than at 300°C; those which formed in greater amounts at both temperatures were propionaldehyde, tetrahydrofuran, and butylformate. Moreover, 2-butenal, benzene, and 2-ethylacrolein (compounds which, however, did not form at 300°C) were also observed. At 400°C, the only by-products obtained (besides those shown in Figure 4.39) were: acrolein, furan, acetic acid, methylvinylketone, tetrahydrofuran, and benzene. These results indicate that 1-butanol is extremely reactive and transforms into a wide range of oxidised compounds, which are typically observed in gas-phase radical oxidations; the presence of a solid in the reactor may facilitate the occurrence of these reactions, especially those involving the oxidative transformations of both the reactant and the products intermediately formed.

When the same experiments were carried out with an oxygen-free feed, but with steatite always filling the reactor, 1-butanol conversion was 40% at 300°C, 88% at 350°C and 98% at 400°C; the prevailing products were butenes (overall selectivity 56%, 68% and 78% at 300, 350 and 400°C, respectively), whereas the selectivity to

butyraldehyde was always lower than 3%. It may be concluded that in the temperature range examined, the thermal dehydrogenation of 1-butanol occurs only to a minor extent; in the presence of oxygen, however, the formation of butyraldehyde becomes much greater. On the other hand, the thermal dehydration of 1-butanol is very common under all the conditions examined.

Because of the significant contribution of the "inert" material used to fill the void in the reactor, we compared the catalytic behaviour obtained with steatite and that shown either in the presence of corundum – another material typically used as an inert filler for catalytic experiments in lab-scale reactors – or without any inert material at all. In the latter case, the aim is that of highlighting the contribution of homogeneous reactions, due to the fact that the glass walls of the reactor should not contribute to 1-butanol conversion. Figure 4.40 compares the results obtained with steatite (data taken from Figure 4.39) and corundum in an empty reactor, at 370°C.

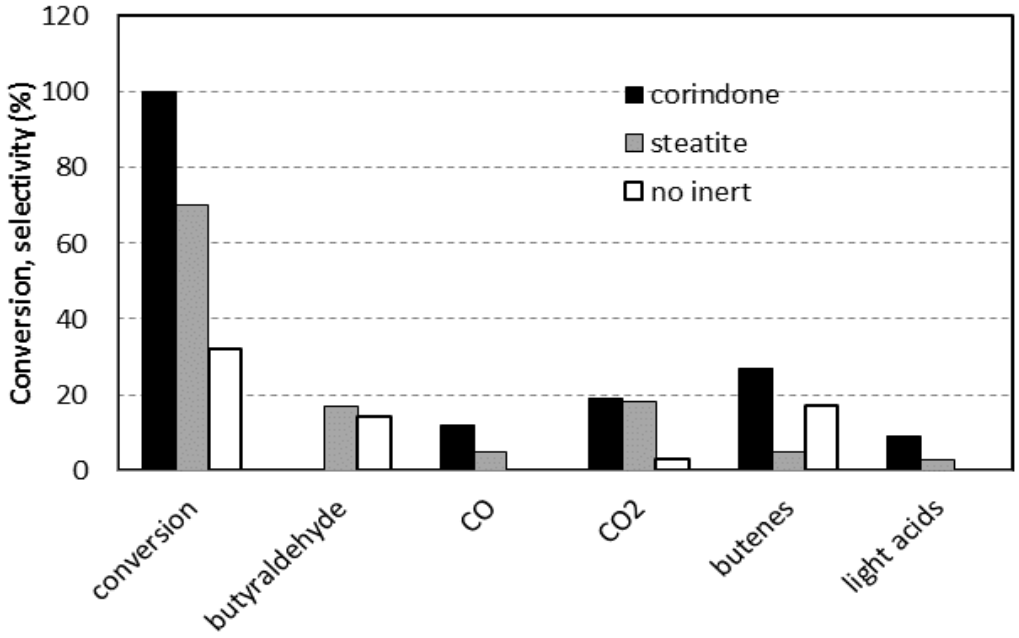

Figure 4.40: Results of reactivity experiments as a function of the inert material filling the reactor (with no catalyst). Conditions: feed 1 mol% 1-butanol, 20% O_2, remaining: N_2. Temperature 370°C.

It can be seen that, with the empty reactor, 1-butanol conversion was lower than that recorded when the inert was filling the reactor. The nature of the products formed was similar in the three cases, but with a different relative amount of the various

compounds. Based on these results, it was decided not to fill the empty space in the reactor with any material during catalytic experiments; since the main role of the inert material was that of inducing the heating of the gaseous flow before reaching the catalytic bed, we modified the set-up of the reactor's pre-treatment inlet feed, in order to achieve an efficient gas feed heating even without the inert material.

The most important outcome of these experiments is that, in order to be selective to MA, a catalyst for 1-butanol oxidative dehydration working in an oxidising atmosphere has to be very efficient in 1-butanol dehydration, in order to further enhance the rate of 1-butene formation with respect to dehydrogenation, thus limiting the parallel formation of butyraldehyde; the latter is the precursor of several of the many by-products identified, but cannot be transformed into MA. Furthermore, butyraldehyde must also be very efficient in 1-butene oxidation into MA. This suggests that vanadyl pyrophosphate (VPP) – the catalyst used industrially for *n*-butane oxidation to MA – is the possible candidate catalyst for this reaction, since not only is VPP selective in butene oxidation into MA [191, 192], but it is also characterised by the acidic properties needed for alcohol dehydration [89, 235]. In fact, 1-butanol has been previously used in some studies as a possible reactant for MA synthesis [236, 237], for the purpose of demonstrating the polyfunctional characteristics of VPP.

4.2.5.2 The effect of temperature

After the blank tests it was possible to choice the best inert filler and the best reactor configuration, so the catalytic tests were carried out using corindone and not filling the empty space of the reactor above the catalytic bed. Vanadyl pyrophospate catalyst furnished by DuPont was suggested as the candidate to study the one-pot oxidehydration of 1-butanol to MA. At first, the reactivity was investigated feeding 1% 1-butanol in air with residence time W/F=1.33 $g \cdot s \cdot ml^{-1}$: Figure 4.41 reports the results obtained using the VPP catalyst, while varying the reaction temperature.

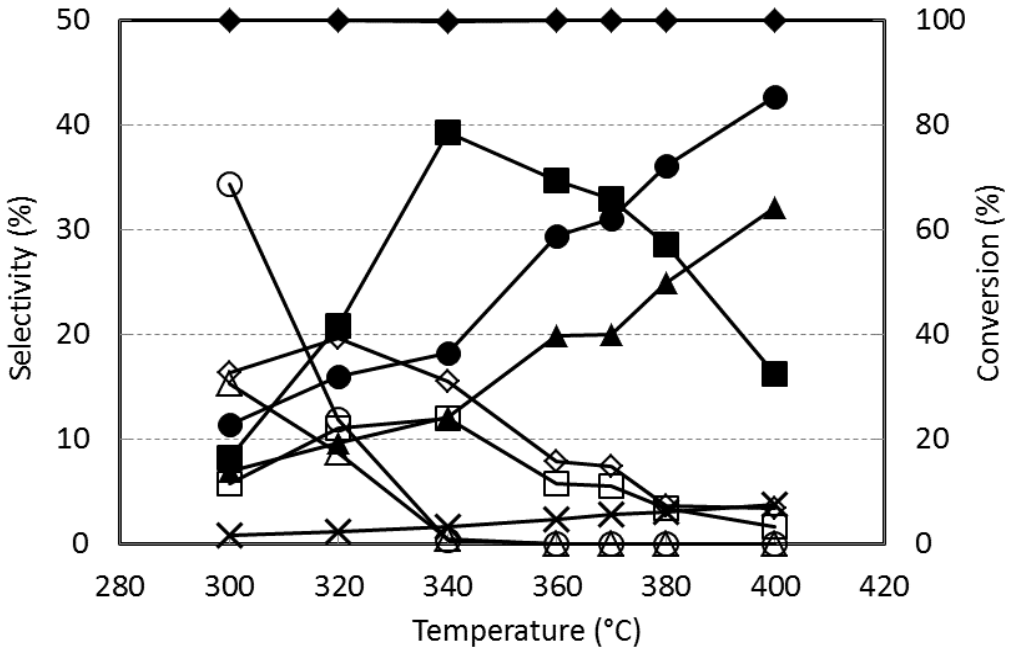

Figure 4.41: Catalytic behaviour of the VPP DuPont catalyst in chemical-1-butanol oxidehydration as a function of temperature. Conditions: feed 1 mol% 1-butanol, 20% O_2, remaining: N_2; W/F 1.33 g·s·mL^{-1}. Symbols: 1-butanol conversion (◆). Selectivity to Maleic Anhydride MA (■), 1-butene (△), 2-butenes (○), acetic acid + acrylic acid (◇), CO (▲), CO_2 (●), Phthalic anhydride PA (□) and "lights" (×).

Under the conditions chosen, the conversion of 1-butanol was completed over the entire range of temperature investigated; products obtained were MA, light acids (acrylic and acetic acid), carbon oxides, phthalic anhydride (PA), and minor amounts of other oxygenated compounds: furan and formaldehyde. Butenes formed at 340°C with a molar ratio between the two positional isomers that was different from the equilibrium value; the latter is close to 3.7 at 330°C for 2-butenes/1-butene molar ratio [217], whereas the experimental one was close to 2 at 300°C, and to 1 at 320 °C and 340°C. The decrease in the molar ratio shown at increasing temperature and the concomitant formation of MA and PA suggest that the isomerisation of 1-butene, the primary product of 1-butanol dehydration, into 2-butenes is slower than the consecutive oxidation occurring upon the olefins, and that 2-butenes are more quickly oxidised than is 1-butene.

The formation of PA, with a maximum yield of 12% shown at 340°C, may occur via a Diels-Alder reaction between the intermediately formed butadiene and MA. In the

case of *n*-butane oxidation, the formation of PA becomes important only under the conditions of surface saturation due to the coverage of active sites by olefinic intermediates, an event that – with the VPP catalyst – only occurs under alkane-rich feed conditions [238, 239, 240]. Under these circumstances, the over-reduction of the V sites leads to the prevailing occurrence of bimolecular reactions, such as the cycloaddition of MA and butadiene, with a minor contribution of olefin oxidation to produce more MA. However, it is worth remembering that, in the case of *n*-pentane oxidation to MA and PA, the mechanism proposed did not involve any Diels-Alder reaction between pentadiene and MA, but rather the oxidation of dialkylaromatics, which are formed by olefin dimerisation, oxidative dehydrocyclisation. and aromatisation [241, 242, 243]. Therefore, it cannot be ruled out that even in the case of 1-butanol oxidation, the formation of PA may indeed occur by the oxidation of *o*-xylene, the latter being formed by the oxidative dehydrocyclodimerisation of butenes. Indeed, it is worth noting that during 1-butanol oxidation the butadiene selectivity recorded was very low, i.e. less than 1%, over the entire temperature range examined (for example, it was 0.2% at 340°C). Even though butadiene can be oxidised to MA, if butadiene were the key reaction intermediate for MA and PA formation, it would have formed in a greater amount, since the reactivity of butenes (which were formed in large amounts, see Figure 4.41) over VPP catalyst is not much different from that of butadiene (both are by far more reactive than *n*-butane) [27, 191, 192].

The highest selectivity to MA was observed at 340°C (39%); in the range 300-340°C, the increase in MA selectivity occurred with a concomitant decrease in selectivity to butenes, whereas at higher temperatures, the MA selectivity decline was due to the prevailing formation of CO and CO_2. Acetic and acrylic acids also formed in relatively high amounts, with a maximum overall selectivity close to 20% at 320°C; the two compounds formed in similar amounts. Butyraldehyde selectivity was very low (e.g. 0.1% at 340°C).

These results indicate that at low temperatures the prevalent reactions were: i) the transformation of 1-butanol into butenes, and ii) the oxidative cleavage of either alcohol or olefins into acetic acid and acrylic acid. When the temperature was raised,

butenes were transformed into MA and PA, whereas the light acids were oxidised into CO_x.

4.2.5.3 The effect of contact time

In order to investigate the scheme of reaction and identify the primary and the secondary products, catalytic tests at different contact times were carried out. The temperature chosen was 340°C, i.e. the condition where the DuPont catalyst showed the highest MA yield. Figure 4.42 plots the effect of contact time on catalytic performance, at 340°C.

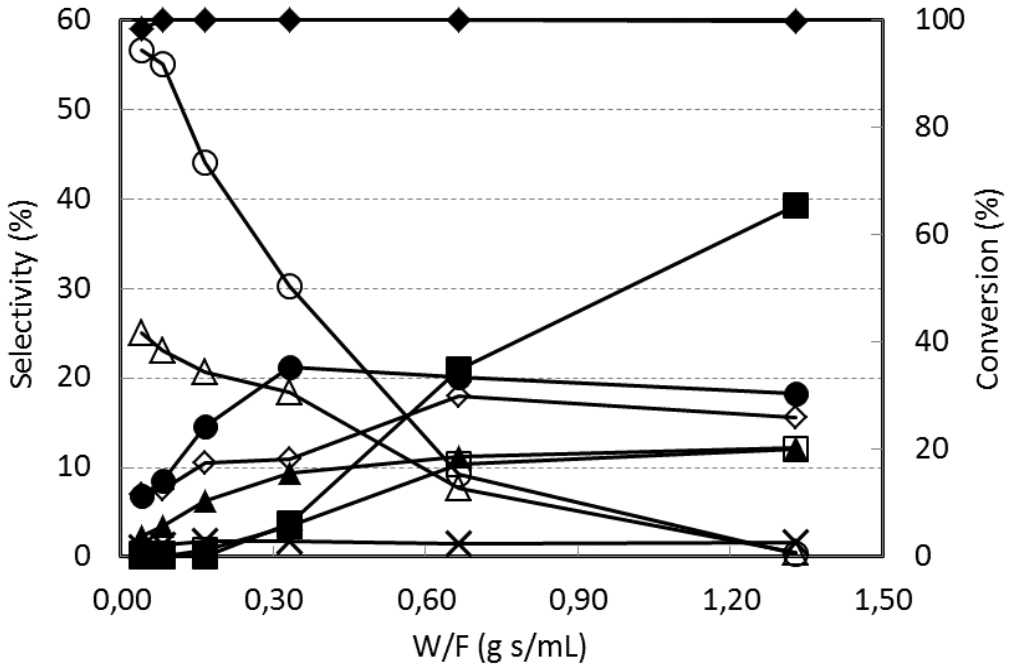

Figure 4.42: Catalytic behaviour of the VPP DuPont catalyst in chemical-1-butanol oxidehydration as a function of the W/F ratio. Conditions: feed 1 mol% 1-butanol, 20% O_2, remaining: N_2; temperature 340°C. Symbols: 1-butanol conversion (◆). Selectivity to Maleic Anhydride MA (■), 1-butene (△), 2-butenes (○), acetic acid + acrylic acid (◇), CO (▲), CO_2 (●), Phthalic anhydride PA (□) and "lights" (×).

From these experiments, the kinetic relationship between butenes and both MA and PA is apparent; in fact, the selectivity to both olefins declined when increasing the contact time, while – at the same time – the selectivity to MA and PA increased. The

molar ratio between 2-butenes and 1-butene decreased from a value close to 2.2 (a value which still is lower than the thermodynamic one), shown for a very short contact time, to a value close to 1. This is a further proof that the isomerisation of 1-butene to butenes is relatively slow at low temperatures, under conditions at which the rate of the consecutive oxidation is negligible. Thereafter, when either the temperature or the contact time is increased, the consecutive oxidehydrogenation into MA occurs at a faster rate on 2-butenes than on 1-butene.

The selectivity to butadiene (not shown in the figure) also decreased, but remained always lower than 1%, even for very short contact times. It can also be seen that the conversion of 1-butanol was less than 100% (but close to 98%) only for extremely short contact times. A surprising effect was that in the W/F range between 0.6 and 1.3 $g \cdot s \cdot mL^{-1}$, the only consecutive reaction was the transformation of butenes into MA, whereas the formation of all the other products, including CO_x and PA, did not show any further increase. This may be due to the fact that under conditions in which the surface coverage is small, because of the low amount of residual butenes, the catalyst becomes very selective in the oxidation of butenes into MA. In other words, the optimal conditions for the VPP catalyst should be those in which a high O_2/(1-butanol + olefins) ratio makes it possible to maintain a clean and selective surface, with a relatively abundant concentration of "free" oxidising sites. These hypotheses will be confirmed by the experiments described below. Another somehow surprising result is that the initial selectivity – that is, the selectivity extrapolated to nil conversion – was almost zero for CO and CO_2. This means that the parallel combustion of 1-butanol gives a marginal contribution to the formation of these compounds, at least at 340°C, whereas the major contribution derives from the consecutive overoxidation of butenes.

4.2.5.4 The effect of oxygen partial pressure

Considering the results obtained in the catalytic experiments in function of contact time, it could be hypothesized that the selective path to MA and PA, instead of the unselective one to CO_x and acids, was function of the availability of V^{5+} sites on the

catalyst surface. This means that when the consecutive transformation of butenes to MA is not kinetically favoured, a great amount of butenes keep adsorbed on the catalyst surface, occupying the active sites and giving a lowering in MA yield; on the other hand, when olefins are converted to the oxidized products rapidly, the concentration of free active sites is higher, giving and enhancement of the catalytic performances. In order to deeply investigate the role of oxidized vanadium sites experiments varying the oxygen partial pressure were carried out. Figure 4.43 shows the effect of oxygen molar fraction on catalytic behaviour.

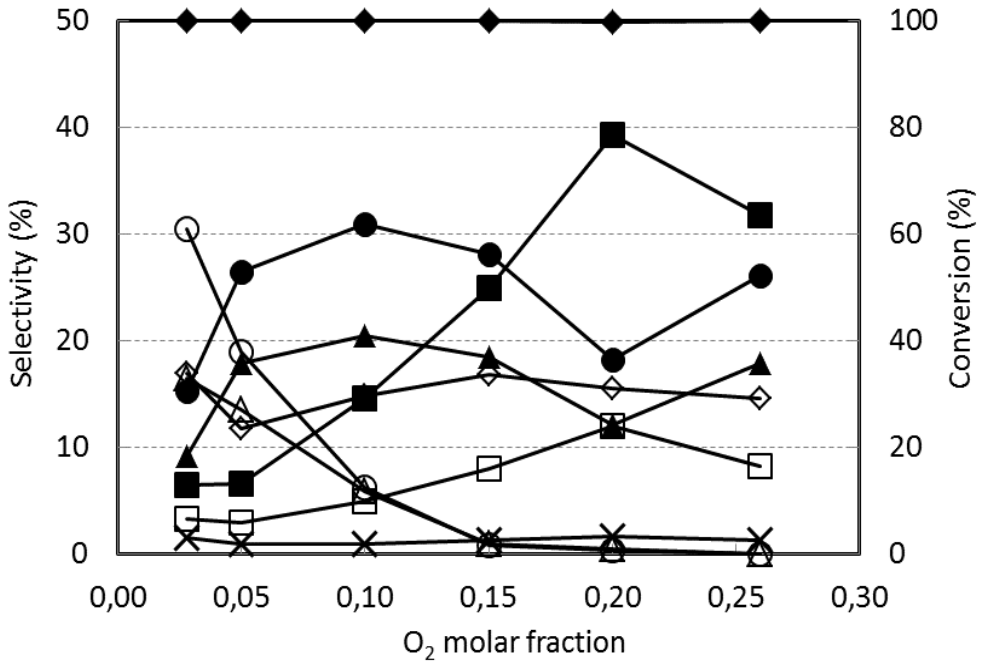

Figure 4.43: Catalytic behaviour of the VPP DuPont catalyst in chemical-1-butanol oxidehydration as a function of the O_2 molar fraction. Conditions: feed 1 mol% 1-butanol; temperature 340°C, W/F 1.33 g s mL^{-1}. Symbols: 1-butanol conversion (◆). Selectivity to Maleic Anhydride MA (■), 1-butene (△), 2-butenes (○), acetic acid + acrylic acid (◇), CO (▲), CO_2 (●), Phthalic anhydride PA (□) and "lights" (×).

Clearly, an increase in the O_2 content led to an increase in both MA and PA selectivity, whereas there was no effect on light acid selectivity (this was confirmed by repeated experiments carried out by increasing and decreasing the temperature; this behaviour turned out to be fully reproducible). Selectivity to CO and CO_2 increased slightly in the range 0.04-to-0.10 O_2 molar fraction, then decreased until the O_2 molar

fraction was equal to 0.20 (at the latter conditions the maximum MA and PA selectivity of 39 and 12%, respectively, was recorded); lastly, both increased again when the O_2 molar fraction was equal to 0.26. It is evident that both low (less than 0.10 molar fraction) and high (more than 0.20) oxygen partial pressure lead to poor selectivity either because of the prevailing selectivity to olefins, or because of the dominant CO and CO_2 formation. Therefore, there is a range where the increased O_2 partial pressure shows a strongly positive effect on both MA and PA yields, because of the decreased selectivity to butenes (precursors for MA and PA formation) and CO_x (formed by the consecutive overoxidation of both MA and PA). It is important to note that such an effect is not observed in the reaction of MA synthesis by *n*-butane oxidation: in this case, in fact, the interaction between the reactant and VPP surface is very weak. Therefore, the saturation of the catalytically active surface is shown only for very high *n*-butane partial pressure (under the so-called hydrocarbon-rich feed); otherwise, being the concentration of adsorbed olefins very low, there is a large availability of oxidising Vanadium sites. In fact, the best selectivity to MA from *n*-butane was observed with the lowest O_2/alkane molar ratio in the feed, when different feed compositions were compared under differential conditions [244]. This could also explain why, under normal conditions, PA forms in traces only during *n*-butane oxidation. Instead, from 1-butene the effect of O_2 partial pressure was similar to that observed with 1-butanol, with a maximum MA selectivity obtained for a O_2/hydrocarbon molar feed ratio close to 30 [191].

In general, it may be concluded that for a consecutive reaction pattern leading in the end to CO_2, with MA and PA as intermediate products, the selectivity to these latter compounds is a function of the fraction of oxidising sites on the catalyst surface which is available under steady state conditions, the latter being, in turn, a function of both the O_2/reactant feed and the nature of the reactant [89, 191, 245].

4.2.5.5 The effect of 1-butanol concentration

As shown by the previous tests, the availability of V^{5+} sites favours the selective oxidation of butenes and butadiene to MA and PA, so theoretically an increase in the

1-butanol partial pressure should produce a reduction on MA selectivity. VPP DuPont catalyst was tested using 2% 1-butanol in function of the temperature, without varying the other reaction conditions (see Figure 4.44).

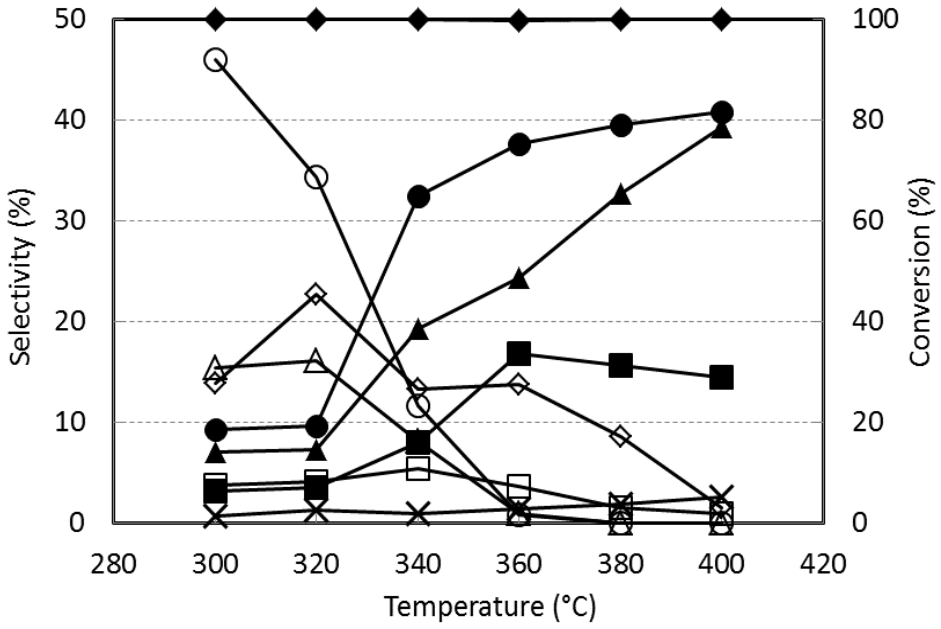

Figure 4.44: Catalytic behaviour of the VPP DuPont catalyst in (chemical)-1-butanol oxidehydration as a function of the temperature. Conditions: feed 2 mol% 1-butanol, 20% O_2, remaining: N_2; W/F 1.33 g s mL^{-1}. Symbols: 1-butanol conversion (◆). Selectivity to Maleic Anhydride MA (■), 1-butene (△), 2-butenes (○), acetic acid + acrylic acid (◇), CO (▲), CO_2 (●), Phthalic anhydride PA (□) and "lights" (×).

The results reported in Figure 4.44 have shown clearly the detrimental effect of the increase of 1-butanol partial pressure, confirming the above-stated: in fact, a comparison of tests carried out with 1-butanol-rich (2%) and 1-butanol-lean (1%) feed shows that the selectivity to both MA and PA was much lower than that seen in experiments carried out with 1% 1-butanol in the feed. In the intermediate temperature range, the selectivity to CO and CO_2 was much higher, while in the low T range the selectivity to olefins was also higher when compared to leaner 1-butanol conditions. These results indicate that, on the one hand, the dehydration of 1-butanol is hindered, again because of the surface saturation which is obviously more significant because of the higher gas-phase concentration of 1-butanol. On the other

hand, it seems that under conditions in which the availability of oxidising sites is scarce, the adsorbed unsaturated intermediates are not oxidised into MA (or PA either), but are instead preferentially transformed into CO and CO_2. It is possible that a direct attack of adsorbed olefins by gas-phase oxygen occurs: an event which has been demonstrated to contribute to overoxidation under conditions of VPP surface saturation [239, 240].

The data obtained highlight that butenes are the intermediates in 1-butanol oxidehydration into MA. Moreover, the catalytic reaction is very selective in the first step of alcohol dehydration into butenes (the initial selectivity to butenes is very high, as shown in Figure 4.41), whereas the kinetically consecutive step of butene oxidation into MA shows a limited selectivity only, because of the several side reactions. Another important result is that most of the by-products observed in thermal experiments (Figure 4.39 and Figure 4.40), are not formed during catalytic experiments. This means that either they are burnt by the catalyst to CO_x, or that the catalytic transformation of 1-butanol into butenes and of butenes into oxidised compounds prevails over thermal reactions. Clearly, a contribution of the thermal, but selective, dehydration of 1-butanol to butenes formation cannot be ruled out.

4.2.5.6 1-butene oxidation to MA

At this point it is clear that butenes are the primary products of the oxidehydration of 1-butanol, so lastly we checked the reactivity of the catalyst in 1-butene oxidation. Results are reported in Figure 4.45.

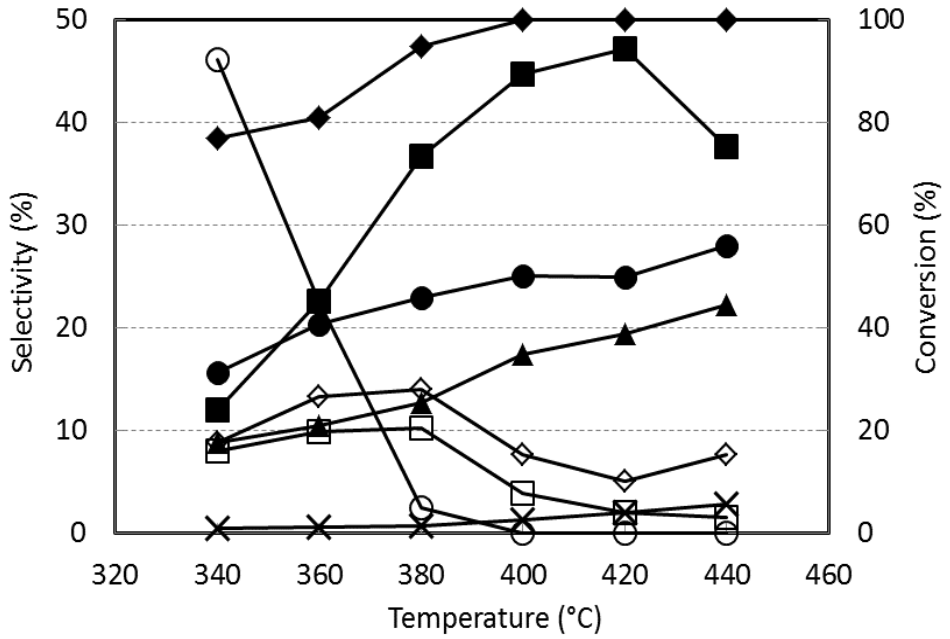

Figure 4.45: Catalytic behaviour of the VPP DuPont catalyst in 1-butene oxidation as a function of temperature. Conditions: feed 1 mol% 1-butene, 20% O_2, remaining: N_2; W/F 1.33 g s mL^{-1}. Symbols: 1-butene conversion (◆). Selectivity to Maleic Anhydride MA (■), 2-butenes (○), acetic acid + acrylic acid (◇), CO (▲), CO_2 (●), Phthalic anhydride PA (□) and "lights" (×).

At low temperature the prevailing products were 2-butenes: their selectivity, however, decreased when the temperature was raised. The highest yield to MA was 46%, slightly higher than that shown from 1-butanol (39%); it is also worth noting that the reactivity of 1-butene was slightly lower when compared to that of 1-butanol. These data can be interpreted by taking into account the different degree of interaction of the two molecules with the VPP surface. The other products obtained were the same as those from 1-butanol: PA, CO, CO_2, acetic acid and acrylic acid.

4.2.5.7 A DRIFTS study of the mechanism of 1-butanol oxidehydration

In order to understand the interaction of 1-butanol with the catalyst surface and investigate on the reaction mechanism, the alcohol was first adsorbed over VPP at 140°C; Figure 4.46 shows the spectra obtained after the alcohol adsorption using

either He or Air as the carrier (8 mL min^{-1}): the experimental conditions are reported in paragraph 3.1.4.

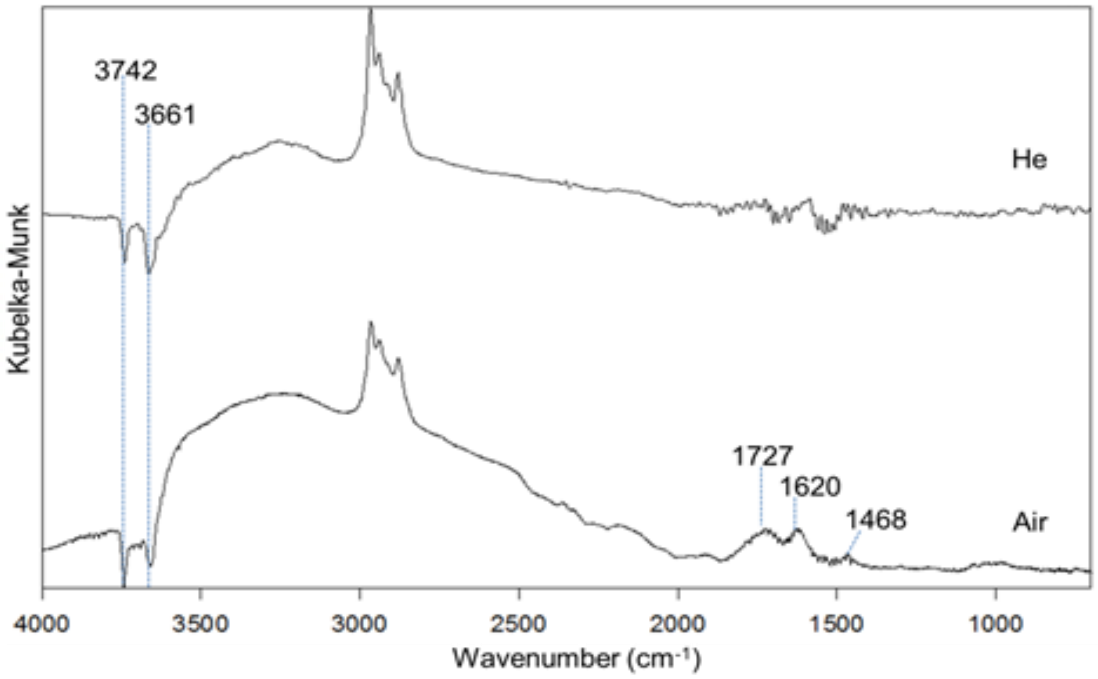

Figure 4.46: DRIFTS spectra for 1-butanol adsorption on VPP DuPont catalyst at 140°C. Carrier: He or air, flow rate 8 mL/min.

In both cases 1-butanol interacted strongly with the OH groups present on the catalyst surface as seen by the negative peaks at 3743 and 3663 cm^{-1}. The positive peaks at around 3250 and 2970-2880 cm^{-1} correspond to the OH and C-H stretching of adsorbed butanol, respectively. In the case of the oxidising atmosphere, the peaks at 1727, 1627, and 1468 cm^{-1} indicate the presence of oxidised species even at this low temperature; these bands may be attributed to either crotonic or maleic acid [246]. These experiments confirm the strong interaction of alcohol with the VPP surface, thus supporting the hypothesis of the saturation of the surface.

When the adsorption was performed at 300°C, differences among spectra recorded under different conditions were more evident (Figure 4.47).

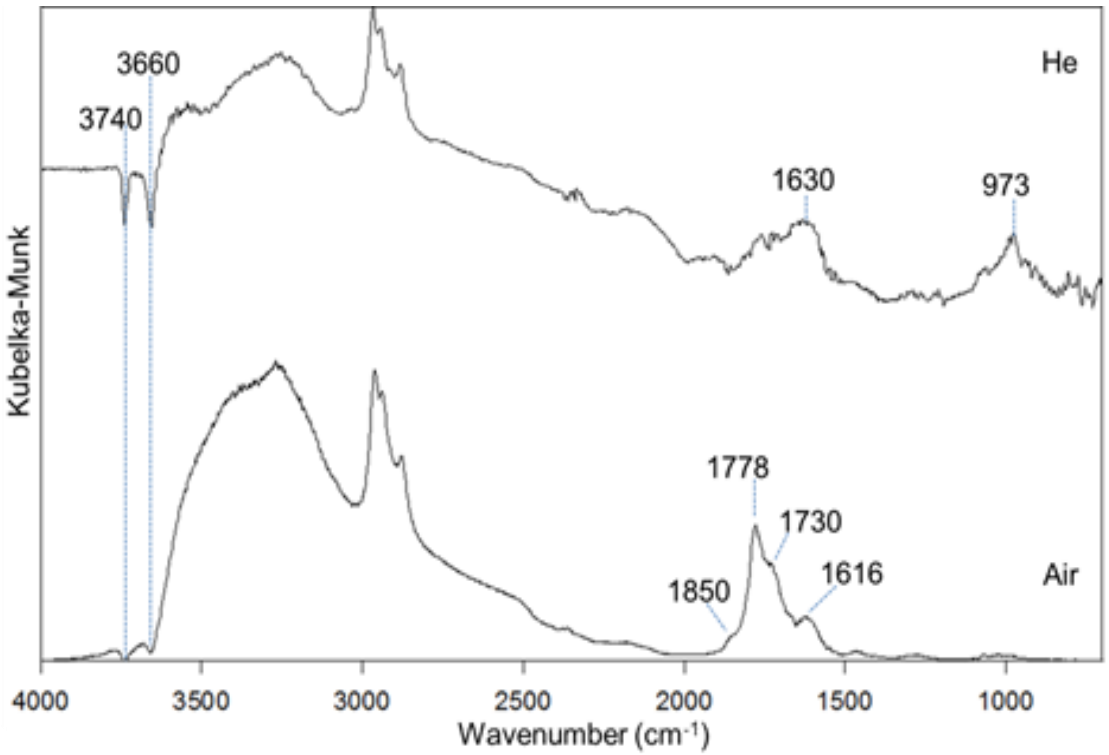

Figure 4.47: DRIFTS spectra for 1-butanol adsorption on VPP DuPont catalyst at 300°C. Carrier: He or air, flow rate 8 mL/min.

In the case of an inert atmosphere, the most important features were the negative peaks at high frequency and broad bands at around 1630 cm^{-1} and 973 cm^{-1}. The former may correspond to a C=C stretching of an olefin (butene) adsorbed on the surface, while the latter is usually attributed to a V=O stretching [247]. Therefore, in this case (when no air is present) the catalyst is able to dehydrate the butanol producing butenes, but this alters the catalyst surface. On the other hand, when air is present, olefins are also formed (butenes and butadiene in this case) but they are further oxidised as evidenced by both the sharp peak present at 1778 cm^{-1} and the shoulder at 1850 cm^{-1}, which have been attributed previously in literature to the O-C=O stretching of adsorbed MA [248]. The bands at 1730 and 1616 cm^{-1} indicate either the presence of species with a C=O and/or C=C bond, such as butyraldehyde, 2-propanal, furan, and alkenals, or some adsorbed unreacted olefins. Since there were no changes in the low frequency range, this confirms that oxygen is necessary to keep the catalyst surface species unaltered. As regards the OH interaction, clearly in

oxidant atmosphere the bands were less intense and this agrees with the fact (observed in reactivity tests) that air (O_2) is needed in order to have a less adsorbed and thus more reactive molecule, which is more quickly oxidised because of the greater availability of V^{5+} sites.

Temperature programmed desorption (TPD) experiments were also carried out. In this set of experiments, 1-butanol adsorption over VPP DuPont catalyst was performed at 140°C and then stopped to monitor the reactive transformations of the adsorbed species with temperature, either in He or in air. The evolution of the surface modifications were followed by collecting DRIFTS spectra in He (Figure 4.48) and in air (Figure 4.49).

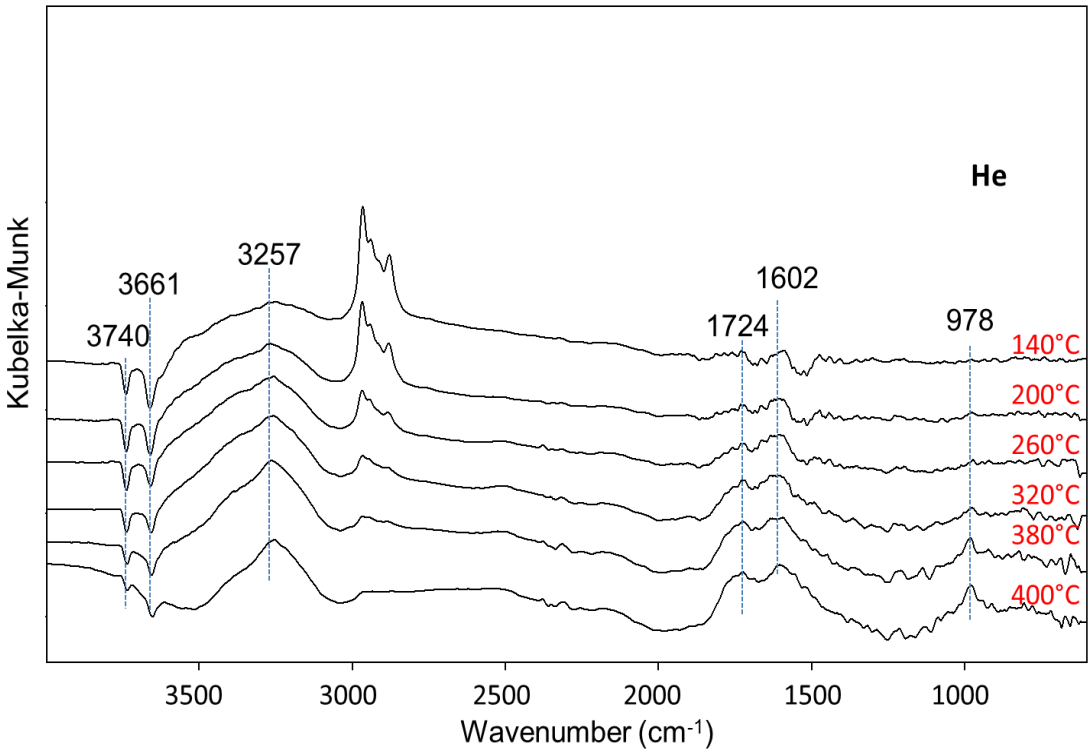

Figure 4.48: DRIFTS spectra for 1-butanol adsorption on VPP catalyst at 140°C and its desorption with temperature (TPD) in inert atmosphere (He).

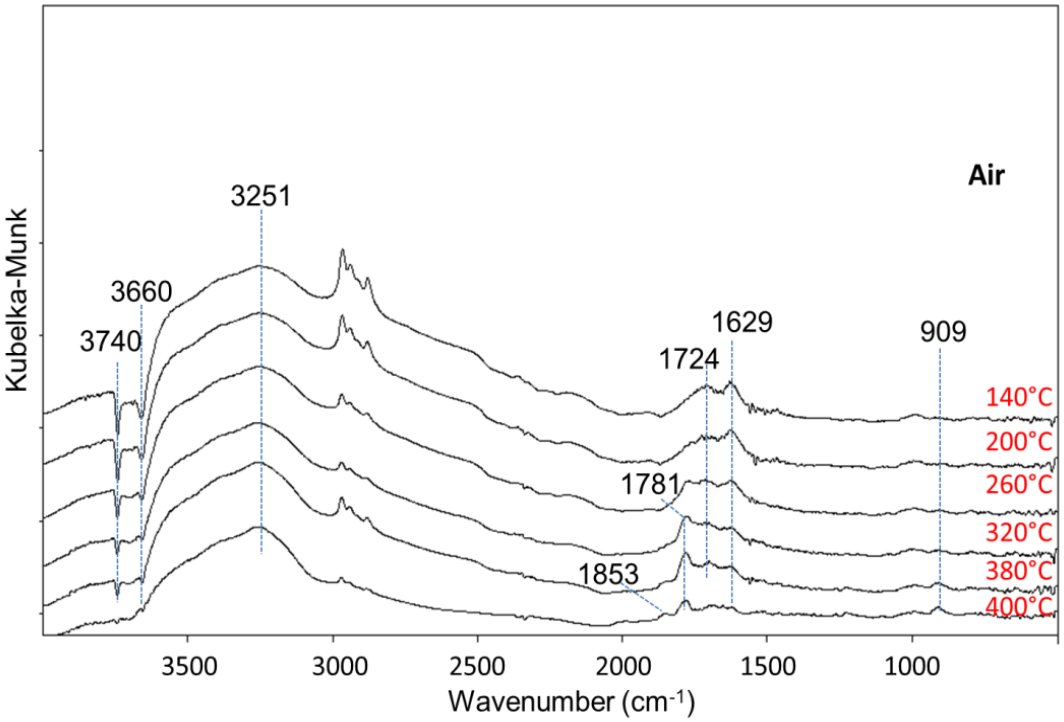

Figure 4.49: DRIFTS spectra for 1-butanol adsorption on VPP catalyst at 140°C and its desorption with temperature (TPD) in oxidising environment..

As observed from the spectra, in the case of inert atmosphere (Figure 4.48) the adsorbed 1-butanol evolved mainly towards butadiene (broad band centred at 1602 cm^{-1}) but then other olefins and carbonylic species also formed (C=C and C=O bands around 1630-1724 cm^{-1}); this occurred concomitantly with the increase of the band at 978 cm^{-1}, thus confirming that vanadyl (V^{4+}) surface species developed during the transformation of 1-butanol under inert atmosphere. The OH interaction was so strong that it was maintained throughout the whole temperature program (negative bands); in fact, a slightly decreased intensity was seen only at T>320°C. On the other hand, when air was present (Figure 4.49), oxidised carbonyl species were more readily formed, corresponding to further oxidation compounds; particularly, the bands at around 1780 and 1850 were assigned to adsorbed MA.

Therefore, it may be concluded that the catalyst under anaerobic conditions is able to dehydrate 1-butanol and oxidise olefins until crotonic or maleic acid; however, oxygen from the gas phase becomes necessary because it helps to keep the vanadium

centres effectively oxidised, while also making it possible for the intermediate to dehydrate and desorb, in the end producing MA.

Lastly, operando-mode experiments were also performed by feeding 1-butanol over the VPP catalyst at 360°C, with and without air: these results are presented in Figure 4.50 and Figure 4.51.

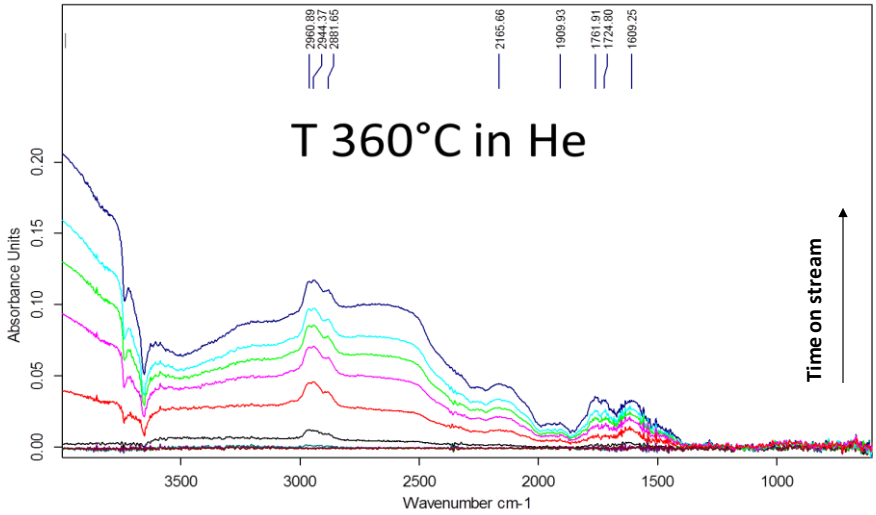

Figure 4.50: *Operando*-DRIFTS spectra collected during the feeding of 1-butanol at 360°C in anaerobic atmosphere (He) over VPP DuPont catalyst, at increasing time-on stream of adsorption.

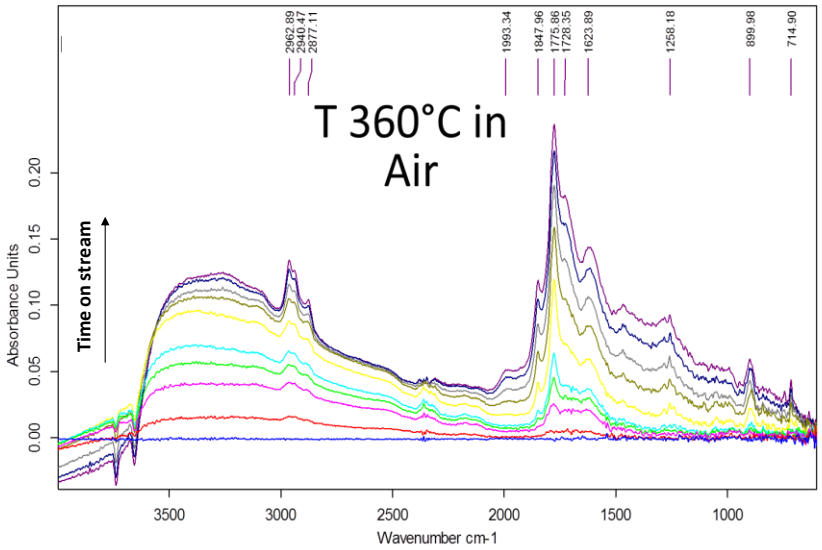

Figure 4.51: *Operando*-DRIFTS spectra collected during the feeding of 1-butanol at 360°C in air over VPP DuPont catalyst, at increasing time-on stream of adsorption.

These tests have shown not only the bands previously attributed, but also their gradually formation during time-on stream of adsorption, confirming the essential role of oxygen for the success of the reaction. Moreover, the relative amounts of the products desorbed from the catalyst surface were detected during the *operando*-tests: results are reported in Figure 4.52.

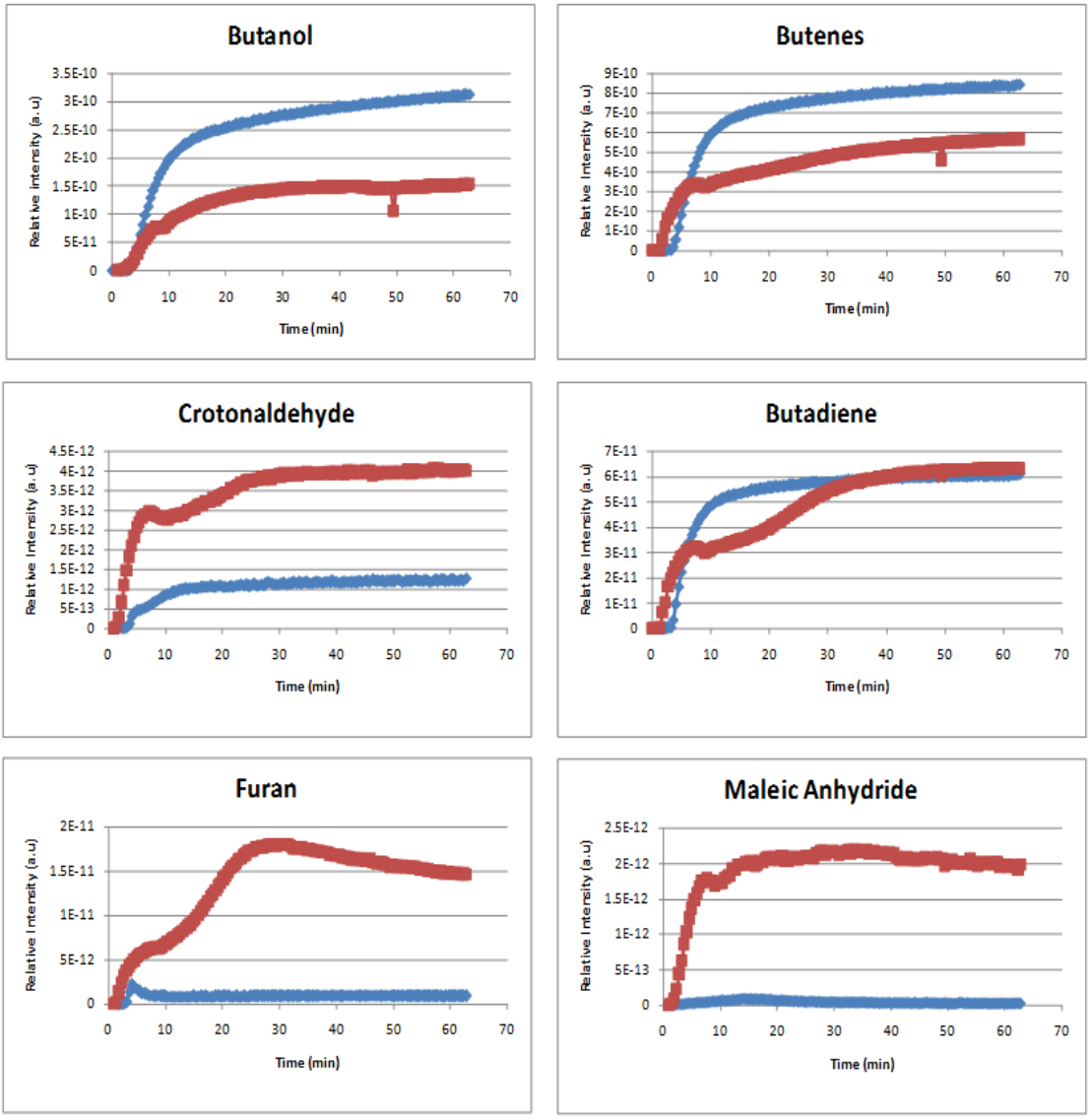

Figure 4.52: Comparison of the relative amount of the main products detected during the feeding of 1-butanol at 360°C in anaerobic atmosphere (blue) and in presence of oxygen (red).

In line with the previous tests, they confirmed that MA could be formed only when air was present; in addition, with oxygen in the feed, the relative amounts of butenes

were smaller (less accumulation), whereas those of other intermediates such as crotonaldehyde and furan, were larger.

4.2.5.8 The reactivity of intermediates and the reaction mechanism: the role of crotonaldehyde

At this point, the reactivity tests and the DRIFTS experiments have suggested that crotonaldehyde may be a key intermediate in the mechanism of 1-butanol oxidehydration to MA, in order to investigate the possible reaction mechanism. Therefore, we carried out experiments feeding crotonaldehyde (as reactant) and air over the VPP catalyst; we used a very diluted feed of the aldehyde, 0.2 mol% in air, in order to simulate the low concentration of the adsorbed compound during 1-butanol oxidation.

The results obtained are plotted in Figure 4.53; as a matter of fact, the yield to MA was close to 50%, with by-products CO, CO_2, acetic acid, acrylic acid, and furan, the latter being found at 260 and 280°C only.

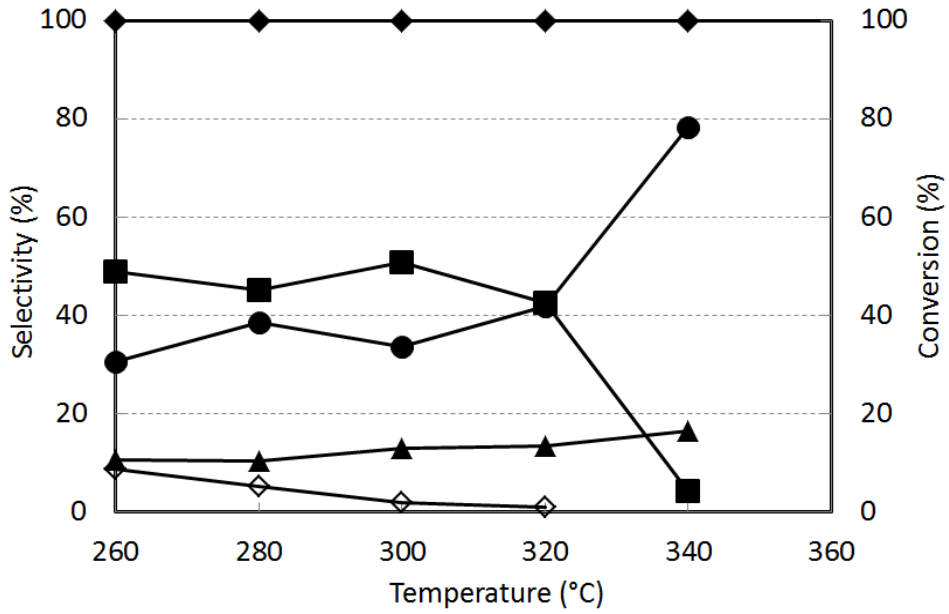

Figure 4.53: Catalytic behaviour of the VPP DuPont catalyst in crotonaldehyde oxidation in function of temperature. Conditions: feed 0.3 mol% crotonaldehyde, 20% O_2, remaining: N_2; W/F 1.33 g s mL^{-1}. Symbols: crotonaldehyde conversion (◆). Selectivity to maleic anhydride MA (■), acetic acid + acrylic acid (◇), CO (▲), and CO_2 (●).

The rapid decline in selectivity seen at 340°C – which, conversely, is the temperature at which the best selectivity to MA from 1-butanol was seen – may be ascribed to an enhanced combustion rate of crotonaldehyde. Indeed, once again the oxidation properties of VPP may be strongly affected by the reactant-to-oxygen ratio in the feed. With crotonaldehyde, which is expected to show a weaker interaction with the catalyst surface compared to 1-butanol, the use of a low crotonaldehyde-to-oxygen feed ratio may lead to a catalyst overoxidation at 340°C, which is responsible, in the end, for the high selectivity to CO_2. This hypothesis was confirmed by catalytic tests carried out in order to show the effect of the inlet molar fraction of crotonaldehyde on MA selectivity. Results are reported in Figure 4.54.

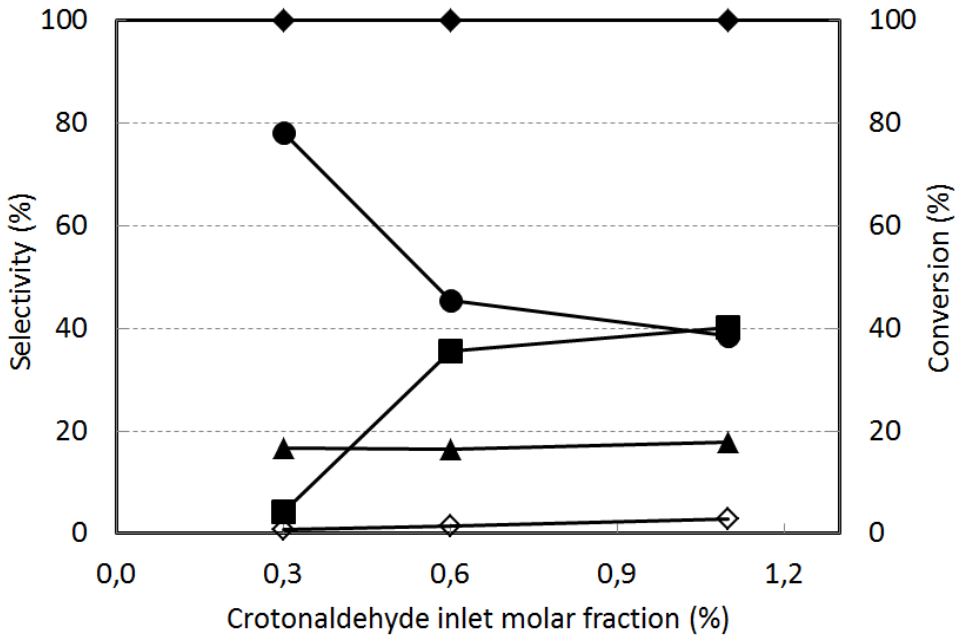

Figure 4.54: Catalytic behaviour of the VPP DuPont catalyst in crotonaldehyde oxidation in function of inlet molar concentration of crotonaldehyde. Conditions: 20% O_2, remaining: N_2; W/F 1.33 g s mL^{-1}; temperature 340°C. Symbols: crotonaldehyde conversion (◆). Selectivity to maleic anhydride MA (■), acetic acid + acrylic acid (◇), CO (▲), and CO_2 (●).

It can be seen that an increased feed ratio led to a remarkable increase in selectivity, with a yield to MA shown at a high crotonaldehyde inlet molar fraction similar to that achieved from 1-butanol under similar reaction conditions (i.e. at similar reactant-to-oxygen feed ratio).

As for the hypothesis of crotonaldehyde as the key reaction intermediate in C_4 oxidation to MA, this possibility has already been described in literature. In fact, it has been reported that crotonaldehyde can be oxidised to maleic acid by using a catalyst based on V/Mo/O supported on pumice, with 46% yield [249]. Cicmanec et al. [250] reported that, with a similar catalyst, crotonaldehyde follows two parallel pathways of oxidation, where the *trans* form is oxidised to crotonic acid, while the latter is then oxidised to MA, whereas the *cis* form is oxidised to furan; the latter may then be oxidised to MA via 2(3H)-furanone and 2(5H)-furanone intermediates. The mechanism involving crotonic acid as the intermediate in crotonaldehyde oxidation was also formerly proposed by Church and Bitha [251], using various types of V oxide catalysts. Xue and Schrader [252] suggested that in *n*-butane oxidation over VPP the main route for MA formation occurs with crotonaldehyde as the key reaction intermediate. However, it cannot be ruled out, as suggested by Wenig and Schrader [248], that the formation of crotonaldehyde or crotonic acid is due to the oxidation of butadiene and not of butene. Crotonaldehyde can also be oxidised to furan with high selectivity by using polyoxometallate catalysts [253]. Indeed, furan is another molecule which was proposed as an intermediate during C_4 oxidation with VPP catalyst. For example, Guliants et al. [236, 237] reported that the oxidation of 2-butene occurs via the formation of furan, which is then oxidised to MA with the generation of a furan endoperoxide produced by reaction with a V^{5+}-OO• species.
Through a dedicated experiment we also confirmed that furan can be oxidised with 59% yield to MA, by using 0.3% furan in air as inlet feed.

Another set of experiments was carried out using crotonaldehyde as the reactant, while varying the contact time, in order to detect the possible formation of furan as an intermediate during crotonaldehyde oxidation to MA (Figure 4.55).

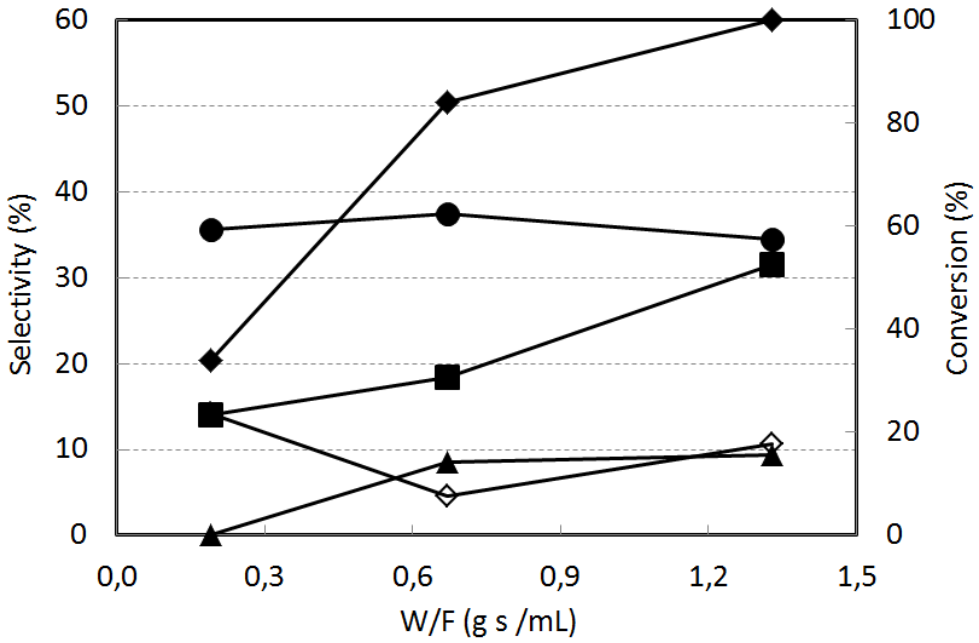

Figure 4.55: Catalytic behaviour of the VPP DuPont catalyst in crotonaldehyde oxidation in function of contact time W/F. Conditions: 0.3% crotonaldehyde, 20% O_2, remaining: N_2; W/F 1.33 g s mL^{-1}; temperature 260°C. Symbols: crotonaldehyde conversion (◆). Selectivity to maleic anhydride MA (■), acetic acid + acrylic acid (◇), CO (▲), and CO_2 (●).

Our results demonstrated that, indeed, furan forms directly from the aldehyde. However, it was also shown that the C balance was poor, especially at low values of contact time.

We characterised the used catalyst after the experiment carried out at low contact time and recorded the IR spectra by means of DRIFT spectroscopy. The analysis are reported in Figure 4.56.

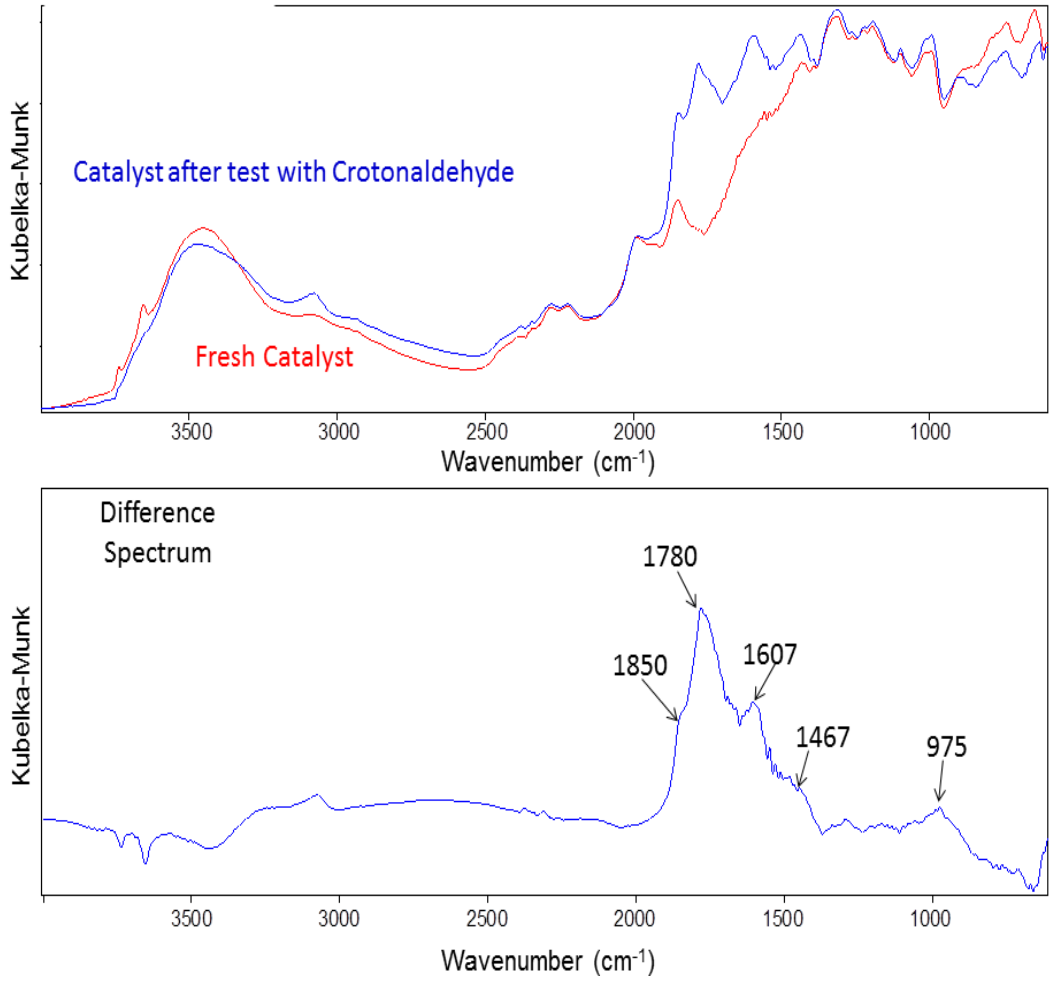

Figure 4.56: Top: Diffuse-Reflectance IR spectra of the fresh catalyst and of the spent catalyst after reactivity experiments with crotonaldehyde at 0.18 s contact time (Figure 4.55). Bottom: difference spectra.

As shown in Figure 4.56, the spectra highlighted the presence of several compounds at the adsorbed state, such as MA, crotonic acid, maleic acid, butenes and butadiene. The catalyst spent after reaction at longer contact time, conditions at which the C balance was improved, showed the presence of minor amounts of these adsorbed compounds. Therefore, at low contact time the catalyst retained adsorbed molecules which are precursors for the formation of MA: crotonic acid and maleic acid. When the contact time was increased, the selectivity to MA increased too; this was due to both the oxidation of furan - the selectivity of which in fact decreased -, and of maleic acid, which was retained on the catalyst surface at low contact time but desorbed as

MA when the contact time was increased, with concomitant improvement of the C balance.

In the following table (Table 4.1) the assignments of the main bands detected are reported.

Band, cm^{-1}	Intensity (KM)	Assigned to
1467	0,265	Crotonic acid
1601	0,515	Butadiene
1672	0,160	Butene
1725	0,322	Maleic acid
1780	0,893	Maleic anhydride
1853	0,247	Maleic anhydride

Table 4.1: Table with assignment of main bands detected in DRIFTS experiments. Band attributions were given based on refs [246, 248].

All these experiments demonstrated that the mechanism for MA formation likely occurs with crotonaldehyde as the key intermediate compound. The latter undergoes two parallel reactions of transformation, one leading to furan, and the other to maleic acid, possibly via crotonic acid. Both furan and maleic acid are intermediates for MA formation, via oxidation or via dehydration, respectively. The relative importance of the two parallel ways is likely a function of the degree of surface availability of oxidising V sites, and thus of the degree of surface coverage by adsorbed species. Another important difference is that furan desorbs easily from the VPP surface, as demonstrated by DRIFTS-MS *operando* experiments, which showed no proof for the retention of furan at the adsorbed state, while furan was detected in a relatively large amount in the gas phase. Conversely, maleic acid was strongly interacting with the catalyst surface; in order to desorb this compound it was necessary to use conditions which fostered the development of a clean and oxidised surface.

Figure 4.57 summarises the proposed reaction network for the transformation of 1-butanol to MA, as inferred by combining our DRIFTS and reactivity experimental results.

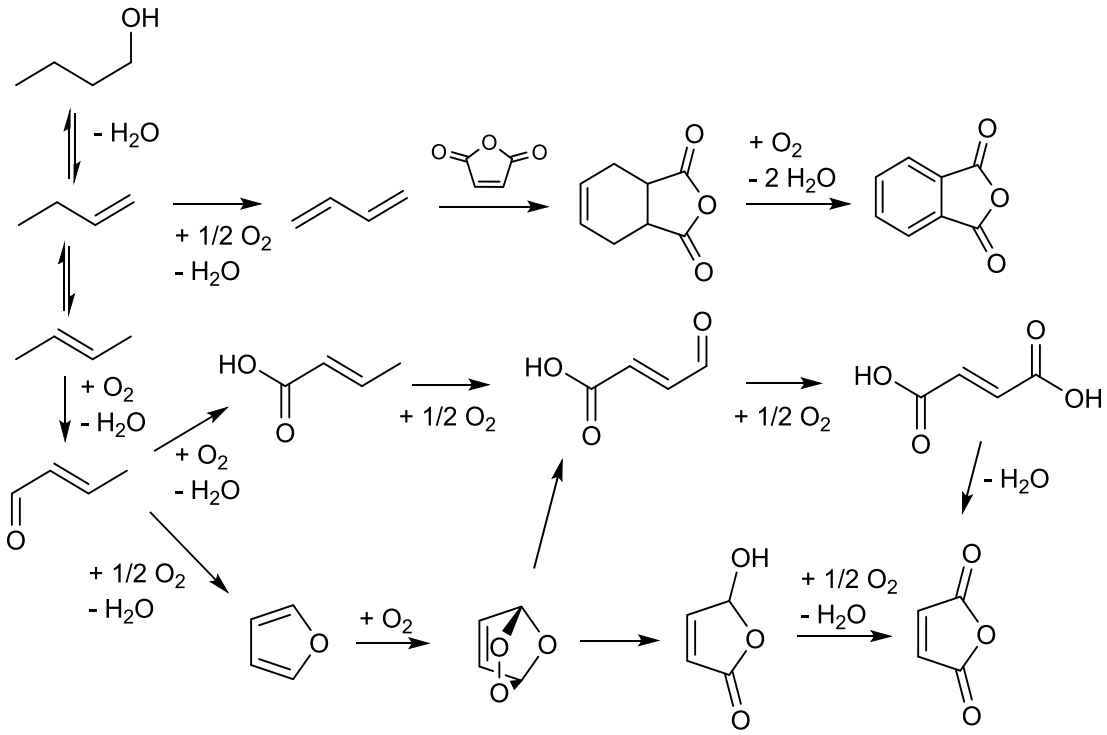

Figure 4.57: Reaction scheme for 1-butanol oxidehydration to MA.

The mechanism involves the dehydration of 1-butanol to 1-butene, the isomerisation to 2-butenes, and the oxidation of the latter to crotonaldehyde. Crotonaldehyde can either cyclises to yield furan or be oxidised until maleic acid. Maleic acid desorbs in the form of MA, whereas furan can desorb and be consecutively re-adsorbed and further oxidised to MA. It is also important to note that the endoperoxide compound formed by furan oxidation can rearrange either into 5-hydroxy-2(5*H*)-furanone [237], or 4-oxo crotonic acid, which is also a precursor of maleic acid; this way, the two parallel reactions would share the same intermediate, maleic acid, as also suggested by DRIFTS experiments.

4.2.6 Bio-butanol to maleic anhydride

After having established the effect of the main reaction parameters on catalytic behaviour using a chemically sourced 1-butanol (CB), we conducted experiments using three different types of BB, whose main impurities are shown in Table 3.1, compared with those of CB. It is important to note that all the samples had purity degrees higher than 99.5%, with a residual water content that in all cases was less than 1%; the latter is expected to have a negligible effect on reactivity behaviour, since the amount of water generated during the reaction was much greater than that present in 1-butanol. However, there were differences in the amount and type of impurities present, and the following rank of impurity contents may be assumed (as from a semi-quantitative assessment inferred from GC and GC-MS analysis): BB1 > BB2 > BB3. It is also worth noting that the pH of the aqueous solution obtained by dissolving 1 ml of BB in 14 ml of water was slightly different in the 3 samples (Table 3.1). Lastly, we also searched for metallic impurities in BB samples by means of detailed ICP and XRF analysis, but no traces of them were found.

The catalytic behaviour shown by sample BB1 (the one containing the greater amount of impurities) is reported in Figure 4.58.

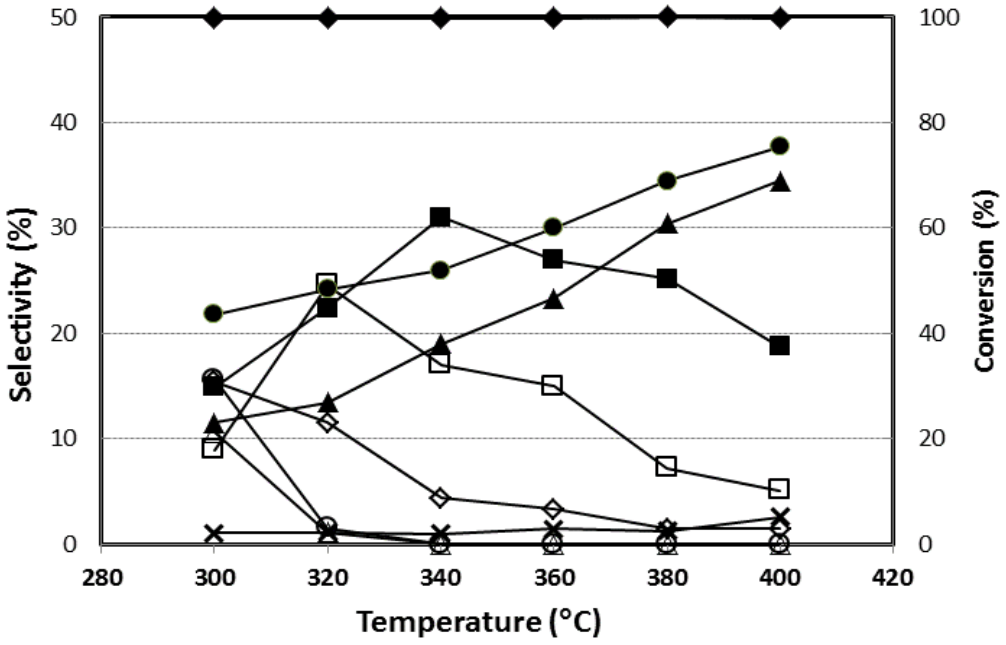

Figure 4.58: Catalytic behaviour of the VPP DuPont catalyst in oxidehydration of BB1.

Symbols: 1-butanol conversion (◆). Selectivity to Maleic Anhydride MA (■), 1-butene (△), 2-butenes (○), acetic acid + acrylic acid (◇), CO (▲), CO_2 (●), Phthalic anhydride PA (□) and "lights" (×).

A comparison with the behaviour shown by the CB sample (Figure 4.41) highlights the following differences:

- With BB1, the maximum yield to MA shown was only 31%, at 340°C (vs 39% for CB, at 340°C). On the other hand, the selectivity to PA was higher than that shown with CB; at 320°C, the PA yield was 25%, and 17% at 340°C; with CB, the PA yield was no higher than 12%. Therefore, the best overall selectivity to MA+PA, at total 1-butanol conversion, was 51% with CB, and 48% with BB1.
- With BB1, the selectivity to CO + CO_2 was greater at low temperatures, but similar (or even slightly lower) at high temperatures, compared to the selectivity obtained with CB.
- The selectivity to light acids and butenes was also lower with BB1. Moreover, traces of other by-products were found, such as lighter aldehydes, which probably formed from small amounts of alcohols other than 1-butanol, which were contained as impurities in BB.

In order to explain the drop in MA selectivity shown with bio-butanol, we monitored the performances during the time-on-stream, comparing the effect on VPP DuPont catalyst for chemical-butanol (CB) and for bio-butanol (BB1). Time-on-stream experiments are reported in Figure 4.59 and Figure 4.60.

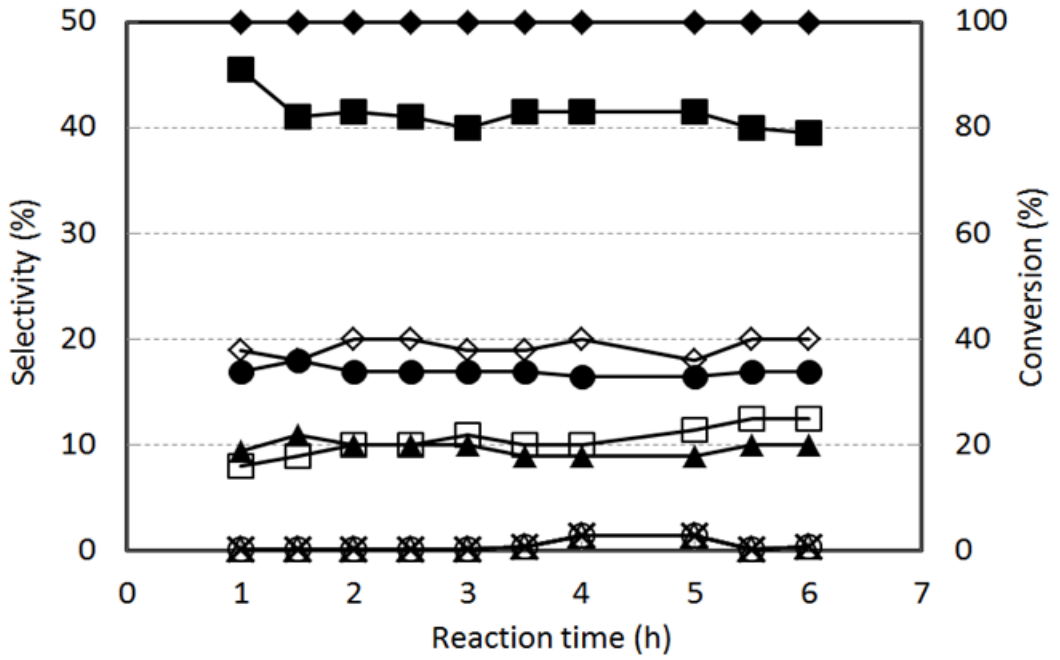

Figure 4.59: Catalytic behaviour of the VPP DuPont catalyst in chemical-1-butanol (CB) oxidehydration. Symbols: 1-butanol conversion (◆). Selectivity to Maleic Anhydride (■), 1-butene (△), 2-butenes (○), acetic acid + acrylic acid (◇), CO (▲), CO_2 (●), Phthalic anhydride (□) and "lights" (×). Temperature 340°C.

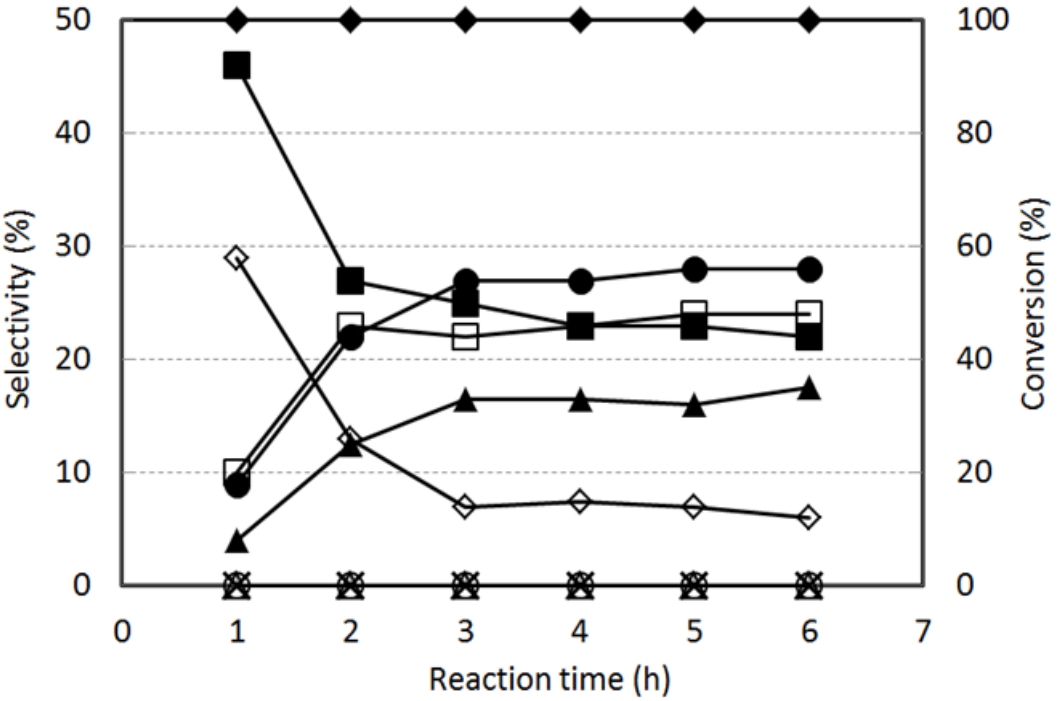

Figure 4.60: Catalytic behaviour of the VPP DuPont catalyst in bio-1-butanol (BB1) oxidehydration. Symbols: 1-butanol conversion (◆). Selectivity to Maleic Anhydride (■), 1-butene (△), 2-butenes

(○), acetic acid + acrylic acid (◇), CO (▲), CO_2 (●), Phthalic anhydride (□) and "lights" (×).Temperature 340°C.

These results demonstrated that the difference in the catalytic behaviour between the two reactants was likely related to some impurities present in BB1, which accumulated on the catalyst surface and modified the surface properties during the first hours of reaction time. In fact, the two reactants gave a similar performance at the beginning of the experiment time (reaction conditions having been fixed at 340°C); however, in the case of the CB feed, the performance remained quite stable, whereas in the case of BB1 the performance progressively changed, with a decline in selectivity to MA and a corresponding increased selectivity to PA.

It may be concluded that the progressive change in the catalyst surface characteristics had an effect mainly on the variation of the PA/MA yield ratio, but affected the overall yield to the two compounds to a lower extent; it is worth reminding that PA formed from a consecutive reaction on MA.

In regards to the nature of the impurities which might be responsible for the poisoning effect, it should be noted that most of the impurities had characteristics not much different from those of the reaction products obtained during 1-butanol oxidehydration. The only exception was a carbazole compound, whose tentatively identified formula was 5H-Naphtho[2,3-C]carbazole-5-methyl. Carbazoles are antibiotics which can be released by microorganisms during the final period of the fermentation process [254].

Lastly, the different reactivity behaviours of bio-butanols reported in Table 3.1 were tested over VPP DuPont catalyst. The first sample was BB1pur: the bio-butanol was purified to lower the impurity content, by means of adsorption over bleaching earth enriched with activated charcoal (see *Experimental*). The catalytic results are reported in Figure 4.61.

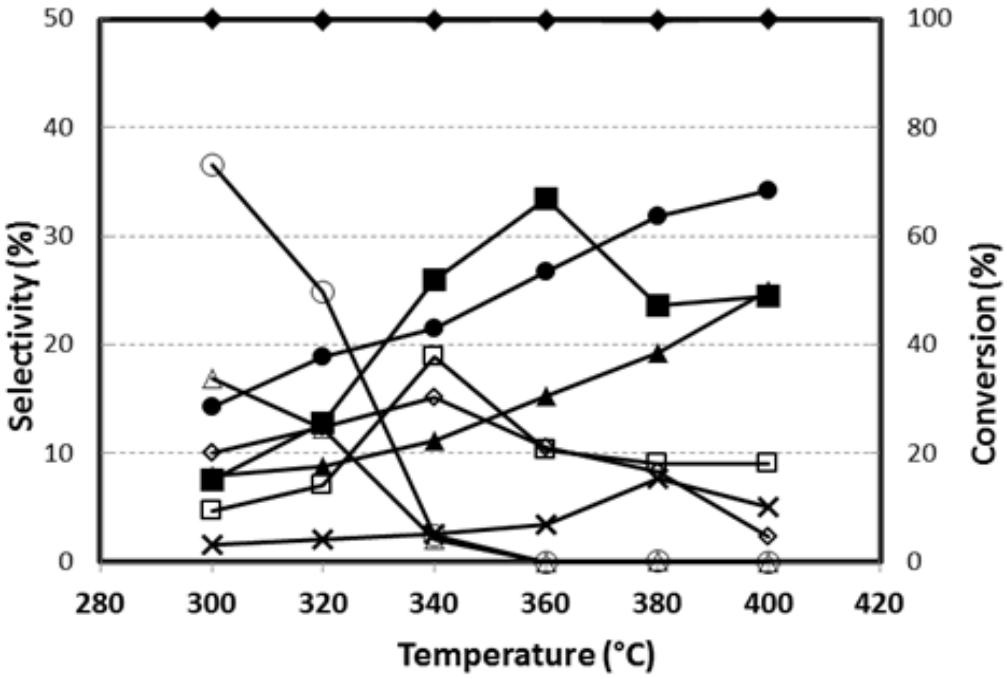

Figure 4.61: Catalytic behaviour of the VPP DuPont catalyst in BB1pur oxidehydration. Symbols: 1-butanol conversion (◆). Selectivity to Maleic Anhydride (■), 1-butene (△), 2-butenes (○), acetic acid + acrylic acid (◇), CO (▲), CO_2 (●), Phthalic anhydride (□) and "lights" (×).

Comparing these results with the test carried out with BB1, we can observe that the purification was only partially successful, since the maximum yield to MA increased from 31% at 340°C to 33% at 360°C, keeping far from the 39% of yield obtained with CB. For this reason the sample BB1 was purified again with a stronger treatment, consisting in a double amount of bleaching earth used (0.06 g instead of 0.03) and a longer time of stirring (24 h instead of 6 h): the bio-butanol obtained was named BB1-superpur. In order to check if the second purification was successful the sample BB1-superpur was tested with VPP DuPont in the same reaction condition: the results of the catalytic test are reported in Figure 4.62.

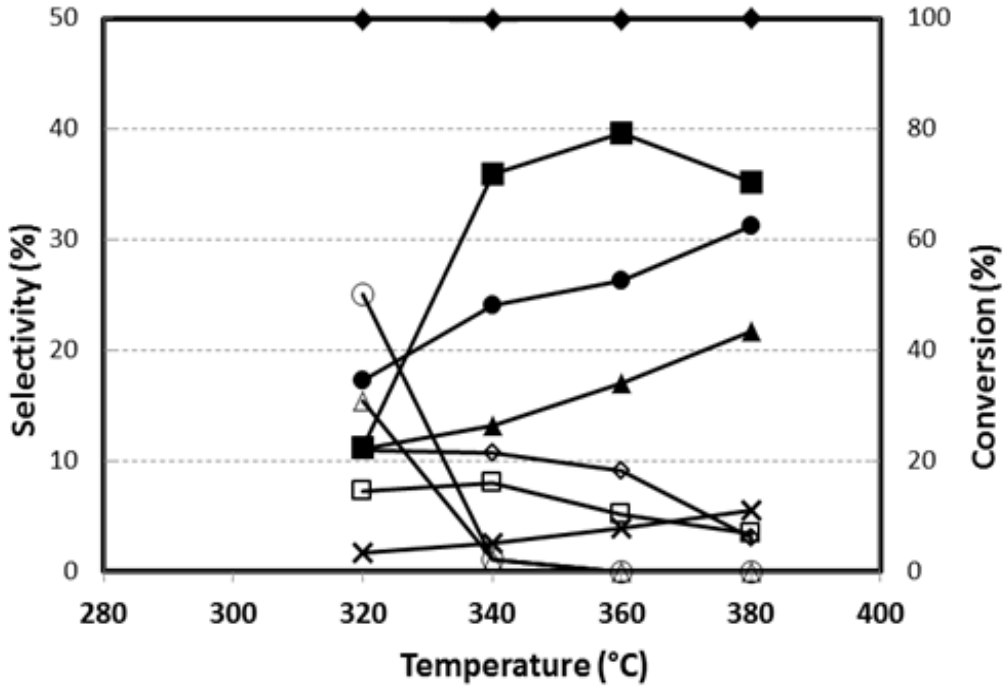

Figure 4.62: Catalytic behaviour of the VPP DuPont catalyst in BB1-superpur oxidehydration. Symbols: 1-butanol conversion (◆). Selectivity to Maleic Anhydride (■), 1-butene (△), 2-butenes (○), acetic acid + acrylic acid (◇), CO (▲), CO_2 (●), Phthalic anhydride (□) and "lights" (×).

The catalytic test demonstrated that the removal of the impurities was efficient, since at 360°C the same value of yield to MA obtained with CB was shown. This results confirmed again that the worsening of the performances shown with bio-butanol was due to the presence of some impurities which accumulates on the catalytic surface. Moreover, with an efficient purification treatment they could be removed giving results quite similar to that one obtained with CB.

We continued the reactivity experiments testing the behaviour of other two types of bio-butanol, the BB2 and the BB3: the results are reported respectively in Figure 4.63 and Figure 4.64.

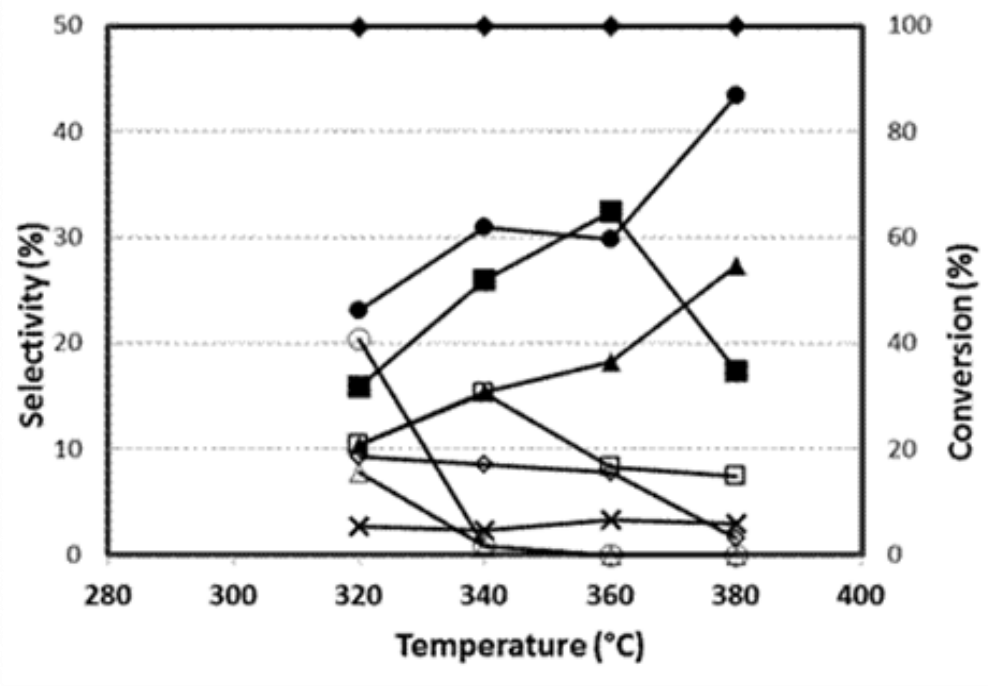

Figure 4.63: Catalytic behaviour of the VPP DuPont catalyst in BB2 oxidehydration. Symbols: 1-butanol conversion (◆). Selectivity to Maleic Anhydride (■), 1-butene (△), 2-butenes (O), acetic acid + acrylic acid (◇), CO (▲), CO_2 (●), Phthalic anhydride (□) and "lights" (×).

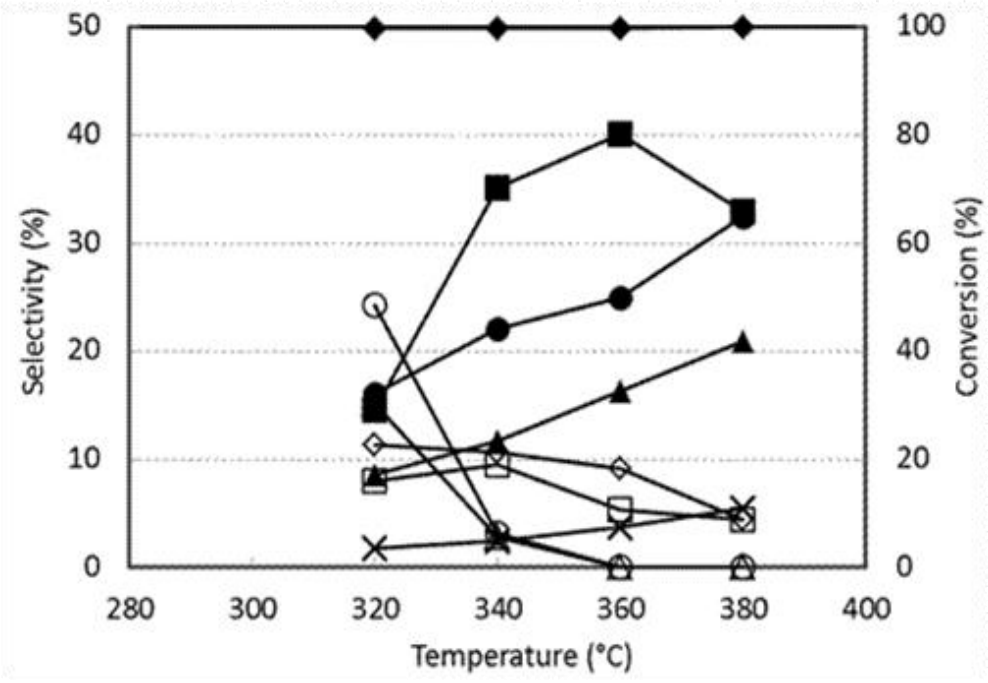

Figure 4.64: Catalytic behaviour of the bulk VPP catalyst in BB3 oxidehydration.

Symbols: 1-butanol conversion (◆). Selectivity to Maleic Anhydride (■), 1-butene (△), 2-butenes (○), acetic acid + acrylic acid (◇), CO (▲), CO_2 (●), Phthalic anhydride (□) and "lights" (×).

These samples exhibits different values of yields to MA, 32% for BB2 and 40% for BB3, both at 360°C (see Table 3.1). These results confirmed again that the presence of impurities greatly affect the catalytic response of bio-butanol over VPP DuPont catalysts.

To summarize, Figure 4.65 compares the best yield to MA and the best MA+PA yield (in all cases at total 1-butanol conversion, at 340-360°C).

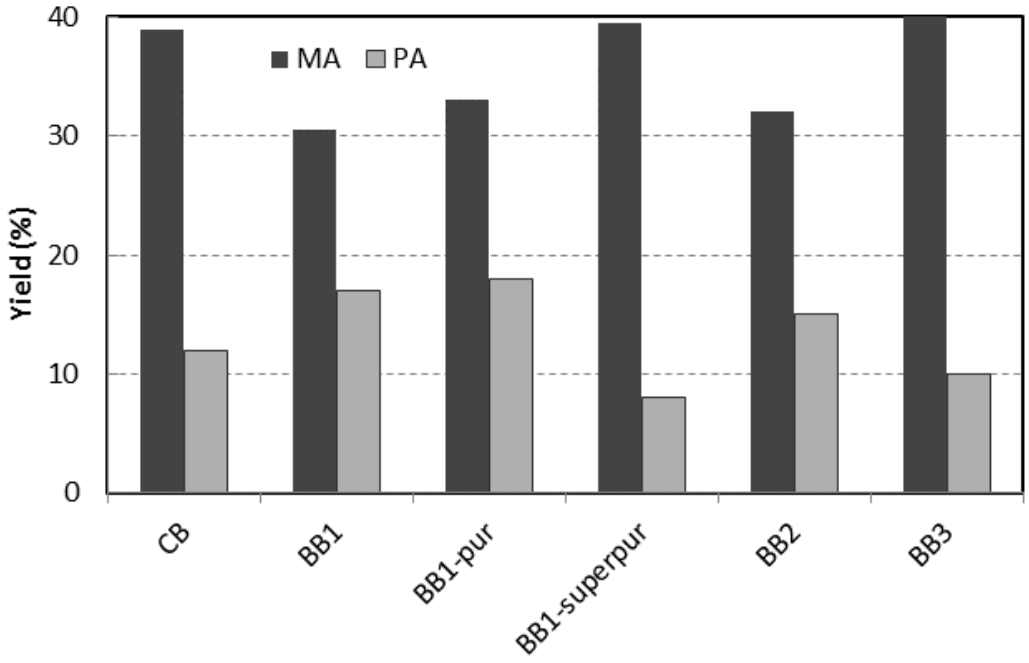

Figure 4.65: Best MA and PA yields obtained with VPP DuPont catalyst feeding either chemical 1-butanol (CB), or bio-1-butanol. Reaction conditions as in Figure 4.41.

It is apparent that samples BB1 and BB2 both led to lower yields if compared to CB, but the BB3 sample (the purest amongst the BB samples) showed a catalytic behaviour quite similar to CB. The purification of BB1 led to an increased yield to MA, with a corresponding lower yield to PA; lastly, sample BB1-superpur, which had undergone a prolonged treatment for the removal of heavier impurities, showed the same behaviour as CB.

In conclusions the impurities contained in bio-butanol affected the overall process selectivity; however, a purification treatment made it possible to obtain a yield to MA which was similar to that achieved from chemically sourced 1-butanol.

4.2.7 VPP DuPont catalyst characterization

The catalyst used for the reactivity tests with 1-butanol and bio-butanol was an industrial catalyst delivered by DuPont, composed by 90%wt. of vanadyl pyrophosphate and 10%wt. of silica. The catalyst was characterized by Raman spectroscopy, X-ray diffractometry and BET surface area analysis; the conditions are reported in the *Experimental* section. The samples were analyzed before reactivity tests (fresh) and after (spent).

Raman analysis

Raman spectroscopy is a very powerful analysis for VPO-based catalysts, because these materials are well known to show typical and well-defined Raman bands. In fact, it is possible to distinguish the main phase $(VO)_2P_2O_7$, the precursor $VOHPO_4 \cdot 0{,}5\ H_2O$ and the several V^{3+} and V^{+5} phases, in particular α_I, α_{II}, β, δ, ε, γ, ω-$VOPO_4$, and hydrated phases $VOPO_4 \cdot nH_2O$. In order to verify which kinds of phases are present on VPP DuPont catalysts, we collected a series of spectra changing the focused position over the sample. The spectra of fresh catalyst are reported in Figure 4.66. The same analysis was conducted over spent VPP DuPont catalyst: examples of the Raman spectra are reported in Figure 4.67.

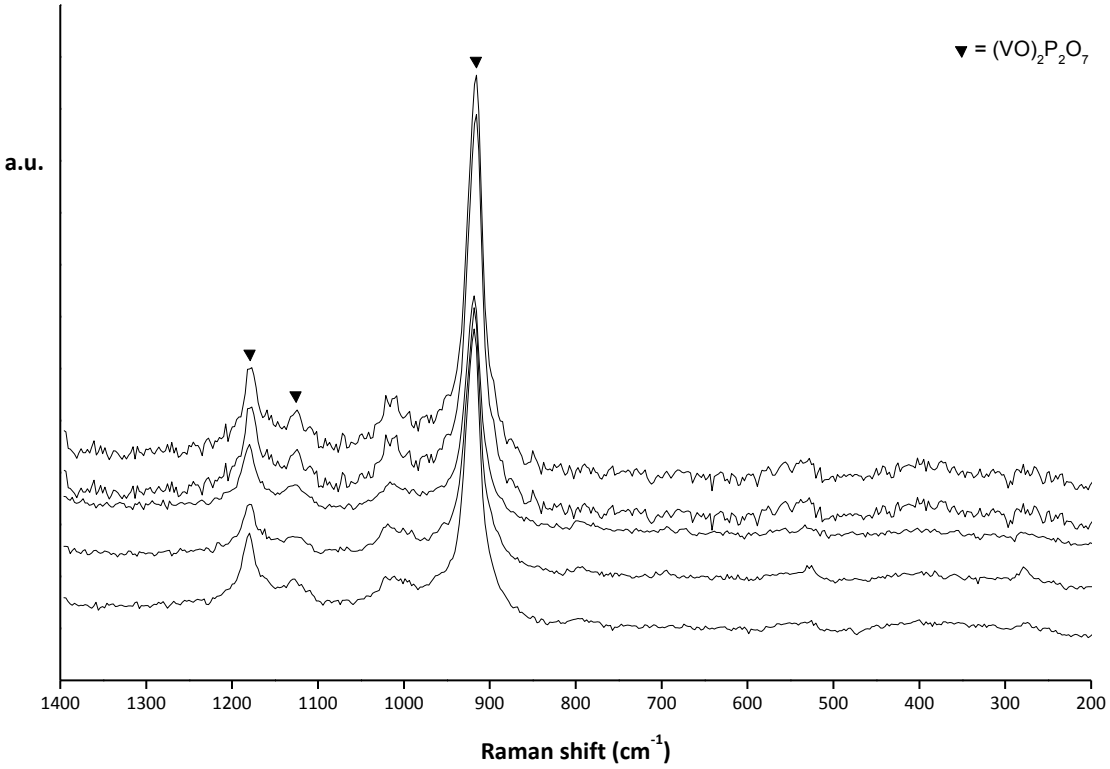

Figure 4.66: Raman spectra of fresh VPP DuPont catalyst.

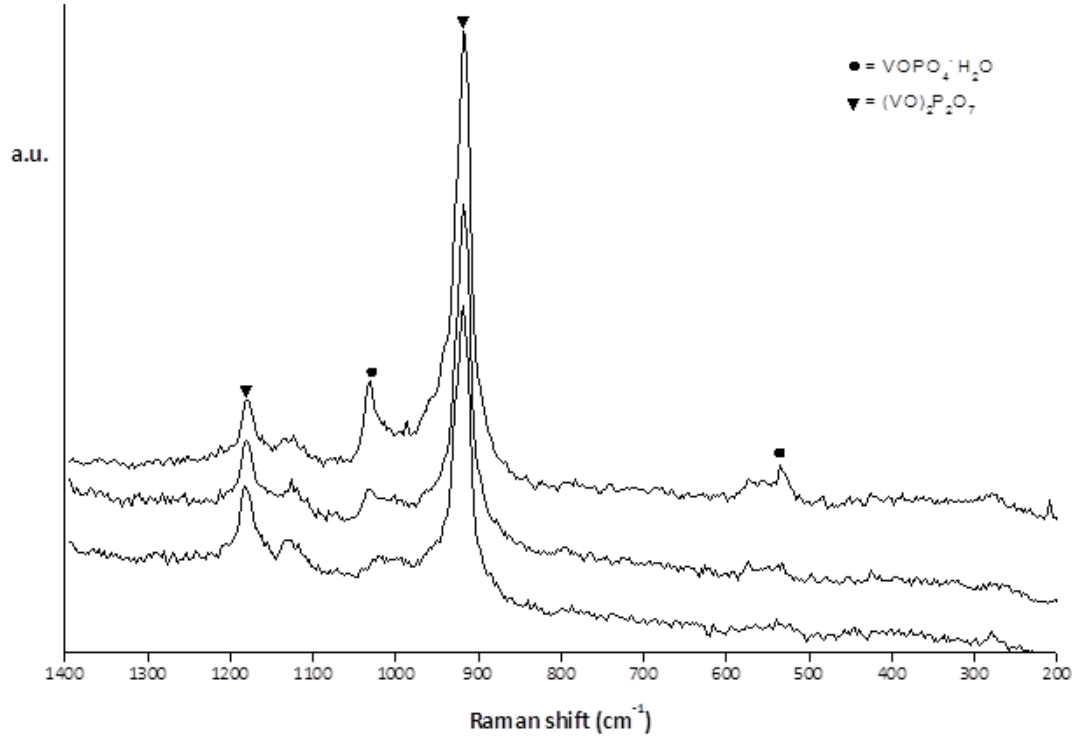

Figure 4.67: Raman spectra of spent VPP DuPont catalyst after reaction feeding 1%1-butanol in air.

As expected, the analysis on the fresh catalyst has confirmed that vanadyl pyrophosphate is the main phase, since only in few points the presence of minor amount of the oxidized and hydrated phase $VOPO_4 \cdot nH_2O$ has been detected.

The Raman spectra of the spent sample have confirmed that VPP is still the main phase, accompanied with the some traces of $VOPO_4 \cdot H_2O$: this means that the catalytic tests did not substantially change the active phase of the catalyst.

X-ray diffraction analysis

XRD-diffraction analysis on fresh and spent VPP DuPont catalyst are reported in Figure 4.68. Comparing the two diffractograms it is possible to note that the diffraction patterns are the same, confirming the predominant presence of the vanadyl pyrophosphate crystalline phase.

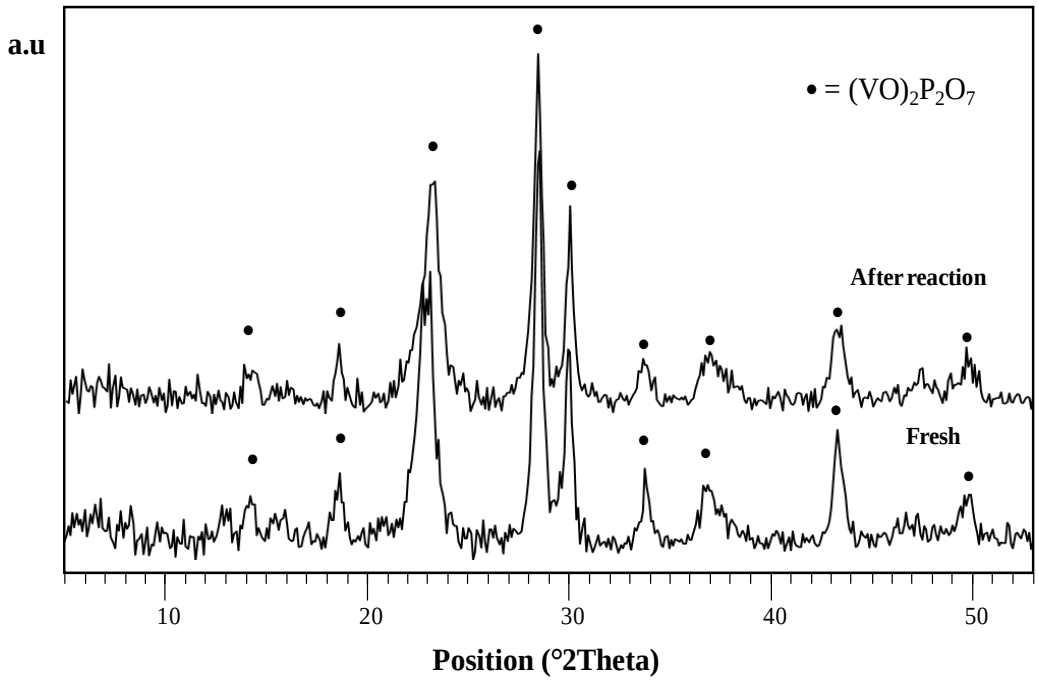

Figure 4.68: XRD diffractograms of fresh (red) and spent (blue) VPP DuPont catalysts.

BET surface area analysis

The surface area of the samples have been measured by BET method. For the fresh catalyst this value is 40 m^2/g, while for the spent one is 38 m^2/g. For this reason we can confirm that the catalytic tests have not altered the material in terms of surface area.

5 Conclusions

The synthesis of maleic anhydride (MA) has received for decades a special attention due to its commercial viability and to its demand in the global market as an intermediate chemical product. Its production has been commercialized mainly by means of the partial oxidation of *n*-butane, a process catalyzed by a vanadium-phosphorous-oxide (VPO) catalyst, typically vanadyl pyrophosphate $(VO)_2P_2O_7$. Otherwise, in recent years an increased interest to produce MA from renewable materials has been observed. In this context my PhD thesis was focused on the improvement of the selective oxidation of *n*-butane into maleic anhydride (MA), investigating the behavior the industrially-produced vanadyl pyrophosphate catalyst (VPP), and on the study of a new process for the synthesis of MA starting from a bio-based building block, 1-butanol.

The first part financially and scientifically supported by Polynt SpA dealed with the improvement of the synthesis of maleic anhydride starting from *n*-butane. The reactivity tests were carried out in order to correlate how the catalytic behavior of VPP (A catalyst) and Nb doped-VPP (X catalyst) could be affected by the reaction conditions passing from plant-scale to the lab-scale. The A and X catalysts tested in hydrocarbon-lean and rich conditions have shown that the differences between the two samples could be observed in lab-scale only when an high concentration of *n*-butane is fed. In fact, working at 1.7% *n*-butane in air (the concentration typically used in fixed-bed reactors) the two catalysts did not differ and in laboratory scale they could be considered equivalent, although their different composition. On the other hand, working at 4% *n*-butane in air (the concentration typically used in fluidized-bed reactors) the presence of Nb as dopant is needed to enhance the oxidative power of the catalyst, becoming more reducing the environment. The improvement exhibited by Nb-doped catalyst was explained by the formation of discete amount of δ-$VOPO_4$, which is known to be a selective V^{5+} phase. *In-situ* Raman analysis carried out on

both A and X catalyst confirmed that Nb enhances the formation of δ-$VOPO_4$, in fact in the un-doped catalyst the phase was obtained only in traces and through the co-feeding of water, which acted as promoter for the oxidation. In this context, the key role of water in the modifications of the catalyst surface was investigated, being steam an important co-product of the reaction. The co-feeding of steam in hydrocarbon-lean condition over the A catalyst showed to have an improving effect on the performances, since a significant increase in terms of selectivity to MA was registered.

The study of vanadyl pyrophosphate as industrial catalyst for the selective oxidation of *n*-butane to MA was continued focusing our attention on the catalyst ageing, in terms of both performances and surface modification of the material. The gradual deactivation of vanadyl pyrophosphate was monitored by reactivity tests and by Raman spectroscopy: the analysis demonstrated that the ageing is a complex process characterized by the formation of different V/P/O-based phases and by the retention of adsorbed organic compounds that could alter the accessibility to the active sites. More in details, the formation of the vanadyl metaphosphate $VO(PO_3)_2$, hydrated phases ($VOHPO_4 \cdot nH_2O$), β-$VOPO_4$ and coke deposits occurred. The presence of vanadyl metaphosphate, characterized by a P/V ratio twice than the VPP one, indicated that one of the effect of the ageing is the phosphorus surface enrichment and it is one of the causes of the significant drop in activity registered. Together with $VO(PO_3)_2$ phase, also the unselective and detrimental phase β-$VOPO_4$ was responsible of the worsening of the catalytic performances. Moreover, the ageing proceeded through the alteration the desorption properties of the material, since the water co-produced by the reaction led formation of hydrated phases ($VOHPO_4 \cdot nH_2O$) and the organic compounds were strong adsorbed forming carbon deposits and causing the blockage of the active sites.

The second part of my PhD thesis was focused on the study a new process for the synthesis of MA starting from a bio-based building block, 1-butanol. This alcohol is recently attracting attention, because it can be obtained from biomass and also used an alternative fuel in place of bioethanol, since it may be also advantageously utilized to

produce chemicals. The reaserch was supported by the FP7 programm of the EC (EuroBioRef).

We examined the different possible configurations in order to carry out the reaction in two steps or in one step: in particular we studied the dehydration of 1-butanol to butenes using acid catalysts (Keggin polyoxomethalates and $VOPO_4 \cdot 2H_2O$) and the "one-pot" reaction (oxidehydration) using vanadyl pyrophosphate as multifunctional catalyst.

The experiments carried out using Keggin polyoxomethalates supported on silica (POM) demonstrated that these materials could be successfully utilized as catalyst for the dehydration of 1-butanol to butenes: in fact, thanks to their acid properties, POM gave butenes with high selectivity. The samples tested were $Cs_2HPW_{12}O_{40}$, $Cs_3PW_{12}O_{40}$, $K_3HSiW_{12}O_{40}$ and $K_4SiW_{12}O_{40}$. The optimal range of temperature was investigated in order to limitate the phenomena responsible of lack to carbon balance: these materials were affected by the adsorption of the organic compound at low temperature and by the formation of coke at high temperature. Moreover, the effect of the chemical composition of the catalysts was outlined, in particular a key role ise played by the nature of the central atom and by the subtitution of the protons with alkaline cations. The $Cs_2HPW_{12}O_{40}$ catalyst showed the best performance both in terms of activity and selectivity, since it reached the total conversion at 150°C and the highest values of selectivity to butenes. On the other hand, the $K_4SiW_{12}O_{40}$ catalyst was revealed to be the worst, the total conversion being obtained at 290°C with a concomitant low selectivity to the dehydration products.

Concerning the dehydration of 1-butanol, the study was continued testing $VOPO_4 \cdot 2H_2O$ (VPD), since V/P/O based catalysts are known to have acid properties. VPD demonstrated to be a promising catalyst in oxidizing environment: in fact in presence of air it exhibited high activity and selectivity with stable perfomance during time and for this reason it was suggested as a good candidate for the dehydration of 1-butanol in presence of air in the "one-reactor" configuration for the synthesis of maleic anhydride from bio-butanol.

Lastly, we investigated the feasibility of the selective oxidehydration of 1-butanol into maleic anhydride. Experiments carried out with DuPont vanadyl pyrophosphate demonstrated that the material could successfully catalyze the dehydration of 1-butanol and the selective oxidation of butenes to MA, confirming its multifunctional properties. By means of reactivity tests the optimal reaction conditions were found: feeding 1%mol 1-butanol in air, the conversion of 1-butanol was completed over the entire range of temperature and the highest selectivity to MA was observed at 340°C (39%); the reaction also produced butenes, light acids (acrylic and acetic acid), carbon oxides, phthalic anhydride (PA), and minor amounts of other oxygenated compounds (furan and formaldehyde). At low temperatures the transformation of 1-butanol into butenes and the oxidative cleavage of either alcohol or olefins into acetic acid and acrylic acid were the prevalent reactions, while increasing the temperature, butenes were transformed into MA and PA and the light acids were oxidised into CO_x.

The investigation on reaction scheme showed that 1-butene is the primary product of the reaction and while its isomerisation to 2-butenes is relatively slow at low temperatures, at high temperature or high the residence time the consecutive oxidehydrogenation into MA occurs at a faster rate on 2-butenes than on 1-butene. The detrimental effect of the increase of 1-butanol partial pressure and the positive effect of the oxygen partial pressure showed that 1-butanol and butenes are strongly adsorbed on the catalyst surface: this is way an high O_2/(1-butanol + olefins) ratio is needed in order to have a sufficient amount of "free" and oxidized active sites. The strong interaction of alcohol with the VPP surface was demonstrated by DRIFT experiments: in fact, oxygen from the gas phase is essential to keep the vanadium centres oxidised, making possible the dehydration and the desorption of the intermediates and at the end the production of MA.

The detection of crotonic acid in DRIFT experiments suggested that crotonaldehyde may be a key intermediate in the mechanism of 1-butanol oxidehydration to MA. This hypothesis was confirmed by catalytic tests and DRIFT experiments, since crotonaldehyde undergoes two parallel reactions, one leading to furan, and the other to maleic acid. Furan and maleic acid were found to be both intermediates for MA formation, via oxidation or via dehydration, respectively. In conclusion, the

mechanism of the oxidehydration of 1-butanol involves the dehydration of 1-butanol to 1-butene, the isomerisation to 2-butenes, and the oxidation of the latter to crotonaldehyde. Then, crotonaldehyde can either cyclises to yield furan or be oxidised until maleic acid, which then could desorbs forming MA; on the other hand, furan can desorb and be consecutively re-adsorbed and further oxidised to MA.

The study of the oxidehydration of 1-butanol to MA was concluded testing three different types of bio-butanol, produced by fermentation of biomass. The first bio-butanol (BB1), even if it reached the total conversion in the same range of temperature investigated with the chemical 1-butanol (CB), gave an overall worsening of the performances, being increased the selectivity to CO_x and lowered the selectivity to MA and butenes. This behaviour was due to the accumulation on the catalyst surface of some impurities present in bio-butanol, which led to the decline of the performance. In particular, the responsible of the poisoning might be a carbazole compound, an antibiotic produced that by microorganisms during the final period of the fermentation process. With the aim of removing the impurities which negatively affected the performances, bio-butanols were treated by means of adsorption over bleaching earth enriched with activated charcoal: the catalytic test confirmed that the removal of the impurities was efficient, since at 360°C the same value of yield to MA obtained with CB was reproduced with BB1-superpur. In conclusion, the oxidehydration of bio-butanol to maleic anhydride was successfully obtained, demonstrating that also bio-butanol produced by fermentation could be easily utilize to carry out the process, since a simple purification treatment made it possible to remove the impurities present in it.

6 Acknowledgments

The research leading to these results has received funding from the European Union FP7 (FP7/2007-2013) under grant agreement n° 241718 EuroBioRef.

Heartfelt thanks to Polynt SpA for the financial and scientific support, in particular thank to Carlotta, Silvia and Federico.

7 Ringraziamenti

Era l'ultima ora dell'ultimo giorno. Ricordo perfettamente quando suonò la campanella e un senso di liberazione irruppe come non mai, alla sola idea che quei banchi e quei libri sarebbero stati a breve soltanto un ricordo. Avevo deciso di allontanarmi da quel mondo fatto di idee astratte e privo di concretezza; avevo deciso che avrei preso una strada diversa da tutti, per poter toccare con mano quelle parole che finora avevo solo potuto pronunciare o scrivere.
"Siamo schiavi delle leggi, per poter essere liberi". Questa è stata ed è per me la scienza, la chimica. In questo viaggio durato otto anni queste parole le ho sempre portate con me, giorno dopo giorno, insieme alle odi dei poeti, alle invettive dei grandi oratori, ai racconti degli storici e ai pensieri dei filosofi. La scienza mi ha permesso di capire quanto l'uomo possa fare per il mondo, per gli altri, per se stesso. Ne ho amato e ne amerò sempre la sua forza, la sua razionalità, il suo simbolismo e la sua magia. Con la chimica possiamo capire il mondo e quello che ci circonda, ma senza la comunicazione, la passione e la libertà anche la scienza nella sua concretezza può rischiare di rimanere un contenitore sterile. Per questo mi piace pensare di essere entrata a scuola da bambina, e di non esserne mai uscita. Mi piace pensare che i grandi classici in fondo siano così reali e così attuali da poter essere d'aiuto nel trasmettere tutto quello che la chimica fa per il progresso dell'uomo, nel suo pragmatismo e nella sua etica.

In questo viaggio ho avuto la fortuna di incontrare tante persone straordinarie e di aver imparato tantissime cose da ognuna di loro.

Ringrazio il prof. Fabrizio Cavani, per avermi seguito nel percorso del dottorato di ricerca, per avermi dato supporto e fiducia.

Ringrazio Carlotta, Silvia e Federico, per avermi permesso di collaborare con loro, dandomi l'opportunità di arricchire la ricerca scientifica.

Ringrazio tutto il gruppo di Catalisi, professori, ricercatori, dottorandi, borsisti, assegnisti e tesisti. Grazie per essere un meraviglioso esempio di collaborazione su ogni fronte, e per essere soprattutto degli amici prima di essere dei "colleghi".

Grazie Ciccio per l'aiuto enorme che mi hai dato negli ultimi tempi e grazie Juliana per il lavoro al DRIFT.

Grazie a tutti, Carlo, Mattia, Mugno, Taba, Max, Chiara, Diletta, Paris, Dodo, Grazia, Sara, Alice, Paolo, Stefania, Claudia, Juliana, Cristian, Ciccio, Erica, Matte, Davide, Alle, Fede, Beppe, Ale, Manuel, Dayanne, Matty, Ciaba, Silvia, Tommy, Oriella…(sicuramente mi sarò dimenticata qualcuno).

Un ringraziamento speciale va ai miei tesisti, Giovanni, Mattia, Luca ed Alberto, per essere stati la chiave di volta che mi ha permesso di capire quale fosse la strada da prendere: grazie per essere stati una delle mie soddisfazioni più grandi in questi anni di dottorato.

Infine grazie a Paolo, ai miei genitori, a mio fratello, alla mia famiglia e alle mie amiche per essere il centro del mio mondo, per volermi bene, per avermi sopportato pazientemente in questi anni, per essermi accanto e per condividere con me gioie e dolori.

"Si quis in caelum ascendisset naturamque mundi et pulchritudinem siderum perspexisset, insuavem illam admirationem ei fore; quae iucundissima fuisset, si aliquem, cui narraret, habuisset".

"Se un uomo salisse in cielo e contemplasse la natura dell'universo e la bellezza degli astri, la meraviglia di tale visione non gli darebbe la gioia più intensa, come dovrebbe, ma quasi un dispiacere, perché non avrebbe nessuno cui comunicarla".

Cicerone "Laelius de amicitia" 88

Concipere animo non potes quantum momenti afferri mihi singulos dies videam. "Mitte" inquis "et nobis ista quae tam efficacia expertus es." Ego vero omnia in te cupio transfundere, et in hoc aliquid gaudeo discere, ut doceam; nec me ulla res delectabit, licet sit eximia et salutaris, quam mihi uni sciturus sum. Si cum hac exceptione detur sapientia, ut illam inclusam teneam nec enuntiem, reiciam: nullius boni sine socio iucunda possessio est.

Non puoi immaginare quali progressi io mi accorga di compiere giorno per giorno. Tu mi dici: "Riferisci anche a me questo metodo che hai trovato così efficace."Certo, desidero travasare in te tutto il mio sapere e sono lieto di imparare qualcosa appunto per insegnarla. Di nessuna nozione potrei compiacermi, per quanto straordinaria e vantaggiosa, se ne avessi conoscenza per me solo. Se mi fosse concessa la sapienza a condizione di tenerla chiusa in me senza trasmetterla ad altri, rifiuterei: non dà gioia il possesso di nessun bene, se non puoi dividerlo con altri.

Seneca "Epistulae morales ad Lucilium" (liber I, Epistola VI, 4-7)

8 References

[1] MSDS of maleic anhydride

[2] Handbook of Chemistry & Physics, 95th edition, 2014-2015

[3] www.polynt.com Technical data sheet Maleic Anhydride Molten

[4] www.chemical.ihs.com

[5] www.mcgroup.co.uk

[6] Patent EP 1047687 (2006) *Process for the production of gamma-butyrolactone*

[7] Patent US 2772292 (1956) *Hydrogenation of maleic anhydride*

[8] Patent EP 0304696 (2006) *Process for the preparation of 1,4-butanediol and/or tetrahydrofuran*

[9] Patent US 5073650 (1991) *Preparation of 1,4-butanediol*

[10] www.thinking.nexant.com Report Abstract - Maleic Anhydride 07/08-8

[11] Ulmann's Chemical Encyclopedia, Vol A, 16 (2011) 54

[12] K. Lohbeck,.H. Haferkorn, W. Fuhrmann, N. Fedtke, "Maleic and Fumaric Acids", *Ullmann's Encyclopedia of Industrial Chemistry* (2000)

[13] D. Lgs. n° 155 del 13/08/2010 "Attuazione della direttiva 2008/50/CE relativa alla qualità dell'aria ambiente e per un'aria più pulita in Europa"

[14] F. Trifirò, R. K. Grasselli, *Top. Catal.*, 57 (2014) 1188 - 1195

[15] T. A. Bither Jr, to E. I. Du Pont de Nemours and Company US Patent 4442226 (1984)

[16] F. Cavani, F. Trifirò, *Chem. Tech*., 24 (1994) 18

[17] P. Arpentier, F. Cavani, F. Trifirò, *"The technology of catalytic oxidation"*, Edition TECHNIP, Paris (2001)

[18] G. Centi, F. Cavani, F. Trifirò, *"Selective oxidation by heterogeneous catalysis"*, Edition Kluwer Academic Plenum Publishers (2001)

[19] F. Centi, F. Trifirò, J. R. Ebner and V. Franchetti, *Chem. Rev.*, 88 (1988) 175

[20] F. Cavani, F. Trifirò, *Appl. Catal. A*, 88 (1992) 115

[21] R. M. Contractor, A. W. Sleight, *Catal. Today*, 3 (1988) 175

[22] N. F. Dummer, J. K. Bartley, G. J. Hutchings, Adv. Catal., 54 (2011) 189

[23] E. A. Lombardo, C. A. Sanchez, L. M.Cornaglia, *Catal. Today*, 15 (1992) 407

[24] G. Poli, I. Resta, O. Ruggeri, F. Trifirò, *Appl. Catal. A Gen.*, 95 (1993) 117

[25] N. H. Batis, H. Batis, A. Ghorbel, J. C. Vedrine, J. C. Volta, J. Catal. 128 (1991) 248

[26] M. O' Connor, F. Dason, B. K. Hodnett, *Appl. Catal. A Gen.*, 64 (1990) 161

[27] F. Cavani, G. Centi, F. Trifirò, *Appl. Catal.*, 9 (1984) 191-202

[28] H. S. Horowitz, C. M. Blackstone, A. W. Sleight, G. Teufer, *Appl. Catal.*, 28 (1988) 1963

[29] J. W. Johnson, D. C. Johnston, A. J. Jacobson, J. F. Brody, *J. Am. Chem. Soc.*, 106 (1984) 8123

[30] G. J. Hutchings, R. Higgins, Appl. Catal. A Gen., 154 (1997) 103

[31] S. Albonetti, F. Cavani, S. Ligi, F. Pierelli, F. Trifirò, F. Ghelfi, G. Mazzoni, *Stud. Surf. Sci.Catal.*, 143, (2002) 963

[32] E. C. Milberger, N. J. Bremer, D. N. Dria to Sohio (1982) US Patent 4350639

[33] M. E. Leonowicz, J. W. Johnson, J. F. Brody, H. F. Shannon, J. M. Newsam. *J. Solid State Chem.*, 56 (1985) 370

[34] J. W. Johnson, A. J. Jacobson, *J. Angew. Chem., Int. Ed. Engl.*, 22 (1983) 412

[35] E. Bordes, P. Courtine, J. W. Johnson, *J. Solid State Chem.*, 55 (1984) 270

[36] G. Busca, F. Cavani, G. Centi, F. Trifirò, *J. Catal.*, 99 (1986) 400

[37] M. R. Thomson, J. R. Ebner in P.Ruyiz and P. Delmon "*New development in selective oxidation by heterogeneous catalysis"*, Edition Elsevier, Amsterdam (1992) 353

[38] L. M. Cornaglia, C. Caspari, E. A. Lombardo, *Appl. Catal.*, 15 (1991) 74

[39] R. M. Contractor, J. R. Ebner, M. J. Mummey in G. Centi and F. Trifirò "*New development in selective oxidations"*, Edition Elsevier Science, Amsterdam (1990) 553

[40] S. Albonetti, F. Budi, F. Cavani, S. Ligi, G. Mazzoni, F. Pierelli, F. Trifirò, *Stud. Surf. Sci.Catal.*, 136 (2001) 141-146

[41] S. A. Linde, Yu E. Gorbunova, *Dokl. Akad. Nauk SSSR*, 245 (1979) 584

[42] P. T. Nguyen, R. D. Hoffman, A. W. Sleight, *Mater. Res. Bull.*, 30 (1995) 1055

[43] Yu E. Gorbunova, S. A. Linde, *Sov. Phys. Dokl.*, 24 (1979) 138

[44] T. Okamura, M. Misono, *Catal. Today*, 16 (1993) 61

[45] R. M. Contractor, Bergna, H. S. Horowitz, C. M. Blackstone, B. Malone, C. C. Torardi, B. Griffiths, U. Chowdhry, A. W. Sleight, *Catal. Today*, 1 (1987) 47

[46] C. C. Torardi, J. C. Calabrese, *Inorg. Chem.*, 23 (1984) 1308

[47] E. Bordes, *Catal. Today*, 1 (1987) 499

[48] E. Bordes, *Catal. Today*, 3 (1987) 163

[49] N. Duvauchelle, E. Kesteman, F. Oudet, E. Bordes, *J. Solid State Chem.*, 137 (1998) 311-324

[50] L. O' Mahony, J. Henry, D. Sutton, T. Curtin, B. K. Hodnett, *Appl. Catal. A Gen.*, 253 (2003) 409

[51] M. Nakamura, K. Kawai, Y. Fujiwara, *J. Catal.*, 34 (1974) 345

[52] T. Shimoda, T. Okuhara, M. Misono, *Bull. Chem. Soc. Jpn.*, 58 (1985) 2163

[53] J. S. Buchanan, J. Apostolakis, S. Sundaresan, *Appl. Catal.*, 19 (1985) 65

[54] B. K. Hodnett, B. Delmon, *J. Catal.*, 88 (1984) 43

[55] A. Caldarelli, M. A. Bañares, C. Cortelli, S. Luciani, F. Cavani, *Catal. Sci. Technol.*, 4 (2014) 419

[56] P. T. Nguyen, A. W. Sleight, N. Roberts, W. W. Warren, *J. Solid State Chem.*, 122 (1996) 259

[57] T. Okumara, K. Inumaru, M. Misono, *ACS Symp. Ser.*, 523 (1993) 156

[58] K. Inumaru, T. Okumara, M. Misono, *Chem. Lett.*, 21(10) (1992) 1955

[59] G. Mazzoni, F. Cavani, G. Stefani to Lonza (2005) US Patent 6956004

[60] Z. Shan, W. S. Frazee, M. J. Mummey, B. A. Horrel, to Hunstman WO 2012033635 Patent

[61] P. Ruiz, P. Bastians, L. Caussin, R. Reuse, L. Daza, D. Acosta, B. Delmon, *Catal. Today*, 16 (1993) 99

[62] F. Garbassi, J. C. J. Bart, F. Montino, G. Petrini, *Appl. Catal.*, 16 (1985) 271

[63] F. Cavani, G. Centi, I. Manenti, F. Trifirò, *Ind.. Eng. Chem. Prod. Res. Dev.*, 24 (1985) 221

[64] H. Morishige, J. Tamaki, N. Miura, N. Yamazoe, *Chem. Lett.*, 19(9) (1990) 1513

[65] G. Centi, *Catal. Today*, 16 (1993) 5-26

[66] P. Mars, D.W. van Krevelen, *Chem. Eng. Sci. Spec. Suppl.*, 3 (1954) 41.

[67] J.-C. Volta, *Catal. Today*, 32 (1996) 29

[68] Y. Schuurman, J. T. Gleaves, *Ind. Eng. Chem. Res.*, 33 (1994) 2935

[69] G. J. Hutchings, A. Desmartin-Chomel, R. Olier, J.C. Volta, *Nature*, 368 (1994) 41

[70] M. Abon, K. Béré, A. Tuel, P. Delichere, *J. Catal.*, 156 (1995) 28

[71] K. Ait-Lachgar, A. Tuel, M. Brun, J.M. Herrmann, J.M. Krafft, J.R. Martin, J.C. Volta, J. Catal., 177 (1998) 224

[72] G. J. Hutchings, C.J. Kiely, M.T. Sananes-Schulz, A. Burrows, J.C. Volta, *Catal. Today*, 40 (1998) 273.

[73] U. Rodemerck, B. Kubias, H.W. Zanthoff, M. Baerns, *Appl. Catal.*, 153 (1997) 203.

[74] U. Rodemerck, B. Kubias, H.W. Zanthoff, G.U. Wolf, M. Baerns, *Appl. Catal.*, 153 (1997) 217

[75] E. Bordes, *Catal. Today*, 16 (1993) 27.

[76] E. Bordes, P. Courtine, *J. Catal.*, 57 (1979) 236

[77] B. Jordan, C. Calvo, *Can. J. Chem.*, 51 (1973) 2621

[78] D. Ballutaud, E. Bordes, P. Courtine, *Mater. Res. Bull.*, 17 (1982) 519

[79] M. Tachez, F. Theobald, J. Bernard, A. W. Hewat, *Rev. Chim. Miner.*, 19 (1982) 291

[80] E. Bordes, P. Courtine, *J. Chem. Soc. Chem. Comm.*, 34 (1985) 294

[81] F. B. Ben Abdelouahab, R. Oliver, N. Guilhaume, F. Lefebvre, J.-C Volta, J. Catal., 134 (1992) 151

[82] F. Girgsdies, M. Schneider, A. Brückner, T. Ressler, R. Schlögl, *Solid State Sciences*, 11(2009) 1258-1264

[83] P. Amorós, G. S. Patience, J. R. Fernandez, M. J. Lorences, F. Díez, A. Vega, R. Cenni, *Catal. Today*, 118 (2006) 32-38

[84] G. W. Coulston, S.R. Bare, H. Kung, K. Birkeland, G.K. Bethke, R. Harlow, N. Herron, P.L. Lee, *Science*, 275 (1997) 191

[85] P. L. Gai, K. Kourtakis, D.R. Coulson, G.C. Sonnichsen, *J. Phys. Chem. B*, 101 (1997) 9916.

[86] R. Mallada, S. Sajip, C. J. Kiely, M. Menendez, J. Santamaria, *J. Catal.*, 196 (2000) 1

[87] S. Mota, M. Abon, J.C. Volta, J.A. Dalmon, *J. Catal.*, 193 (2000) 308.

[88] G. Busca, G. Ramis, V. Lorenzelli, *J. Mol. Catal.*, 50 (1989) 231

[89] F. Cavani, F. Trifirò, *Appl. Catal. A Gen.*, 157 (1997) 195

[90] L. M. Cornaglia, E. A. Lombardo, *Stud. Surf. Sci. Catal.*, 90 (1994) 429

[91] G. Centi, G. Gollinelli, G. Busca, *J. Phys. Chem.*, 94 (1990) 6813

[92] J. C. Vedrine, J. M. M. Millet, J.-C. Volta, *Catal. Today*, 32 (1996) 115-123

[93] D. J. Thompson, I. M. Ciobîcă, B. K. Hodnett, R. A. Van Santen, M. O. Fanning, *Surf. Science*, 547 (2003) 438-451

[94] Y. Schuurman, J. T. Gleaves, Catal. Today, 33 (1997) 25-37

[95] G. S. Patience, R. E. Bockrath, J. D. Sullivan, H. S. Horowitz, *Ind. Eng. Chem. Res.*, 46 (2007) 4374-4381

[96] P. G. Pries de Oliveira, J. G. Eon, M. Chavant, A. S. Richè, V. Martin, S. Caldarelli, *Catal. Today*, 57 (2000) 177-186

[97] V. V. Guliants, *Catal. Today*, 51 (1999) 255

[98] R. A. Overbeek, P.A. Warringa, M.J.D. Crombag, L.M. Visser, A.J. van Dillen, J.W. Geus, *Appl. Catal. A*, 135 (1996) 209

[99] R. A. Overbeek, A.R.C.J. Pekelharing, A.J. van Dillen, J.W. Geus, *Appl. Catal. A*, 135 (1996) 231

[100] M. Ruitenbeek, R.A. Overbeek, A.J. van Dillen, D.C.Koningsberger, J.W. Geus, *Recl. Trav. Chim. Pays-Bas*, 115 (1996) 519

[101] M. Nakamura, K. Kawai, Y. Fujiwara, *J. Catal.*, 34 (1974) 345

[102] M. J. Ledoux, C. Crouzet, C. Pham-Huu, V. Turines, K. Kourtakis, P. Mills and J.J. Lerou, *J. Catal.*, 203 (2001) 495

[103] R. A. Overbeek, P.A. Warringa, M.J.D. Crombag, L.M. Visser, A.J. van Dillen and J.W. Geus, *Appl. Catal. A*, 135 (1996) 209

[104] F. Cavani, D. De Santi, S. Luciani, A. Lofberg, E. Bordes-Richard, C. Cortelli, R. Leanza, *Appl. Catal. A*, 376 (2010) 66–75

[105] M. Abon, J.M. Herrmann, J.C. Volta, *Catal. Today*, 71 (2001) 121

[106] L. Cornaglia, S. Irusta, E.A. Lombardo, M.C. Durupty, J.C. Volta, *Catal. Today*, 78 (2003) 291

[107] J. G. Hutchings, *Appl. Catal.*, 72 (1991) 1

[108] G. J. Hutchings, R. Higgins, *J. Catal.*, 162 (1996) 153

[109] F. Cavani, C. Fumagalli, F. Ghelfi, C. Mazzoni, F. Pierelli to Lonza (2005) EP 1514598 A1 Patent

[110] D. Ye, A. Satsuma, T. Hattori, Y. Marakami, Appl. Catal., 69 (1991) L1

[111] D.-Q. Ye, M.-L. Fu, L. Hong, S.-Z. Rong, S. Cheng, X. Pang, *Res. Chem. Intermed.*, 29 (2003) 271

[112] G. J. Hutchings, *Catal. Today*, 16 (1993) 139

[113] V. V. Guliants, J. B. Benziger, S. Sundaresan, I. E. Wachs, *Stud. Surf. Sci. Catal.*, 130B (2000) 1721

[114] H. Liang, D.-Q. Ye, W.-M. Lin, *J. Yun. Univ.*, 28 (2006) 68

[115] N. Ballarini, F. Cavani, C. Cortelli, S. Ligi, F. Pierelli, F. Trifirò, C. Fumagalli, G. Mazzoni, T. Monti, *Top. Catal.*, 38 (2006) 147

[116] I. Matsuura, T. Ishimura, S. Hayakawa, N. Kimura, *Catal. Today*, 28 (1996) 133-138

[117] V. V. Guliants, J. B. Benziger, S. Sundaresan, I. E. Wachs, A. M. Hirt, *Catal. Lett.*, 62 (1999) 87-91

[118] P. A. Agaskar, R. K. Grasselli, D. J. Buttrey, B. White, *Stud. Surf. Sci. Catal.*, 110 (1997) 219-226

[119] A. M. Duarte de Farias, W. De A. Gonzalez, P.G. Pries de Oliveira, J. G. Eon, J.M. Herrmann, M. Aouine, S. Loridant, J.-C. Volta, *J. Catal.*, 208 (2002) 238-246

[120] M. Eichelbaum, R. Stößer, A. Karpov, C.-K. Dobner, F. Rosowski, A. Trunschke, R. Schlögl, *Phys. Chem. Chem. Rev.*, 14 (2012) 1302-1312

[121] R. Fricke, H.-G. Jerchekewitz,, G. Lischke, G. Z. Ohlmann, *Anorg. Allg. Chem.*, 23 (1979) 448

[122] F. Trifirò, *Catal. Today*, 16 (1993) 91

[123] B. K. Hodnett, B. Delmon, *Appl. Catal.*, 15 (1985) 141

[124] L. Morselli, F. Trifirò, L. Urban, *J. Catal.*, 75 (1982) 112

[125] M. Ai, *J. Catal.*, 67 (1981) 110

[126] G. Centi, G. Fornasari and F. Trifirò, *J. Catal.*, 89 (1984) 44

[127] S. Albonetti, F. Cavani and F. Trifirò, *Catal. Rev. Sci. Eng.*, (1996) 413

[128] D. J. Thompson, I.M. Ciobîca, B.K. Hodnett, R.A. van Santen, M.O. Fanning, *Surface Science*, 547 (2003) 438

[129] D. J. Thompson, I.M. Ciobîca, B.K. Hodnett, R.A. van Santen, M.O. Fanning, *Catal. Today*, 91 (2004) 177

[130] G. Busca, E. Finocchio, G. Ramis, G. Ricchiaroli, *Catal. Today*, 32 (1996) 1330

[131] V. A. Zazhigalov, J. Haber, J. Stoch, V. M. Belousov, *Appl. Catal.*, 96 (1993) 135

[132] M. R. Thompson, J. R. Ebner in P. Ruyiz, B. Delmon *"New Developments in Selective Oxidation by Heterogeneous Catalysis"*, Edition Elsevier, Amsterdam, 1992, page 353

[133] P. L. Gai, K. Kourtakis, *Science*, 267 (1995) 661

[134] P. L. Gai, *Topics Catal.*, 8 (1999) 97

[135] P. A. Agaskar, L. De Caul, R. K. Grasselli, *Catal. Lett.*, 23 (1994) 339

[136] Z. Du, J. Ma, F. Wang, J. Liu, J. Xu, *Green Chem.*, 13 (2011) 554-557

[137] H. Guo, G. Yin, *J. Phys. Chem. C*, 115 (2011) 17516-17522

[138] N. Alonso-Fagündez, M. López Granados, R. Mariscal, and M. Ojeda, *ChemSusChem*, 5 (2012) 1984-1990

[139] H.-D. Hahn, G. Dämbkes, N. Rupprich, H. Bahl, *Ullmann's Encyclopedia of Industrial Chemistry, Vol. 6*, Wiley-VCH Verlag GmbH & Co. KGaA, Weinheim (2012**)** pp. 417-430.

[140] T. Tsuchida, J. Kuboa, T. Yoshioka, S. Sakuma, T. Takeguchi, W. Ueda, *J. Catal*., 259 (2008) 183-189

[141] C. Yang, Z. Meng, *J. Catal.*,142 (1993**)** 37-44

[142] A. S. Ndou, N. Plint, N.J. Coville, *Appl. Catal. A*, 251 (2003) 337-345

[143] M. León, E. Díaz, A. Vega, S. Ordóñez, A. Auroux, *Appl. Catal. B*, 102 (2011**)** 590–599

[144] B. G. Harvey, H. A. Meylemans, *J. Chem. Technol. Biotechnol.*, 86 (2011) 2

[145] N. Qureshi, T. C. Ezeji, Biofuels, *Bioprod. Bioref.*, 2 (2008) 319

[146] M .R. Harper, K. M. V. Geem, S. P. Pyl, S. S. Merchant, G. B. Marin, W. H. Green, *Combust. Flame*, 158 (2011**)** 2075

[147] R. Horyń, R. Klimkiewicz, *Appl. Catal. A*, 370 (2009) 72-77

[148] C. Cobzaru, S. Oprea, E. Dumitriu, V. Hulea, *Appl. Catal. A*, 351 (2008) 253-258

[149] A. Ungureanu, S. Royer, T. V. Hoang, D. Trong On, E. Dumitriu, S. Kaliaguine, *Micropor. Mesopor. Mater*., 84 (2005) 283-296.

[150] H. Hattori, *Appl. Catal. A*, 222 (2001) 247-259

[151] J. Raskó, J. Kiss, *Appl. Catal. A: Gen*., 285 (2005) 252–260

[152] J. S. Kruger, R. Chakrabarti, R.J. Hermann, L.D. Schmidt, *Appl. Catal. A*, 411–412 (2012) 87–94

[153] A. A. Shoaibi, A.M. Dean, *J. Fuel Cell Sci. Technol*, 7 (2010) 041015-041018

[154] A. Iriondo, M.B. Guemez, J. Requies, V.L. Barrio, J.F. Cambra, P.L. Arias, J.L.G. Fierro, *Stud. Surf. Sci. Catal.*, 175 (2010) 453-456

[155] M. A. Parent, J.B. Moffat, *Catal. Lett.*, 48 (1997) 135-143

[156] J. Macht, M.J. Janik, M. Neurock, E. Iglesia, *J. Am. Chem. Soc.*, 130 (2008) 10369-10379

[157] K. Hashimoto, Y. Matsumura, M. Fukuchi, Y. Kera, *Catal. Lett.*, 19 (1993) 375-381

[158] M. R. Mostafa, A.M. Youssef, *Mater. Lett.*, 34 (1998) 405-410

[159] F. M. Bautista, B. Delmon, *Appl. Catal. A*, 130 (1995) 47-65

[160] V. Macho, M. Králik, E. Jurecekova, J. Hudec, L. Jurecek, *Appl. Catal. A*, 214 (2001) 251–257

[161] S. J. Joris, C.H. Amberg *J. Fuel Cell Sci. Technol*.,76 (1971) 3167-3171

[162] G. Guiu, P. Grange, *J. Catal.*, 168 (1997) 463-470

[163] A. Gil, M.A. Vicente, S.A. Korili, *J. Catal*., 229 (2005) 119-126

[164] S. Delsarte, M. Florea, F. Maugé, P. Grange, *Catal. Today*, 116 (2006) 216–225

[165] R. A. Hernandez, U. S. Ozkan, *Ind. Eng. Chem. Res.*, 29 (1990) 1454

[166] U.S. Ozkan, G.L. Schrader, *J. Catal.*, 95 (1985) 137

[167] J. McMurry, Chimica Organica, Ed. Piccin, 2009

[168] M. Perissinotto, M. Lenarda, L. Storaro, R. Ganzerla, *J. Molec. Catal. A: Chem.*, 121 (1997) 103-109

[169] G. Chen, S. Li, F. Jiao, Q. Yuan, *Catal. Today*, 125 (2007) 111-119

[170] P. Vazquez, L. Pizzio, C. Caceres, M. Blanco, H. Thomas, E. Alesso, L. Finkielsztein, B. Lantano, G. Moltrasio, J. Aguirre, *J. Molec. Catal. A: Chem.*, 161 (2000) 223-232

[171] M. J. Janik, J. Macht, E. Iglesia, M. Neurock, *J. Phys. Chem.*, 113 (2009) 1872-1885

[172] P. Berteau, B. Delmon, J.-L. Dallons, A. Van Gysel, *Appl. Catal.*, 70 (1991) 307-323

[173] M. A. Makarova, E. A. Paukshtis, J. M. Thomas, C. Williams, K.I. Zamaraev, *Stud. Surf. Sci. Catal.*, 75 (1993) 1711-1714

[174] L. Matachowski, A. Drelinkiewicz, E. Lalik, D. Mucha, B. Gil, Z. Brozek-Mucha, Z. Olojniczak, *Microporous Mesoporous Mater.*, 144 (2011) 46-56

[175] M. Ammam, *J. Mater. Chem. A*, 1 (2013) 6291-6312

[176] S. Lis, *J. Alloys and Compounds*, 300-301 (2000) 88-94

[177] X. Lopez, L. Vila-Nadal, X. Aparicio-Angles, J. M. Poblet, *Phys. Procedia*, 8 (2010) 94-103

[178] M. Sadakane, E. Steckhan, *Chem. Rev.*, 98 (1998) 219-237

[179] I. A. Weinstock, *Chem. Rev*., 98 (1998) 113-170

[180] A. S. Dias, M. Pillinger, A. A. Valente, *Appl. Catal. A: Gen.*, 285 (2005) 126-131

[181] V. Palermo, G. P. Romanelli, P. G. Vazquez, *J. Molec. Catal. A: Chem.*, 373 (2013) 142-150

[182] L. Jing, J. Shi, F. Zhang, Y. Zhong, W. Zhu, *Ind. Eng. Chem. Res.*, 52 (2013) 10095-10104

[183] P. Xiao, F. Dumur, M. A. Tehfe, B. Graff, J. P. Fouassier, D. Gigmes, J. Lalevee, Macromol. *Chem. Phys.*, 214 (2013) 1749-1755

[184] J. T. Rhule, C. L. Hill, D. A. Judd, R. F. Schinazi, *Chem. Rev.*, 98 (1998) 327-357

[185] J. Berzelius, *Ann. Phys. Chem.*, 82 (1826) 369

[186] M. T. Pope, *"Heteropoly and Isopoly oxometalates"*, Ed. Springer, 1983

[187] C. L. Hill, *Chem. Rev.*, 98 (1998) 1-2

[188] L. Pauling, *J. Am. Chem. Soc.*, 51 (1929) 2868

[189] J. F. Keggin, *Nature*, 131 (1933) 908

[190] A. Corma, A. Martinez, C. Martinez, *J. Catal.*, 164 (1996) 422-432

[191] T. Okuhara, T. Nishimura, H. Watanabe, M. Misono, *J. Mol. Catal.*, 74 (1992) 247256

[192] N. F. Dummer, W. Weng, C. Kiely, A.F. Carley, J.K. Bartley, C.J. Kiely, G.J. Hutchings, *Appl. Catal. A*, 376 (2010) 47–55

[193] L. Griesel, J. K. Bartley, R. P. K. Wells, G. J. Hutchings, *J. Mol. Cat. A: Chem*., 220 (2004) 113

[194] G. Mazzoni, G. Stefani, F. Cavani, EP 804963 Patent (1997), assigned to Lonza group

[195] F. Cavani and J. H. Teles, *ChemSusChem*, 2 (2009) 508–534

[196] M. S. Haddad, R. A. Gustaferro, to Ineos (2013) US 20130102455 A1 Patent

[197] C. K. Dobner, S. Altwasser, W. Hagen, F. Rosowski, to BASF (2011) US 20110257414 A1 Patent

[198] A. Caldarelli, F. Cavani, F. Folco, S. Luciani, C. Cortelli, R. Leanza, *Catal. Today*, 157 (2010) 204-210

[199] H. Bluhm, M. Hävecker, E. Kleimenov, A. Knop-Gericke, A. Liskowski, R. Schlögl, D. S. Su, *Top. Catal.*, 23 (2003) 99-107

[200] M. Hävecker, A. Knop-Gericke, H. Bluhm, E. Kleimenov, R. W. Mayer, M. Fait, R. Schlögl, *Appl. Surf. Sci*., 230 (2004) 272-282

[201] M. Hävecker, R.W. Mayer, A. Knop-Gericke, H. Bluhm, E. Kleimenov, A. Liskowski, D. S. Su, R. Follath, F. G. Requejo, D. F. Ogletree, M. Salmeron, J. A. Lopez-Sanchez, J. K. Bartley, G. J. Hutchings, R Schlögl, *J. Phys. Chem. B*, 107 (2003) 4587-4596

[202] H. W. Zanthoff, M. Sananes-Schultz, S. A. Buchholz, U. Rodemerck, B. Kubias, M. Baerns, *Appl. Catal.* A, 172 (1998) 49‑58

[203] E. W. Arnold, S. Sundaresan, *Appl. Catal.*, 41 (1988) 225-239

[204] R. M. Contractor, H. S. Horowitz, G. M. Sisler, E. Bordes, *Catal. Today*, 37 (1997) 51-57

[205] E. Bordes, J. W. Johnson, A. Raminosova, P. Courtine, *Mater. Sci. Monograph.*, 28B (1985) 887

[206] G. Stefani, P. Fontana to Lonza, US Patent 4181628 (1980)

[207] German Patent 2353136 (1973)

[208] K. R. Bakshi, US Patent 4123442 (1978)

[209] R. C. Edwards, P. H. Kilmer, C. A. Hudovich, P. L. Stauffenberg, *Eur. Pat. Appl.*, EP123467 (1984)

[210] B. K. Hodnett, *Catal. Rev.-Sci. Eng.*, 27 (1985) 373

[211] I. Mastuura, M. Yamazaki in G. Centi and F. Trifirò *"New Developments in Selective Oxidation"*, Edition Elsevier, Amsterdam (1990) 563

[212] V. A. Zazhigalov, *Teor. And Experim. Chem.*, 35 (1999) 265

[213] M. Pawlyta, J.-N. Rouzaud, S. Duber, *Carbon*, 84 (2015) 479-490

[214] A. C. Ferrari, J. Robertson, *Phys. Rev. B*, 61 (2000) 14095

[215] G. F. Froment, *Stud. Surf. Sci. Catal.*, 6 (1980) 1

[216] M. Guisnet, P. Magnoux, *Stud. Surf. Sci. Catal.*, 88 (1994) 53

[217] D. M. Golden, K. W. Egger, S. W. Benson, J. Amer. Chem. Soc., 86 (1964) 5416

[218] L. Matachowski, A. Drelinkiewicz, E. Lalik, D. Mucha, B. Gil, Z. Brozek-Mucha, Z. Olojniczak, *Microporous Mesoporous Mater*., 144 (2011) 46-56

[219] P. Berteau, M. Runet, B. Delmon, *Acta Chim. Hung.*, 124 (1987) 25

[220] Y. H. Taufiq-Yap, M. H Looi, M. Z. Hussein, Z. Zainal, *Asian Jour. Chem.*, 14 (2002) 1494-1502

[221] I. J. Ellison, G. J. Hutchings, M. T. Sananes, J. C. Volta, *J. Chem. Soc. Chem. Commun.*, 9 (1994) 1093

[222] Y. H. Taufiq-Yap, A. A. Rownaghi, M. Z. Hussein, R. Irmawati, *Catal. Lett.*, 119 (2007) 64

[223] N. Yamamoto, N. Hiyoshi, T. Okuhara, *Chem. Mater*., 14 (2002) 3882

[224] N. Hiyoshi, N. Yamamoto, N. Ryumon, T. Okuhara, *J. Catal.*, 221 (2004) 225-233

[225] G. Ladwig, *Z. Anorg. Allg. Chem*., 338 (1965) 266

[226] M. Trchová, P. Čapková, P. Matějka, K. Melánová, L. Beneš, E. Uhlıřová, *J. Solid State Chem.*, 148 (1999) 197

[227] C. J. Kiely, A. Burrows, S. Sajip, G. J. Hutchings, M. T. Sananes, A. Tuel, J. C. Volta, *J. Catal.*, 162 (1996) 31

[228] S. J. Puttock, C. H. Rochester, *J. Chem. Soc. Faraday Trans. I*, 82 (1986) 2773

[229] G. Busca, G. Centi, F. Trifirò, *J. Am. Chem. Soc*., 107 (1985) 7757

[230] M. Ai, *J. Catal.*, 116 (1989) 23

[231] G. Centi, D. Pesheva, F. Trifirò, *Appl. Catal.*, 33 (1987) 343

[232] A. Martin, B. Lücke, H. Seeboth, G. Ladwig, *Appl. Catal.*, 49 (1989) 205

[233] G. Centi, F. Trifirò, *J. Molec. Catal.*, 35 (1986) 255

[234] G. Centi, J. L. Nieto, F. Ungarelli, F. Trifirò, Catal. Letters, 4 (1990) 309

[235] M. Ai, S. Suzuki, *Bull. Chem. Soc. Jpn*., 47 (1974) 3074-3077

[236] V. V. Guliants, J.B. Benziger, S. Sundaresan, *Stud. Surf. Sci. Catal*., 101 (1996) 991-1000

[237] V. V. Guliants, S.A. Holmes, *J. Mol. Catal. A*, 175 (2001) 227-239

[238] F. Cavani, F. Trifirò, *Catal. Today*, 51 (1999) 561-580

[239] Ph. Arpentinier, F. Cavani, F. Trifirò, *Catal. Today*, 99 (2005) 15-22

[240] N. Ballarini, F. Cavani, C. Cortelli, F. Gasparini, A. Mignani, F. Pierelli, F. Trifirò, C. Fumagalli, G. Mazzoni, *Catal. Today*, 99 (2005) 115-122

[241] F. Cavani, A. Colombo, F. Giuntoli, E. Gobbi, F. Trifirò, P. Vazquez, *Catal. Today*, 32 (1996) 125-132

[242] M. López Granados, J.L.G. Fierro, F. Cavani, A. Colombo, F. Giuntoli, F. Trifirò, *Catal. Today*, 40 (1998) 251-261

[243] G. Bignardi, F. Cavani, C. Cortelli, T. De Lucia, F. Pierelli, F. Trifirò, G. Mazzoni, C. Fumagalli, T. Monti, *J. Molec. Catal. A*, 244 (2006) 244-251

[244] F. Cavani, G. Centi, A. Riva, F. Trifirò, *Catal. Today*, 1 (1987) 17-26

[245] F. Cavani, G. Centi, F. Trifirò, R.K. Grasselli, *Catal. Today*, 3 (1988) 185-198

[246] R. Wenig, G. Schrader, *J. Phys. Chem*., 91 (1987) 5674–5680

[247] B. Sakakini, *J. Catal*., 189 (2000) 253–262

[248] R. W. Wenig, G. L. Schrader, *J. Phys. Chem*., 91 (1987) 1911-1918

[249] S. K. Bhattacharyya, A. K. Kar, *J. Catal*., 1 (1962) 293-300

[250] P. Cicmanec, K. Syslova, J. Tichy, *Topics Catal*, 45 (2007) 229-232

[251] J.M. Church, P. Bitha, *Ind. & Eng. Chem. Prod. Res. & Dev.*, 2 (1963) 61-66

[252] Z.-Y. Xue, G.L. Schrader, *J. Catal.*, 184 (1999) 87-104

[253] M. Ai, T.-h. Tsai, A. Ozaki, *Bull. Chem. Soc. Jpn*., 53 (1980) 2647-2650

[254] P. Ruanpanun, Z. Teklemariam Dame, H. Laatsch, S. Lumyong, *FEMS Microbiol Lett*, 322 (2011) 77–81